



Hull Structural Safety Assessment -of Aged Non-ice Class Container Vessels -in an Arctic Operation

Yun-Tzu, Huang

Master Thesis

presented in partial fulfillment

of the requirements for the double degree:

“Advanced Master in Naval Architecture” conferred by University of Liege

“Master of Sciences in Applied Mechanics, specialization in Hydrodynamics,

Energetics and Propulsion” conferred by Ecole Centrale de Nantes

developed at West Pomeranian University of Technology, Szczecin

in the framework of the

“EMSHIP”

Erasmus Mundus Master Course

in “Integrated Advanced Ship Design”

Ref. 159652-1-2009-1-BE-ERA MUNDUS-EMMC

Supervisor: Prof. Zbigniew Sekulski, West Pomeranian University of
Technology, Szczecin

Internship Supervisor: Prof. Jeom-Kee Paik, National Busan University, Korea

Reviewer: Prof. Hervé Le Sourne, ICAM Nantes

Szczecin, February 2017



CONTENTS

CONTENTS	3
ABSTRACT	5
LIST OF FIGURES	7
LIST OF TABLES	10
ABBREVIATIONS	11
NOMENCLATURES	11
1. INTRODUCTION	13
2. LITERATURE REVIEW	17
2.1 REGULATIONS	17
2.2 THEORY OF ULTIMATE STRENGTH	19
2.3 STUDIES RELATED TO STRUCTURE SAFETY FOR CONTAINER VESSELS	21
2.4 PROCEDURE FOR HULL STRUCTURE SAFETY ASSESSMENT	21
3. MODELLING OF STRUCTURES AND ANALYSIS ASSUMPTIONS	23
3.1 GEOMETRIC MODEL OF STIFFENED PANELS	23
3.2 GEOMETRIC MODEL OF HULL GIRDERS	27
3.3 MATERIAL PROPERTIES	32
3.4 CORROSION WASTAGE	34
3.5 INITIAL DEFLECTIONS	38
4. ULTIMATE STRENGTH CALCULATIONS	40
4.1 ULTIMATE STRENGTH OF STIFFENER PANELS	40
4.1.1 ANALYSIS RESULTS FOR STIFFENER PANELS	40
4.1.2 DISCUSSION THE RESULTS FOR STIFFENER PANEL ANALYSIS	61
4.2 ULTIMATE STRENGTH OF HULL GIRDERS	62
4.2.1 ANALYSIS RESULTS FOR HULL GIRDERS	62
4.2.2 DISCUSSION THE RESULTS FOR HULL GIRDERS ANALYSIS	77
5. COLLISION ANALYSIS	81
5.1 METHODS FOR COLLISION PROBLEMS	82
5.2 APPLIED EXAMPLES FOR COLLISION	86
5.3 COLLISION ANALYSIS RESULTS	90
5.4 DISCUSSION	94
6. CONCLUSION AND FUTURE WORK	98
DECLARATION OF AUTHORSHIP	99
ACKNOWLEDGEMENTS	101

REFERENCES	103
APPENDICES	107

ABSTRACT

Within the industries development, the situation of melting ice in Arctic Ocean become more disastrously and the global warming phenomenon affect the temperature to induce the sea level increasing. For these reasons that the undiscovered nature resource and route of operating in Arctic Ocean can be used more sufficiently at present.

Nowadays, the ship industry try to find the way to operating in Northern Sea Routes (NSR) which has lower fuel wastage and shorter time of passing through the Arctic Ocean rather than south one. But the existing iced class ship is in short supply, and each construction time of new iced class ship proceed long time, therefore ship owners would like to understand the structure strengths of aged non-iced class container ships when operating in Arctic Ocean.

To evaluate the safety of large container hull structures under low temperatures, the priority issues are ultimate and fracture strengths. Especially after the MOL accident, it gave a rise to concentrate the ultimate strength problem of ultra-large vessels. As well as the impact damage of hull structures in ship collision will induce environment catastrophe and cargo loss.

Different from previous studies for ultimate strengths which focused on the low temperature or aged plates separately, under the realistic situation that both need to be as references. Consequently, both corrosion of aged ship structures and low temperature effect were undertaken as a main factors for ultimate strength analysis in this paper.

The ultimate strengths were estimated by Maestro software with the idealized structural unit method (ISUM) which verified stiffened panels for different locations and hull girder structures applied on a 13,000 TEU container ship. Furthermore, the fracture effect and structure resistance according to low temperatures were estimated by nonlinear dynamics impact analysis with LS-DYNA code.

Key word: ultimate strength, fracture strength, ice-class, aged container ship, collision, Arctic, NSR (Northern Sea Routes)

LIST OF FIGURES

Fig. 1.1 Scheme of Arctic Ocean area.....	13
Fig. 1.2 Photos of the MOL accident	15
Fig. 2.1 Infographic of the safety requirements of Polar Code (IMO Polar Code).....	17
Fig. 2.2 Calculating the ultimate strength of plates in ALPS/ULSAP	19
Fig. 2.3 Collapse modes of stiffened panel from Paik research.....	20
Fig. 2.4 Scheme of hull structure safety assessment and applied analysis.....	22
Fig. 3.1 Scheme of the locations for each analysis cases on ship section view	24
Fig. 3.2 Example model of applied stiffened plates (ISUM model)	25
Fig. 3.3 Applied loading model for stiffened plates (ISUM model)	25
Fig. 3.4 Schematic of stiffener panel for different four locations	27
Fig. 3.5 Area definition of cross-section for container ship.....	27
Fig. 3.6 Cross-section of container ship.....	28
Fig. 3.7 Properties of stiffeners and hull cross-sectional data.....	29
Fig. 3.8 Schematic diagram of attached plate consideration in MAESTRO ALPS/HULL	30
Fig. 3.9 ALPS/HULL analysis model for 13000 container ship.....	30
Fig. 3.10 Hull girder sectional load components from Meastro user manul	31
Fig. 3.11 Trend of yielding stress under different temperatures (Park, 2015)	33
Fig. 3.12 Stress-strain diagram for AH32 steel, t=12.0 mm (Park, 2015)	33
Fig. 3.13 Nominal design corrosion values for container ships (ABS rules, 2013).....	34
Fig. 3.14 Nominal design corrosion values for container ships (ABS rules, 2013).....	35
Fig. 3.15 Schematic of the corrosion process for marine structures (Paik, 2003)	36
Fig. 3.16 Comparison of annualized corrosion rate formulas, together with the measured corrosion data for seawater ballast tanks (Paik, 2004).....	37
Fig. 3.17 Assumption of corrosion ratio with consideration of age plates for two different area	38
Fig. 3.18 Schematic of initial deflection on plates	39
Fig. 3.19 Schematic of initial deflection on stiffeners	39
Fig. 4.1 Schematic of stiffener panel of upper deck.....	40
Fig. 4.2 Ratios of ultimate strength for different aged upper deck plates under low temperatures	42
Fig. 4.3 Ratios of ultimate strength for upper deck plates with same temperature consideration according to ages.....	43
Fig. 4.4 Schematic of stiffener panel of bottom plate in pipe duct area.....	43

Fig. 4.5 Ratios of ultimate strength for different aged bottom plates (in pipe duct area) under low temperatures	45
Fig. 4.6 Ratios of ultimate strength for bottom plates (in pipe duct area) with same temperature consideration according to ages	46
Fig. 4.7 Schematic of stiffener panel of inner bottom plate in pipe duct area	46
Fig. 4.8 Ratios of ultimate strength for different aged inner bottom plates (in pipe duct area) under low temperatures	48
Fig. 4.9 Ratios of ultimate strength for inner bottom plates (in pipe duct area) with same temperature consideration according to ages	49
Fig. 4.10 Schematic of stiffener panel of bottom plate with stiffener 1* in tank area.....	49
Fig. 4.11 Ratios of ultimate strength for different aged bottom plates with stiffener*1 (in ballast tank area) under low temperatures	51
Fig. 4.12 Ratios of ultimate strength for bottom plates with stiffener*1 (ballast tank area) with same temperature consideration according to ages	52
Fig. 4.13 Schematic of stiffener panel of bottom plate with stiffener 2* in tank area.....	52
Fig. 4.14 Ratios of ultimate strength for different aged bottom plates with stiffener*2 (in ballast tank area) under low temperatures	54
Fig. 4.15 Ratios of ultimate strength for bottom plates with stiffener*2 (ballast tank area) with same temperature consideration according to ages	55
Fig. 4.16 Schematic of stiffener panel of inner bottom plate with stiffener 3* in tank area..	55
Fig. 4.17 Ratios of ultimate strength for different aged inner bottom plates with stiffener*3 (in ballast tank area) under low temperatures.....	57
Fig. 4.18 Ratios of ultimate strength for inner bottom plates with stiffener*3 (ballast tank area) with same temperature consideration according to ages	58
Fig. 4.19 Schematic of stiffener panel of inner bottom plate with stiffener 4* in tank area..	58
Fig. 4.20 Ratios of ultimate strength for different aged inner bottom plates with stiffener*4 (in ballast tank area) under low temperatures.....	60
Fig. 4.21 Ratios of ultimate strength for inner bottom plates with stiffener*4 (ballast tank area) with same temperature consideration according to ages	61
Fig. 4.22 Distribution of Von Mises stress for hogging and sagging conditions in each age consideration (20°C)	64
Fig. 4.23 Distribution of Von Mises stress for hogging and sagging conditions in each age consideration (0°C)	65
Fig. 4.24 Distribution of Von Mises stress for hogging and sagging conditions in each age consideration (-20°C).....	67

Fig. 4.25 Distribution of Von Mises stress for hogging and sagging conditions in each age consideration (-40°C).....	68
Fig. 4.26 Distribution of Von Mises stress for hogging and sagging conditions in each age consideration (-60°C).....	70
Fig. 4.27 Ultimate hull girder longitudinal strength with different low temperatures and same age consideration under vertical bending moment.....	73
Fig. 4.28 Ultimate hull girder longitudinal strength with different structure ages with same temperature consideration under vertical bending moment	76
Fig. 4.29 Summary of the bending moment of ultimate strength under temperature and aged plates effect (hogging condition).....	77
Fig. 4.30 Summary of the bending moment of ultimate strength under temperature and aged plates effect (sagging condition)	78
Fig. 4.31 Summary of the ultimate bending moment under temperature and aged plates effect (hogging condition).....	79
Fig. 4.32 Summary of the ultimate bending moment under temperature and aged plates effect (sagging condition).....	80
Fig. 5.1 External internal mechanics in grounding problems (Simonsen, 1997).....	81
Fig. 5.2 Flow chart for the collision mechanics (Paik, 2007)	82
Fig. 5.3 Regression curve based on the collision cases (Minorsky, 1959)	83
Fig. 5.4 Grounding analysis of VLCC (Kuroiwa, 1996).....	84
Fig. 5.5 Experiment test of cutting plate by Cone wedges (Simonsen, 1997).....	84
Fig. 5.6 Collision analysis on a cylinder, Alexander (1959).....	85
Fig. 5.7 Simulation model of side ship collision by ISUM analysis (Paik and Pedersen, 1996)	86
Fig. 5.8 Schematic diagram of collision analysis (isometric view)	86
Fig. 5.9 Schematic diagram of collision analysis (Front view).....	87
Fig. 5.10 Schematic diagram of collision analysis (Top view)	87
Fig. 5.11 Engineering stress-strain curve of Mild steel.....	88
Fig. 5.12 Engineering stress-strain curve of High tensile steel (AH)	88
Fig. 5.13 Normalized dynamic failure strain versus strain rate for mild steel (Paik and Thayamballi, 2003)	89
Fig. 5.14 Ignored contact area during collision analysis.....	90
Fig. 5.15 Von Mises stress contours of struck ship on side shell with room temperature (20°C)	91

Fig. 5.16 Von Mises stress contours of struck ship on side shell with -60°C	92
Fig. 5.17 Von Mises stress contours of struck ship on inner shell with room temperature (20°C)	93
Fig. 5.18 Von Mises stress contours of struck ship on inner shell with -60°C	93
Fig. 5.19 Comparison the start point of rupture on side shell between room temperature and -60°C	94
Fig. 5.20 Comparison the start point of rupture on inner shell between room temperature and -60°C	95
Fig. 5.21 Total reaction force with indentation depth for five different temperatures.....	95
Fig. 5.22 Internal energy with indentation depth for five different temperatures	96
Fig. 5.23 Internal energy history before inner shell ruptured.....	96

LIST OF TABLES

Table 1.1 Distances and potential days saved for Asian transport from Kirkenes (Norway) and Murmansk (Russia) Source: Tschudi Shipping Company A/S	14
Table 2.1 Polar Class descriptions (IACS Polar rules, 2016)	18
Table 3.1 Description of the analytical location and compartment for analysis cases.....	24
Table 3.2 List of scantling and material for analysis cases	26
Table 3.3 Corrosion wastage assumption for different analysis cases with ages.....	26
Table 3.4 Hull cross-sectional properties of analysis models	30
Table 3.5 Formulas for calculating yielding stresses (in a range from -80°C to 20°C).....	32
Table 3.6 The ratio of yielding stresses from temperature 20°C to -80°C (Park, 2015).....	32
Table 3.7 Corrosion ratios of ballast tank and void space according to plate ages.....	38
Table 4.1 Formulas for calculating the ultimate vertical bending moment ratio (Hogging condition)	78
Table 4.2 Formulas for calculating the ultimate vertical bending moment ratio (Sagging condition)	79
Table 4.3 Summary ratio of vertical bending moment with room temperature for hogging and sagging conditions.....	80
Table 5.1 Sample coefficients for the Cowper-Symonds constitutive equation	89

ABBREVIATIONS

ABS	American Bureau of Shipping
AH32	High tensile steel (yielding stress is 315MPa)
AH36	High tensile steel (yielding stress is 355MPa)
ClassNK	NIPPON KAIJI KYOKAI
FB	Flat bar
IMO	International Maritime Organization
ISUM	Idealized Structural Unit Method
MS	Mild steel (yielding stress is 235MPa)
PC	Polar Class
PSPC	Performance Standard for Protective Coatings
RT	Room temperature
SOLAS	International Convention for the Safety of Life at Sea
T*	T-bar
TEU	Twenty-foot Equivalent Unit
UR	Unified Requirements

NOMENCLATURES

a	Panel length
A	Cross-sectional area
b	Stiffener spacing
B	Panel breadth
B_n	Width of the number n structure on struck ship
B_N	Width of the number N structure on striking ship
C (1/s)	Coefficient from test data. 40.4 for mild steel, and 3200 for high tensile steel.
$C1$ and $C2$	Corrosion Coefficient from statistical analysis
d_1, d_2	Coefficients
E	Young's modulus
I (m ⁴)	Second moments of area
L_n	Length of structure of struck ship
L_N	Length of structure of striking ship
M_u	Ultimate vertical bending moment
M_{uo}	Ultimate vertical bending moment of 0 year condition (as-built)
N.A.	Neutral axis
q	Coefficient from test data, normally use 5 for steel.
Ratio; R	Ratio of vertical bending moment
R_v	Ruptured volume of striking and struck ships
r_r	Corrosion rate in mm/year
s	Finite element mesh size (length)
$S1$	Number of structures on striking
$S2$	Number of structures on struck ship
SM	Section modulus
t ; t_p	Plate thickness
t_n	Thickness of struck ship
t_N	Thickness of striking ship
tr ($r=1\sim6$)	Required corrosion margin (mm)
T	Ship age (year)
T_c	Coating life (year)

Tt	Duration of transition (year)
$Temp.$	Temperature
w_{opl}	Initial deflection of plates
w_{oc}	Column Type Initial Distortion of Stiffener
w_{os}	Sideways Type Initial Distortion of Stiffener
W_{BC}	Absorbed energy from damaged bow structures of striking ship
W_C	Total absorbed energy
W_{SC}	Absorbed energy from damaged structures of struck ship
ε	Strain
$\dot{\varepsilon}$	Strain rate
ε_F	Fracture strain
ε_{Fc}	Critical fracture strain
ε_{Fd}	Dynamic fracture strain
σ_x, σ_y	Yielding stress from x and y axis
$\sigma_{eq}; \sigma_Y$	Yielding stress
σ_{Y-RT}	Yielding stress on the room temperature (20°C)
σ_{Yd}	Dynamic yielding stress
τ	Shear force
γ	Correction factor
ΔE	Loss of kinetic energy
β	Ratio from spacing, young's modulus, plate thickness, and yielding stress

1. INTRODUCTION

Arctic Ocean is the smallest and shallowest ocean area all of the world. The area is around 13,986,000 kilometres square, and it almost cover in the Arctic Circle and surrounded with Russia, Iceland, Norway, Canada, Greenland, and the north of United States as shown in Fig. 1.1. In the Arctic Circle, it covered with ice for the most of time in a year. The position of Arctic Ocean made it important during the World War II to shorten the transportation way for military supply. <http://www.7continents5oceans.com/> [Accessed January 2017]

The Arctic Ocean is one of the most unexplored ocean areas in the world, but the resources are hard to obtain due to the low temperature and ice-covered route. As the environmental changed lately, the global warming affect the temperature, and the sea level increased obviously. This phenomenon opened a new access to utilize these Ocean natural resource and trail routes.



Fig. 1.1 Scheme of Arctic Ocean area

From: http://readmt.com/images/content/articles/Arctic_map.jpg.jpg

In Table 1.1 that we can find out the differences of route distance between Suez Canal and Northern Sea Rout from Kirkenes transport to different three main ports in Asia which are Shanghai, Busan and Yokohama.

Table 1.1 Distances and potential days saved for Asian transport from Kirkenes (Norway) and Murmansk (Russia) Source: Tschudi Shipping Company A/S

Destination	Via Suez Canal			Through Northern Sea Route			Days Saved
	Distance (Nm)	Speed (Knots)	Days	Distance (Nm)	Speed (Knots)	Days	
Shanghai, China	12050	14.0	37	6500	12.9	21	-16
Busan, Korea	12400	14.0	38	6050	12.9	19.5	-18.5
Yokohama, Japan	12730	14.0	39	5750	12.9	18.5	-20.5

The environmental factor caused some crack problem that force scientist face the fracture problem by low temperatures since World War II. During the World War II, the navy vessels need to pass through the Arctic Ocean Area as a transportation path of military and food supplies (which is the efficient way for American naval vessel).

Normally, the ship which will pass through the Arctic area should be constructed by polar materials, it is different with traditional material and considered the low temperature effect of structure strength. Furthermore, traditional material is not suitable for brittle fracture that as polar material to be used in construction of vessels operating in Arctic Ocean.

Recently, the research of Arctic Ocean has become popular, not only in the Marine Ecology, but also in ship industries, such as D.K. Park, 2015, and Y.S. Kim, 2014. Also in the previous studies for ultimate strengths which focused on the low temperature or aged plates separately, such as Liu and Amdahl 2010, Liu et al. 2011, Paik et al. 2011, Ehlers and Østby 2012, but under the realistic situation that both need to be as references. According to the demand from ship owner who want to use the existing non-iced ship operating in Arctic Ocean, this study considered the strength of hull structures of aged non-iced class container ship operate in the Arctic Ocean. Consequently, this study considered the strength of hull structures of aged non-iced class container ship operate in the Arctic Ocean. Both corrosion of aged ship structures and low temperature effect will be undertaken as a main factors of ultimate strength analysis.

For saving the transport cost and increasing the ability to carry on much more goods, the trend of constructing ultra large container ship is prevalent from 2006 until now. The largest container ship is MSC Oscar, which can carry on 20,000 TEU and constructed by Daewoo Shipbuilding & Marine Engineering (DSME). With this tendency of large container ships, the ultimate strength becomes more important than smaller vessel.

To evaluate the safety of large container hull structures under low temperatures, the priority issues are ultimate and fracture strengths. Especially after the MOL accident, it gave a rise to

concentrate the ultimate strength problem of ultra-large vessels. As well as the impact damage of hull structures in ship collision will induce environment catastrophe and cargo loss.

The accident of MOL Comfort was that occurred on 17th of June, 2013. A modern 8,110 TEU container vessel break into two parts then sink on the way from Singapore to Jeddah (Saudi Arabia) which was established in 2008. From MOL Comfort official report by ClassNK that we can know the fracture started from the bottom shell which is on the middle of ship, along with the crack progressed up to the side shell plates, the ship break into two parts, fore and stern. The fore part was being towed by a salvage company sank on 11th of July 2013 which was partly destroyed by fire. The related accident photos of MOL Comfort show in Fig.1.2.

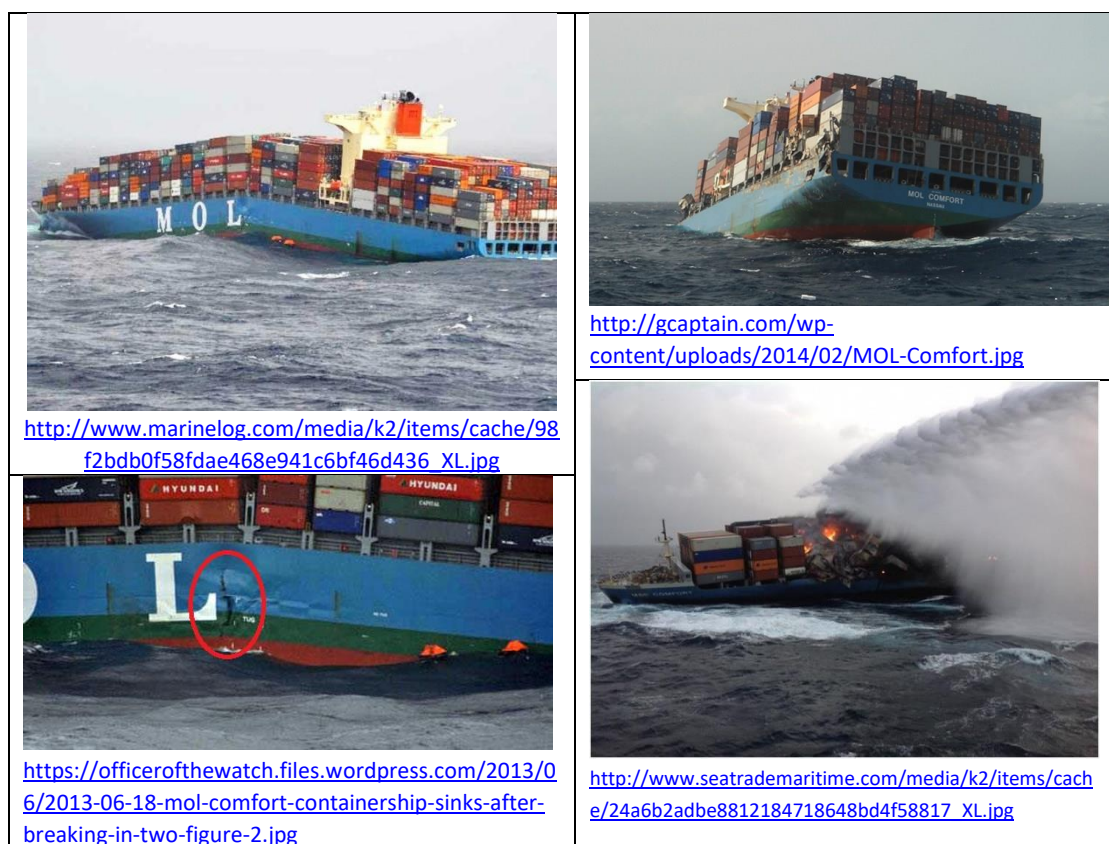


Fig. 1.2 Photos of the MOL accident

This research investigates the problem of material of both ultimate strength under low temperature with the consideration of corrosion ages for stiffened plates and hull girder structures. Also investigate the brittle of material under low temperatures by dynamic collision analysis which considered fracture effect as factor from stress-strain curve.

In this study that we consider three parts to investigate the ultimate strength and fracture influence under consideration of low temperature and aged plates.

First part of this study investigated the strength of hull structural safety of stiffener panels by two main factors: aged plates and the different low temperature environment.

- ✓ The main factor of aged plates are as the corrosion effect with coating life in tank area and average ratio of design life in pipe duct space which we considered.
- ✓ The differences of yielding strength of each low temperatures are supposed as another factor of the affect for material model.

Second part will be included the investigation of the ultimate strength of hull girder structures by the same considerations.

Third part is the collision analysis with low temperature consideration which included the dynamic yielding stress and dynamic fracture strain effect.

The specific contents of each chapter will be shortly introduced as following:

Chapter 1: Present the background of Arctic Ocean during recently decay and propose of this research, also introduce the concept of each chapter.

Chapter 2: Introduce the related regulation of Polar rules and corrosion consideration, applied theory of ultimate strength, safety assessment of structures, and recently research review.

Chapter 3: Presentation of analysis method of ultimate strength, collapse modes of stiffened panel, and model information with material and corrosion wastage

Chapter 4: Applied examples of stiffened plates with different location and hull girder structures on a 13,000 TEU container ship which including the consideration of low temperature effect of yielding stress and aged plates corrosion wastage from as-built structure to 25 years old.

Chapter 5: Collision analysis with different low temperatures which consider the fracture strain as main factor to investigate the brittle of structures.

Chapter 6: The conclusion of this research and further work which will be more complete with this topic.

2. LITERATURE REVIEW

The related literature which will be separated into 4 parts that included the international regulations with ice class and foundation of corrosion wastage assumption, applied theory and latest researches of related topics. These will be introduced in the following subsections.

2.1 REGULATIONS

There are two regulations related to operate in the Arctic Area which are IMO Polar Code and IACS Polar rules. These two rules performed the safety of the ship in structures, equipment, and pollution prevention when operating in such a difficult environment.

➤ IMO Polar Code

To prevent the catastrophe and improve the safety for ship which operating in the polar regions that polar regions that the International Maritime Organization (IMO) adopted the “Polar Code”, which is specifically emphasize the mean of Polar Code for ship safety in main three aspects in Fig. 2.1.

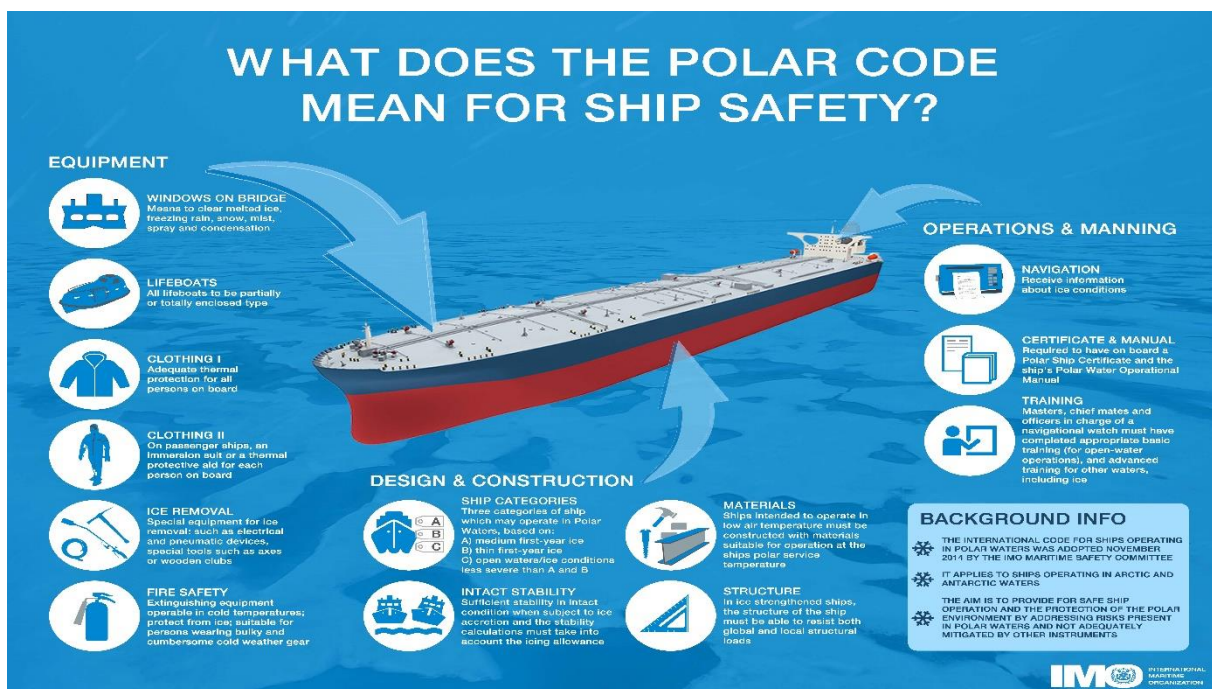


Fig. 2.1 Infographic of the safety requirements of Polar Code (IMO Polar Code)

Polar Code covers all the relevant matters of ships in the water of polar region, including the effect of ship structure, equipment, operational and training, search and rescue and environment protection. The Polar Code includes mandatory measures covering safety part (part I-A) and pollution prevention (part II-A) and recommendatory provisions for both (parts I-B and II-B).

It certificate ships as Category A, B or C type by defining the waters (ice) of operating in Arctic area to apply for a Polar Ship Certification. When the new ship constructed after 1st of January 2017 that will follow Polar Code and related SOLAS amendments, and if the ship was constructed before, it will be required to survey intermediate or renewal after 1st of January 2018. (<http://www.imo.org/en/mediacentre/hottopics/polar/pages/default.aspx>)

➤ **IACS Polar rules : URI1 - I3**

IACS Polar rules are mainly separated into three parts which are UR I1, UR I2 and UR I3.

URI1: Polar Class Descriptions and Application Rev.2 in Apr. 2016, which give the general description of IACS Polar rule, and defined the applied ship and operating area.

URI2: Structural Requirements for Polar Class Ships Rev.3 in Apr. 2016, which including all the consideration for the safety of ship structures, such as hull construction calculation with design ice load and longitudinal strength of hull and design maximum shear force...etc.

URI3: Machinery Requirements for Polar Class Ships Corr.1 in Oct. 2007, which contained all the main machinery equipment effected by temperatures that involved propulsion system and cooling water systems...etc.

The Table 2.1 shows the description of each Polar class level form PC1 to PC7 that based on the different ice conditions.

Table 2.1 Polar Class descriptions (IACS Polar rules, 2016)

Polar Class	Ice descriptions (based on WMO Sea Ice Nomenclature)
PC 1	Year-round operation in all polar waters
PC 2	Year-round operation in moderate multi-year ice conditions
PC 3	Year-round operation in second-year ice which may include multiyear ice inclusions.
PC 4	Year-round operation in thick first-year ice which may include old ice inclusions
PC 5	Year-round operation in medium first-year ice which may include old ice inclusions
PC 6	Summer/autumn operation in medium first-year ice which may include old ice inclusions
PC 7	Summer/autumn operation in thin first-year ice which may include old ice inclusions

➤ **Performance Standard for Protective Coatings (PSPC)**

The International Maritime Organization (IMO) has passed the legislation to follow PSPC requirements on 8th of December, 2006. In SOLAS II-1 3-2 that protected panting of double side of bulk carrier and ballast tank need to be satisfied with all the requirement of PSPC.

Need to be follow with PSPC:

Total weight is equal or large than 500 tons for sea water ballast tanks of all kinds of ship, and double bilge sides of bulk carrier which ship length is over 150 m.

- ✓ Contract date after 1th of July, 2008
- ✓ No identify contract date but establish keel after 1st of January, 2009
- ✓ Delivered time after 1st of July, 2012

2.2 THEORY OF ULTIMATE STRENGTH

Theory of ultimate strength of plates are as follows Fig. 2.2, which represents the different three kinds of deformation of plates, and the equation for calculating the ultimate strength.

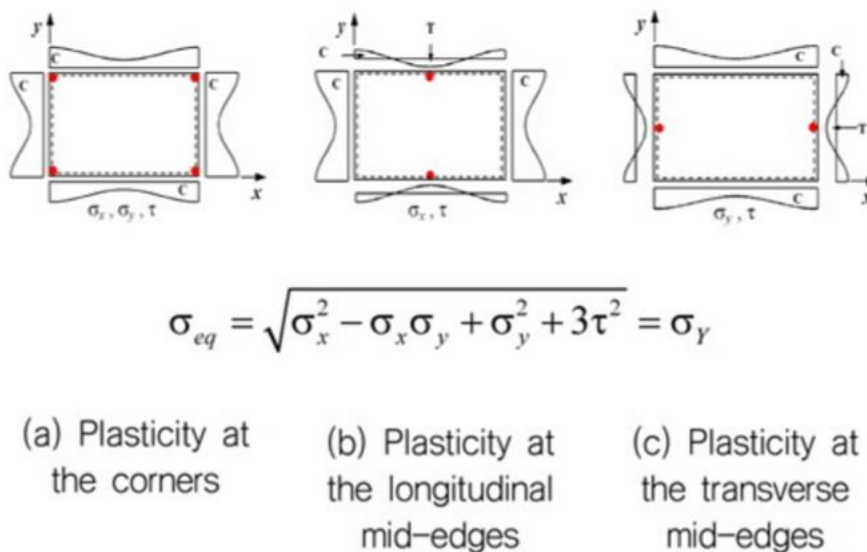


Fig. 2.2 Calculating the ultimate strength of plates in ALPS/ULSAP
(Paik & Thayamballi, 2003)

The Fig. 2.3 show the different 6 types of collapse modes of stiffener panels which including the comparison results of experimental test and simulation.

The mode 1 with both direction stiffeners which show projection in the centre of the plate when the structure obtain the ultimate strength. The mode 2 can show the plate induced collapse and mode 3-6 show the stiffener induced collapse of different stiffener systems. Further, the collapse mode 3 which is induced by stiffeners that we could see the yielded regions in the central of plate under stiffeners. Moving to collapse mode 4 that is similar with mode 3 which induced by stiffeners, but mode 4 comes from the local buckling of the stiffener web. Therefore, the buckling collapse can effect both of the plating and the stiffeners which shows in the fig below. Collapse mode 5 is induced by tripping of stiffener collapse which is the flexural-torsional buckling of stiffeners. (Paik, 2010)

- Mode I: overall collapse of plating and stiffeners as a unit;
- Mode II: biaxial compressive collapse;
- Mode III: beam column type collapse;
- Mode IV: local buckling of stiffener web;
- Mode V: tripping of stiffener;
- Mode VI: gross yielding.

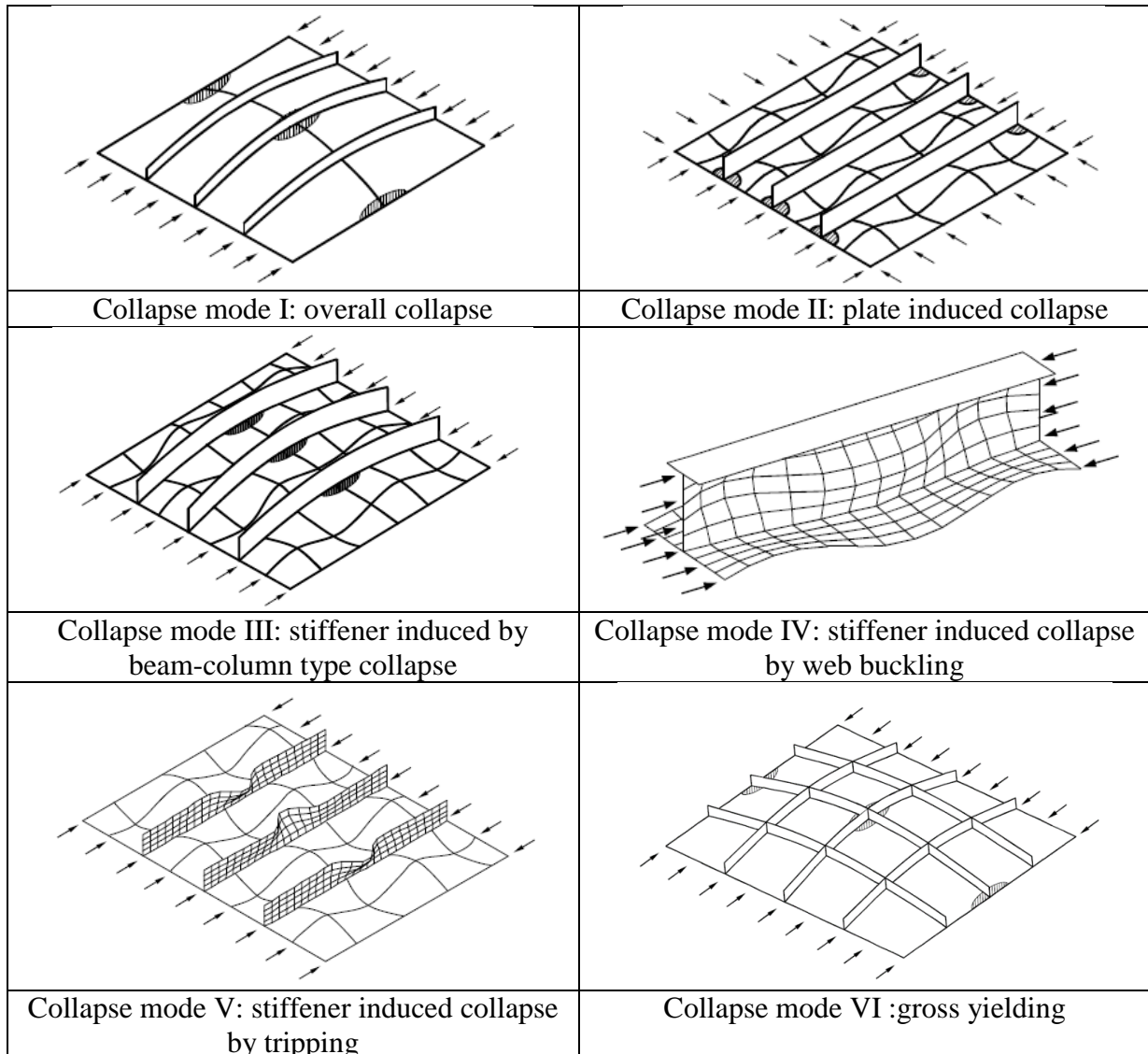


Fig. 2.3 Collapse modes of stiffened panel from Paik research

2.3 STUDIES RELATED TO STRUCTURE SAFETY FOR CONTAINER VESSELS

From 20 century that researchers of naval architecture and ocean engineering have been studied the ultimate limit state of ship structures stated from stiffened plates such as Paik, J.K. and Thayamballi, A.K., 2003 conducted the research with time-variant consideration of ultimate strength, and Paik, J.K., Lee, J.M., Park, Y.I., Hwang, J.S. and Kim, C.W., 2003 studied for corroded bulk carriers.

Also, with the consideration of aged ship structures, the safety assessment of structures are not the same situation as built, it have to be estimated such as Paik, J.K. and Melchers, R.E., 2008. For the aged ship structures that the most important is corrosion effect that Qin, S. and Cui, W., 2003 present the effect of corrosion models on the time-dependent reliability of steel plated elements and Paik, J.K., Thayamballi, A.K., Park, Y.I. and Hwang, J.S., 2004 conducted the research with seawater ballast tank structures. Further, Paik, J.K. and Kim, D.K., 2012 performed an advanced method to predict time-dependent corrosion wastage.

Considering the ultimate longitudinal strength of container ships with corrosion, Kim, D.K., Park, D.K., Kim, H.B., Seo, J.K., Kim, B.J., Paik, J.K. and Kim, M.S., 2012 studied the necessity of applicable of corrosion addition. Soares, C.G., Garbatov, Y., Zayed, A. and Wang, G., 2005 introduced a non-linear corrosion model of steel plates with environmental factors.

2.4 PROCEDURE FOR HULL STRUCTURE SAFETY ASSESSMENT

The risks for a ship when operating at sea that included grounding, extremely weather environment, aged structures, ultimate strength, and fatigue...etc. Some cause from sea water such as wave impact or wave loads, others could happen from the ship operation itself.

Here we focus on the hull structure safety assessment with aged structures consideration under low temperatures of Arctic Ocean area. Fig. 2.4 shows the procedure of consideration the combination of risk and provides the program of evaluating the safety for ship hull structures.

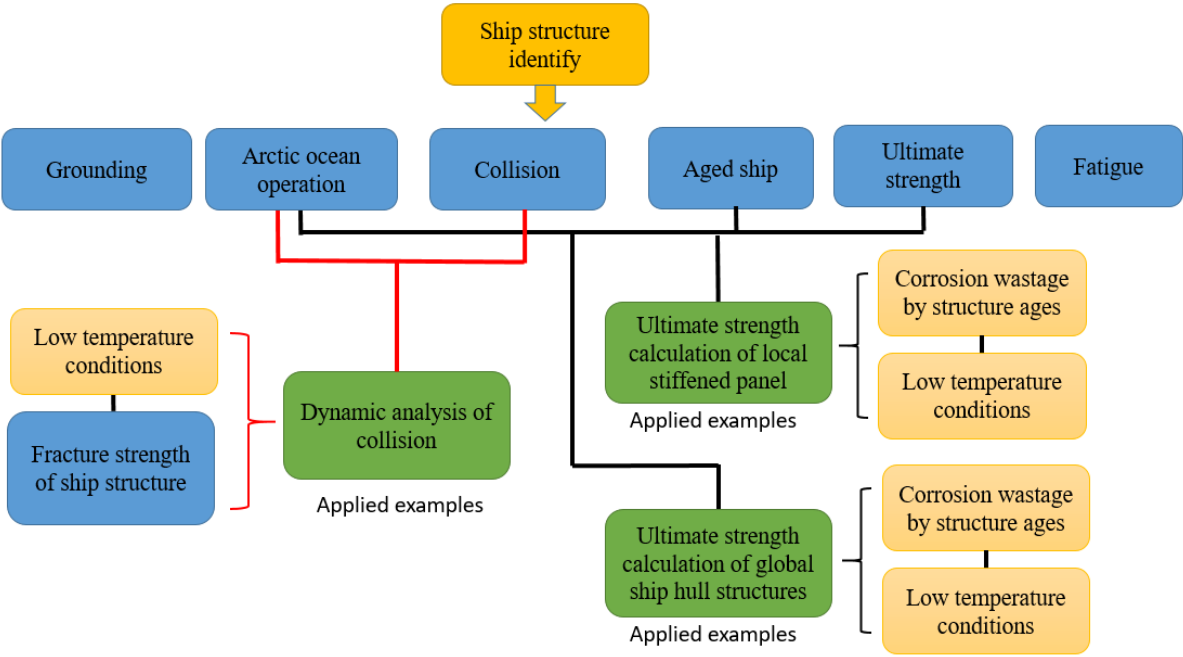


Fig. 2.4 Scheme of hull structure safety assessment and applied analysis

3. MODELLING OF STRUCTURES AND ANALYSIS ASSUMPTIONS

Start from the simple structure model to know the effect of aged and low temperature differences as the first step to understand the structure characteristic. With the consideration of ultra large container ship which ultimate strength is the main calculation point at design stage, therefore, the ultimate strength of stiffened panel and hull girder strength will be evaluated in this research.

A 13,000 TEU ultra large container ship has been used as the target of analysis in this paper. In general, when ship is operating at sea, the external force from wave and wind will apply on the ship hull structures, the bending moment of hull girder will become hogging or sagging condition that cause the tension and compression stress on bottom and upper deck, and the maximum value normally will be occurred on midship section.

In stiffened calculation, accordingly to find out the critical condition of structures that we select the 7 cases of different position which include upper deck, inner bottom and bottom plate with different compartment identify and supporting stiffener scantling.

Especially for large container ship, the ultimate strength calculation for hull girder which means the capacity of structures to support the total loads from waves and cargos. If the ultimate strength is not enough to carry the loads that will cause plate or stiffener buckling even bring cracks. Serious and series of cracks will induce the fracture to loss lives or cargos and cause catastrophe when the oil spread out that polluted environment. Therefore, the calculation of hull girder ultimate strength which will need to be indeed considered under hull girder hogging and sagging conditions.

Step by steps, this research will start from the local structure of stiffened panel to global hull girder structures that will observe the effect from corrosion wastage and temperatures with the combination of comparison from simple to complex.

3.1 GEOMETRIC MODEL OF STIFFENED PANELS

In this section that we discussed the ultimate strength estimation of three positions which included upper deck, bottom plates and inner bottom plates for pipe duct area and tank space. As represented in the following tables, there are 7 cases of different stiffener panels and the related input data for ULSAP software, which a is panel length, B is panel breadth, b is stiffener spacing and tp is plate thickness. Furthermore, the Fig. 3.1 are schematic for stiffener panels of upper deck, bottom plate in pipe duct area, inner bottom plate in pipe duct area, and bottom plate/inner bottom plate in tank area.

Table 3.1 describe the positions of stiffener panels with different compartment consideration and different stiffener combination.

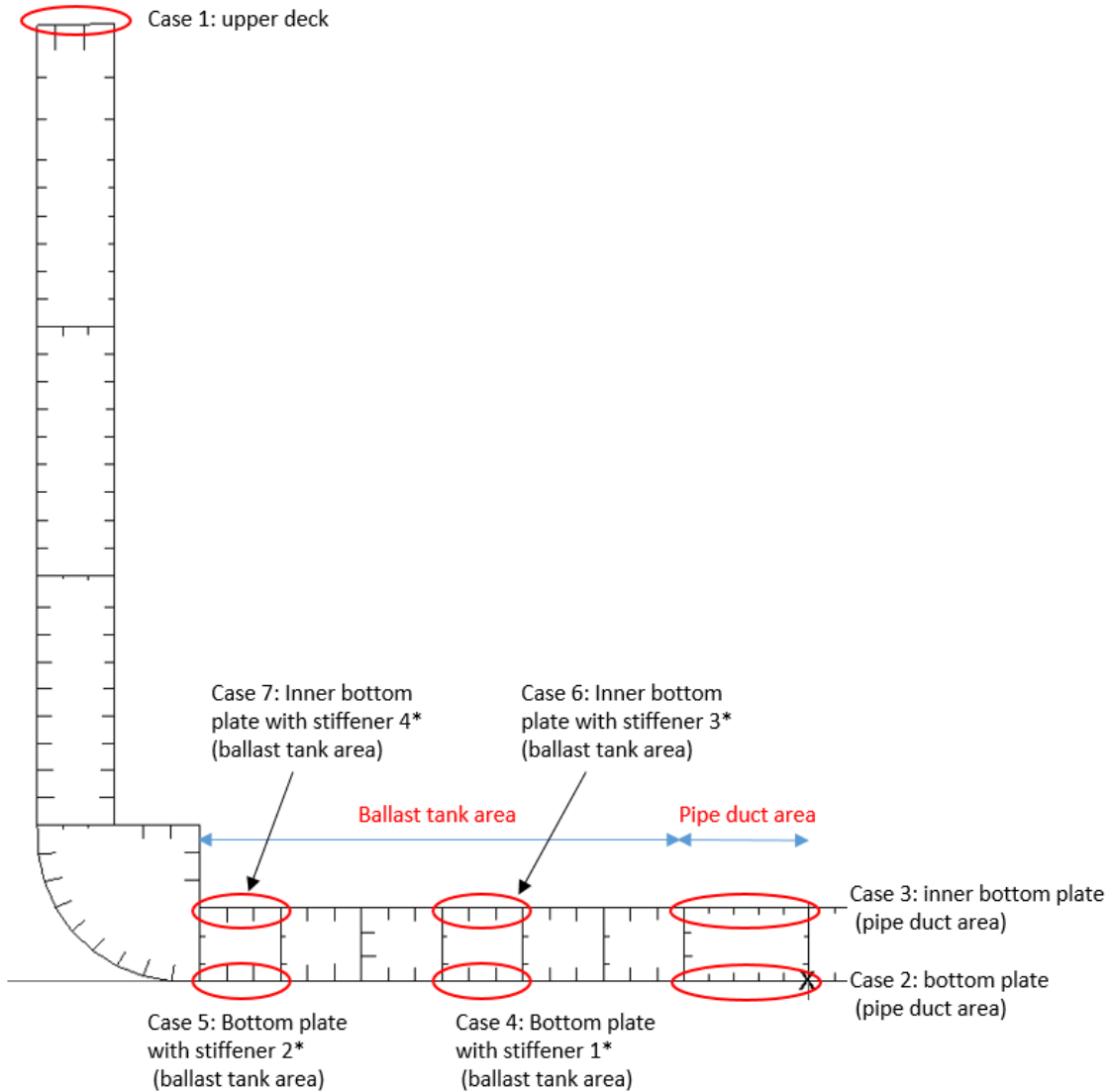


Fig. 3.1 Scheme of the locations for each analysis cases on ship section view

Table 3.1 Description of the analytical location and compartment for analysis cases

Analysis cases	Positions of stiffener panels
Case 1	Upper deck
Case 2	Bottom plate (pipe duct area)
Case 3	Inner bottom plate (pipe duct area)
Case 4	Bottom plate with stiffener 1* (ballast tank area)
Case 5	Bottom plate with stiffener 2* (ballast tank area)
Case 6	Inner bottom plate with stiffener 3* (ballast tank area)
Case 7	Inner bottom plate with stiffener 4* (ballast tank area)

*stiffener 1: 425x140x11/16; stiffener 2: 550x150x12/18; stiffener 3: 400x140x11/16; stiffener 4: 450x150x11/18

Fig. 3.2 and Fig. 3.3 represent the example model of ISUM stiffened panel which include the definition of input data and represent the action of how the assumption loads applied on stiffened panels.

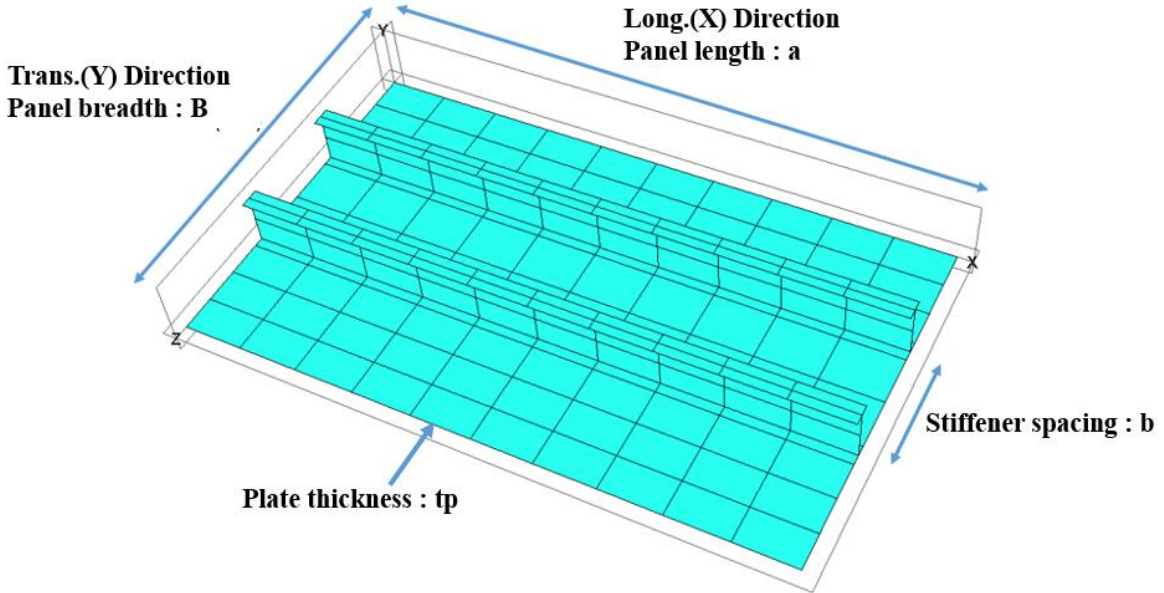


Fig. 3.2 Example model of applied stiffened plates (ISUM model)

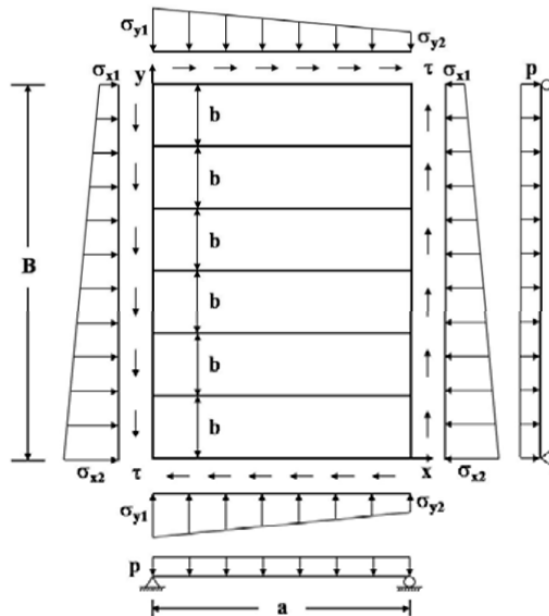


Fig. 3.3 Applied loading model for stiffened plates (ISUM model)

There are the detailed scantling of stiffened panel of each analysis case (position) in Table 3.2 and list out the assumption of corrosion wastage for each case. The example ISUM model of analytical stiffened panel has been shown in Fig. 3.4.

Table 3.2 List of scantling and material for analysis cases

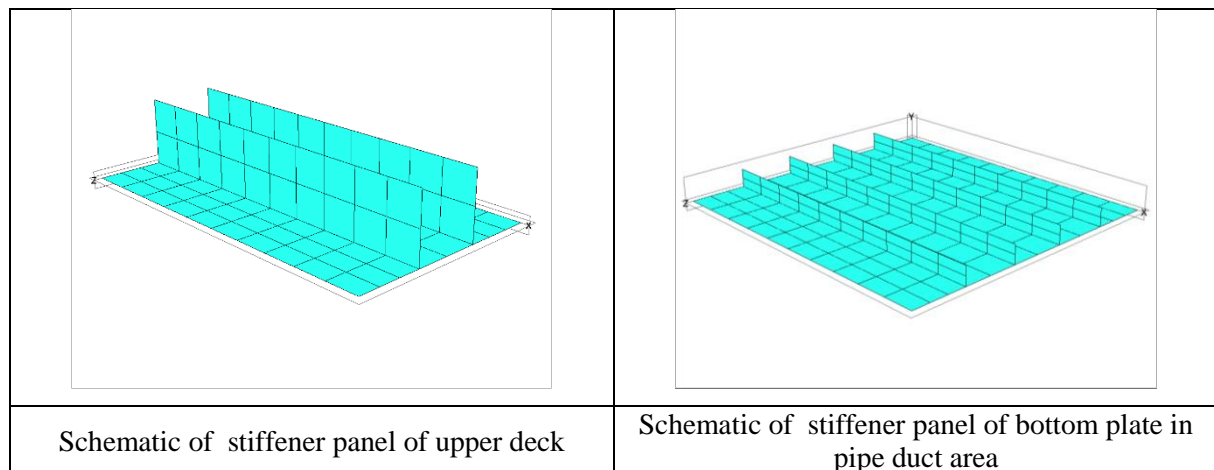
Analysis cases	a	B	b	tp	Stiffener scantling	Material
Case 1	4210	2400	800	78	800x78 (FB)	AH36
Case 2	4210	3910	780	23	250x19 (FB)	AH32
Case 3	4210	3910	780	18	200x25 (FB)	AH32
Case 4	4210	2520	840	22	425x140x11/16 (T*)	AH32
Case 5	4210	2520	840	22	550x150x12/18 (T*)	AH32
Case 6	4210	2520	840	18	400x140x11/16 (T*)	AH32
Case 7	4210	2520	840	18	450x150x11/18 (T*)	AH32

T*: web height x flange breadth x web thickness/ flange thickness (Unit: mm)

Table 3.3 Corrosion wastage assumption for different analysis cases with ages

Analysis cases	Corrosion wastage					
	Original from rules	5 years	10 years	15 years	20 years	25 years
Case 1	1.5	0.375	0.750	1.125	1.500	1.875
Case 2	1.0	0.250	0.500	0.750	1.000	1.250
Case 3	1.0	0.250	0.500	0.750	1.000	1.250
Case 4	1.0	0.000	0.333	0.667	1.000	1.333
Case 5	1.0	0.000	0.333	0.667	1.000	1.333
Case 6	1.5	0.000	0.500	1.000	1.500	2.000
Case 7	1.5	0.000	0.500	1.000	1.500	2.000

(Unit: mm)



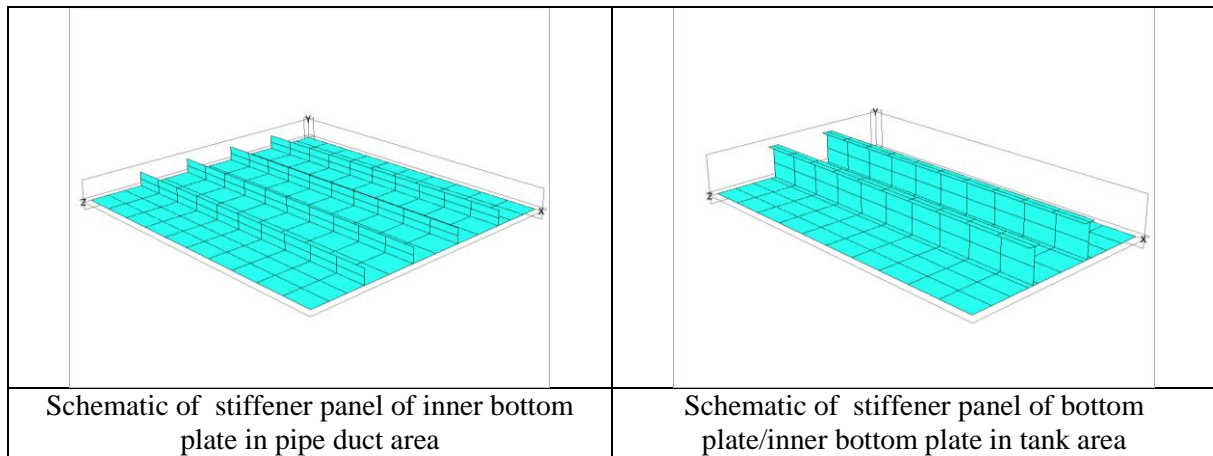


Fig. 3.4 Schematic of stiffener panel for different four locations

3.2 GEOMETRIC MODEL OF HULL GIRDERS

The section view of 13,000 TEU container ship which use as the applied example is shown on the Fig. 3.5 to Fig. 3.7, it also represent the detail of spacing, scantlings, materials, and area definition of ballast tank. Also, the scantlings of all the analysis are based on gross scantling with the consideration of corrosion wastage which is the same as in Chapter 3.1.

In the Fig. 3.5, the identification of different tank area has been shown which use as the corresponding for the corrosion wastage in ballast tank area and dry space.

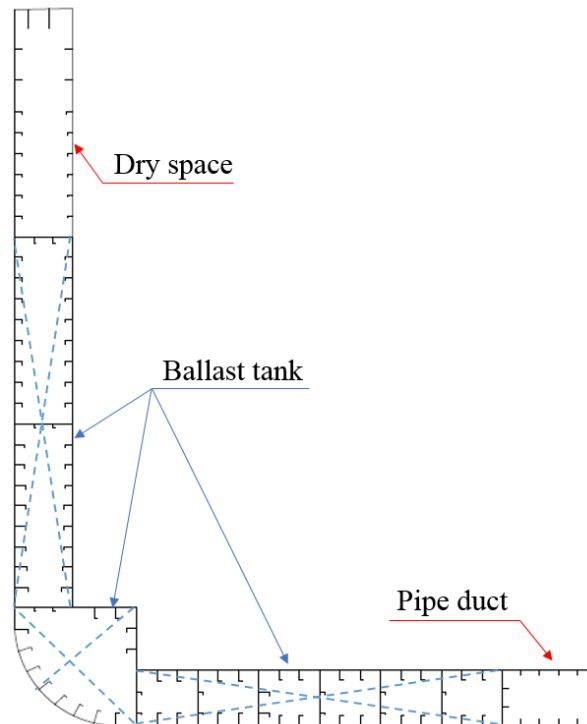


Fig. 3.5 Area definition of cross-section for container ship

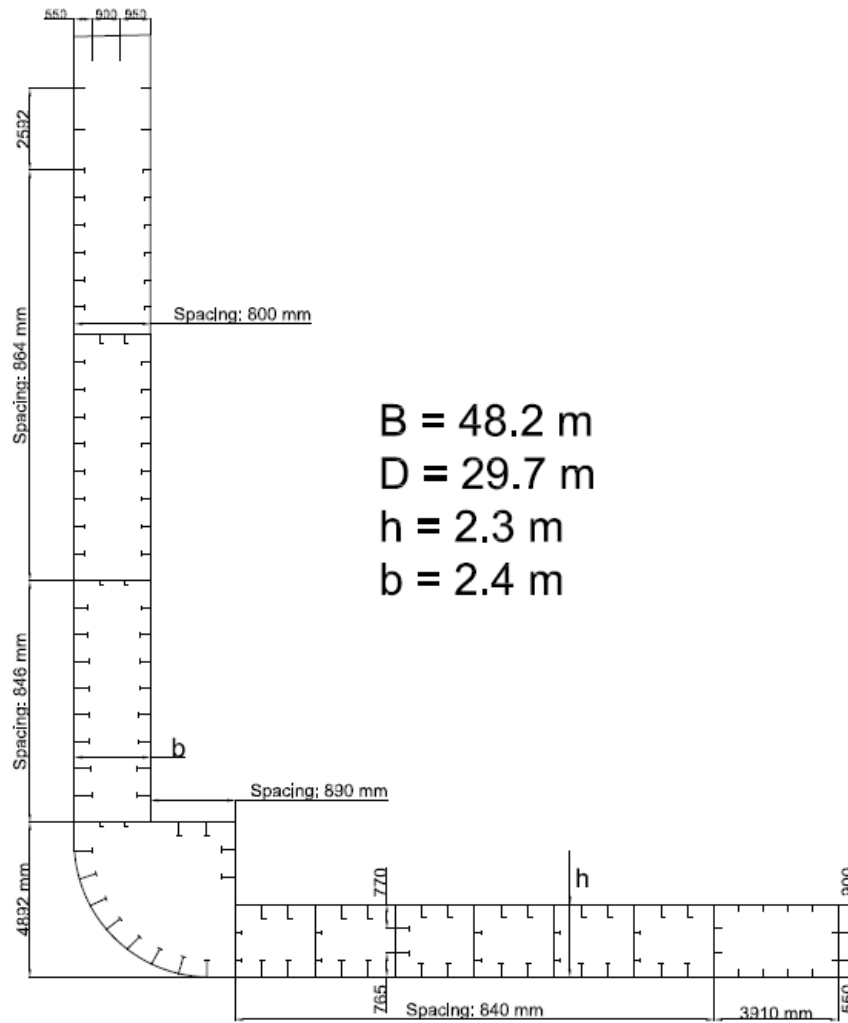


Fig. 3.6 Cross-section of container ship

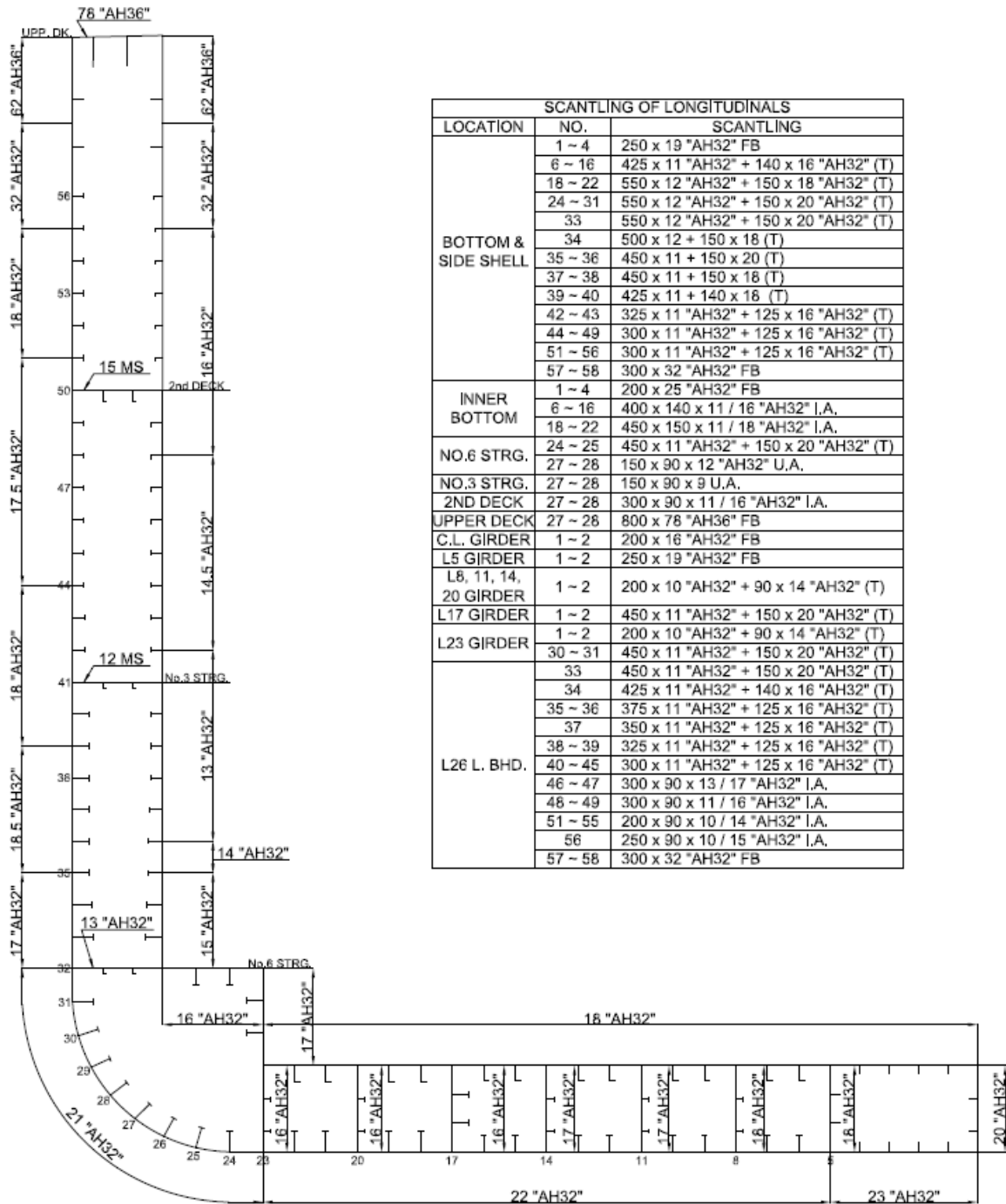


Fig. 3.7 Properties of stiffeners and hull cross-sectional data

The Table 3.4 represents the detailed of hull cross-sectional data differences between considering the corrosion wastage with ages. The decreasing trend of area, moment of inertial and section modulus of both deck and bottom can be found out with the corrosion deductions.

Table 3.4 Hull cross-sectional properties of analysis models

Scantling	A(m ²)	I(m ⁴)	SM(m ³)		N.A.(m)
			Deck	Bottom	
Gross(as-built)	7.01	921.99	50.01	80.40	11.47
5Y	6.99	918.20	49.74	80.22	11.45
10Y	6.83	903.93	49.24	78.29	11.55
15Y	6.67	889.56	48.73	76.36	11.65
20Y	6.51	875.00	48.22	74.42	11.76
25Y	6.35	860.29	47.71	72.46	11.87

The consideration of calculating the ultimate strength by MAESTRO ALPS/HULL, the plate and the stiffeners have been separated into two models as the Fig. 3.8 that the calculation of beam-column elements without considering the attached width of plate elements.

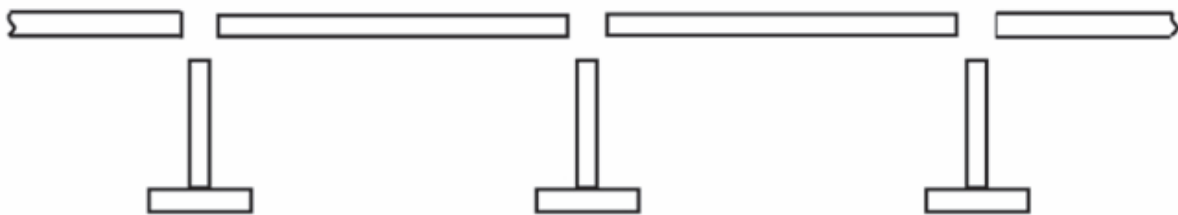


Fig. 3.8 Schematic diagram of attached plate consideration in MAESTRO ALPS/HULL

In the MAESTRO ALPS/HULL that the number of elements, plates and beams of analysis model are as follows, and the ISUM model shows in the Fig. 3.9:

Total number of elements: 535

Number of Plates: 305

Number of Beam-columns: 230

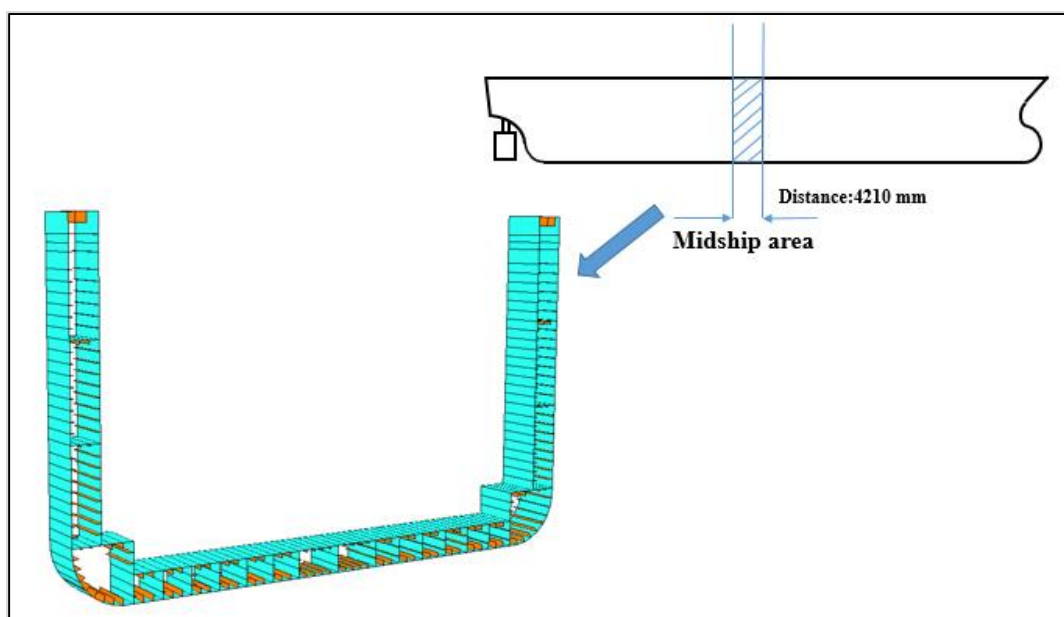


Fig. 3.9 ALPS/HULL analysis model for 13000 container ship

The ALPS/HULL process of this collapse analysis start from the static condition without loading until the ultimate limit state is reached which use the simplified nonlinear finite element method that called ISUM (Idealized Structural Unit Method). The vertical bending, horizontal bending, sectional shear and torsion loadings of hull girder components could be applied in this analysis. In addition, both steel and aluminium of materials can be coped with ALPS/HULL. Furthermore, particular incremental loading steps could be set up with the concern of initial imperfections form the initial deflections and welding residuals.

For this study case which considered the maximum deflection/ thickness as 0.1, the residual stress/yielding stress is 0.0015 for plate initial condition, and the stiffener initial condition for maximum deflection/ length is equal to 0.1.

Various types of structural degradation, e.g., corrosion wastage, fatigue cracking-and local denting are dealt with as parameters of influence.

Ship hulls are subjected to a variety of hull girder or local load components. Of these, vertical bending is a primary hull girder load component. It is known that the horizontal bending may sometimes be large in the magnitude, approaching the magnitude of vertical bending moment when the ship runs at an oblique heading in waves. Fig. 3.10 represents the sectional load components for hull girder. Also, in some vessels such as bulk carriers carrying dense cargo such as iron ore, an uneven alternate hold loading condition is normally applied, and, as a result, large shearing forces will be imposed. Moreover, torsion is normally considered to be important for vessels with low torsional rigidity due to large deck opening such as for instance in container vessels and some large bulk carriers.

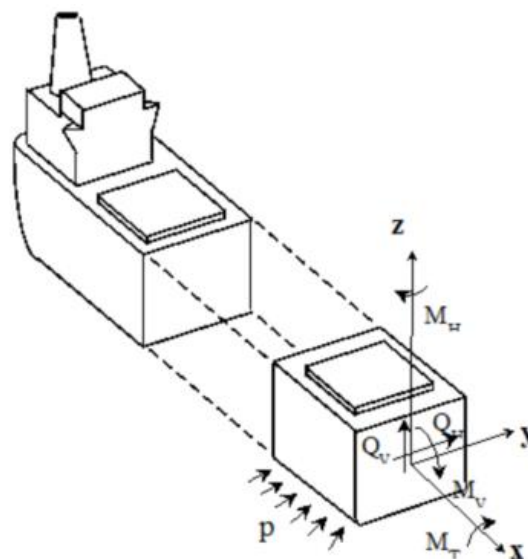


Fig. 3.10 Hull girder sectional load components from Meastro user manual

3.3 MATERIAL PROPERTIES

The applied value of yielding stresses of Grade A and Grade AH steel material from temperature 20°C to -80°C were based on the research of “Operability of non-ice class aged ships in the Arctic Ocean—Part I: Ultimate limit state approach” which were obtained from the material tensile test results as Table 3.6 .

From Fig. 3.11 that we can find out the yielding stresses of high tensile steel that were no effect by the temperature differences during 20°C to 0°C. Then the tendency of yielding stresses increase with the temperature decreased. To sort out the simple way to utilize the yielding stress value for each temperature, here are the formulas from Fig. 3.11 for mild steel, high tensile steel AH32 and AH36 separately and the temperature should be in the range of -80°C to 20°C listed in Table 3.5.

Table 3.5 Formulas for calculating yielding stresses (in a range from -80°C to 20°C)

$\sigma_{Y,AH36} = 0.0071Temp.^2 - 0.0023Temp. + 323.11$ (MPa)	(-80°C ≤ Temp. ≤ 20°C)
$\sigma_{Y,AH32} = 0.0068Temp.^2 - 0.0022Temp. + 313.17$ (MPa)	
$\sigma_{Y,MS} = 0.009Temp.^2 - 0.2064Temp. + 235.59$ (MPa)	

Table 3.6 The ratio of yielding stresses from temperature 20°C to -80°C (Park, 2015)

Temp. (°C)	Grade A			Grade AH		
	Modified σ_Y (MPa)	σ_Y (MPa)	$\sigma_Y/\sigma_{Y-R.T.}$	Modified σ_Y (MPa)	σ_Y (MPa)	$\sigma_Y/\sigma_{Y-R.T.}$
20	235.000	281.158	1.000	315.000	400.669	1.000
0	235.592	-	1.003	315.000	-	1.000
-20	243.328	300.558	1.035	315.315	415.900	1.001
-40	258.209	313.214	1.099	323.789	419.479	1.028
-60	280.233	333.543	1.192	337.806	437.053	1.072
-80	309.401	366.527	1.317	357.368	447.141	1.135

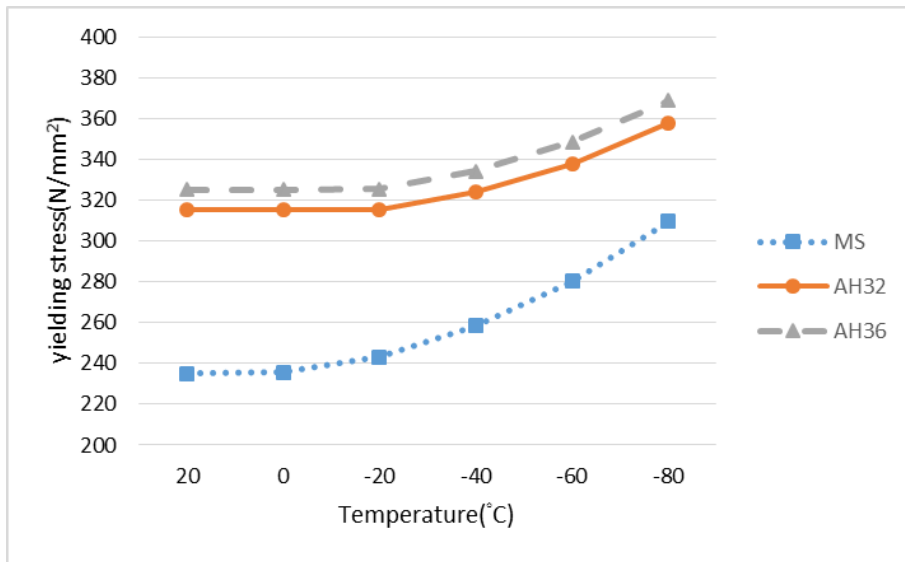


Fig. 3.11 Trend of yielding stress under different temperatures (Park, 2015)

The reference data of Fig. 3.12 is based on the experimental test done by Dr. Park Dae Kyeom in “Nonlinear Structural Response Analysis of Ship and Offshore Structures in Low Temperature” in which the material stress and strain in low temperatures have been evaluated by tensile tests with considering different thickness and types of steel. It represent the stress-strain curve that we could find out when strain is around 0.2 that the lower temperature will have higher stress, and it reached to 600 MPa for AH32 steel under -60°C. On the other hand, at the same strain point, the stress under room temperature (20°C) is around 520 MPa which have 15% differences.

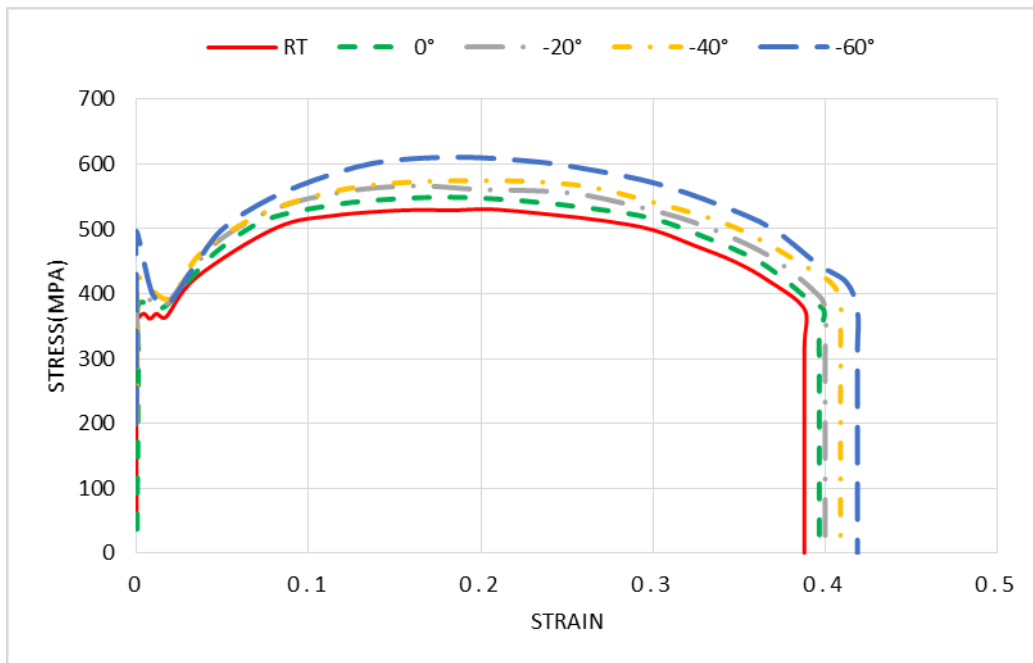


Fig. 3.12 Stress-strain diagram for AH32 steel, t=12.0 mm (Park, 2015)

3.4 CORROSION WASTAGE

The reference of corrosion wastage that came from ABS rules "Building and Classing for Steel Vessels (PART 5C-5, special for Vessels Intended to Carry Containers)" as the Fig. 3.13. Moreover, the two different consideration of corrosion addition can be found out in the Fig. 3.5 which are the applied area of ballast tank and pipe duct/void space.

Nominal Design Corrosion Values (NDCV) (2013)

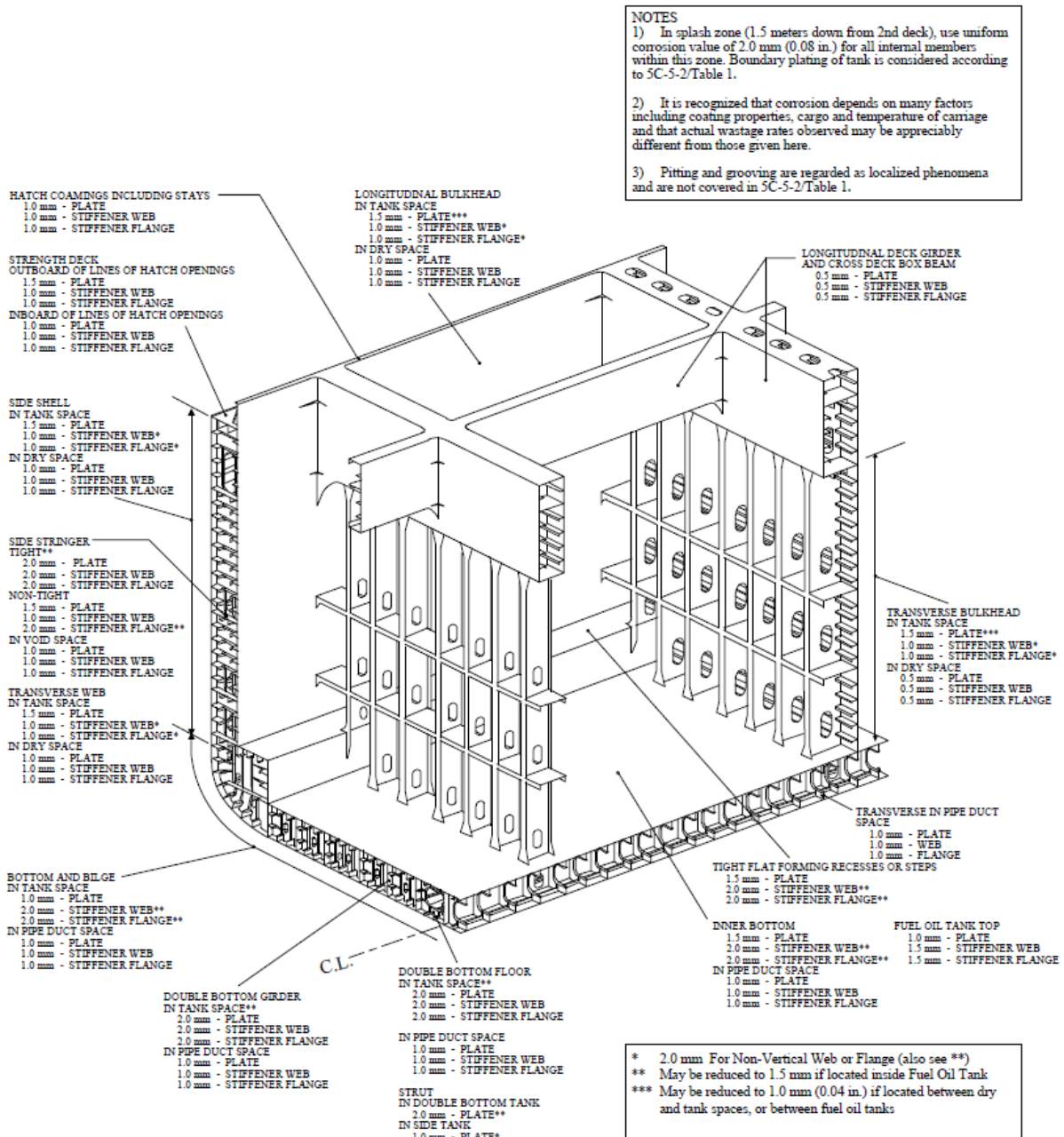


Fig. 3.13 Nominal design corrosion values for container ships (ABS rules, 2013)

**Nominal Design Corrosion Values (NDCV)
for Container Carriers (2013)**

Structural Element/Location		Nominal Design Corrosion Values in mm (in.)		
		Plate	Attached Stiffeners	
			Web	Flange
Strength Deck	Outboard of Lines of Hatch Openings	1.5 (0.06)	1.0 (0.04)	1.0 (0.04)
	Inboard of Lines of Hatch Openings	1.0 (0.04)	1.0 (0.04)	1.0 (0.04)
Side Shell	In Tank Space	1.5 (0.06)	1.0 (0.04) *	1.0 (0.04) *
	In Dry Space	1.0 (0.04)	1.0 (0.04)	1.0 (0.04)
Bottom and Bilge	In Tank Space	1.0 (0.04)	2.0 (0.08) **	2.0 (0.08) **
	In Pipe Duct Space	1.0 (0.04)	1.0 (0.04)	1.0 (0.04)
Inner Bottom	In Tank Space	1.5 (0.06)	2.0 (0.08) **	2.0 (0.08) **
	In Pipe Duct Space	1.0 (0.04)	1.0 (0.04)	1.0 (0.04)
Longitudinal Bulkhead	In Tank Space	1.5 (0.06) ***	1.0 (0.04) *	1.0 (0.04) *
	In Dry Space	1.0 (0.04)	1.0 (0.04)	1.0 (0.04)
Transverse Bulkhead (except for Cross Deck Box Beam)	In Tank Space	1.5 (0.06) ***	1.0 (0.04) *	1.0 (0.04) *
	In Dry Space	0.5 (0.02)	0.5 (0.02)	0.5 (0.02)
Transverse Web	In Tank Space	1.5 (0.06)	1.0 (0.04) *	1.0 (0.04) *
	In Dry Space	1.0 (0.04)	1.0 (0.04)	1.0 (0.04)
Tight Flat forming Recesses or Steps (except 2 nd deck)		1.5 (0.06)	2.0 (0.08) **	2.0 (0.08) **
Side Stringer	Tight **	2.0 (0.08)	2.0 (0.08)	2.0 (0.08)
	Non-Tight	1.5 (0.06)	1.0 (0.04)	2.0 (0.08) **
	In Void Space	1.0 (0.04)	1.0 (0.04)	1.0 (0.04)
Double Bottom Girder	In Tank **	2.0 (0.08)	2.0 (0.08)	2.0 (0.08)
	In Pipe Duct Space	1.0 (0.04)	1.0 (0.04)	1.0 (0.04)
Double Bottom Floor	In Tank **	2.0 (0.08)	2.0 (0.08)	2.0 (0.08)
	In Pipe Duct Space	1.0 (0.04)	1.0 (0.04)	1.0 (0.04)
Transverse in Pipe Duct Space		1.0 (0.04)	1.0 (0.04)	1.0 (0.04)
Longitudinal Deck Girder and Box Beam		0.5 (0.02)	0.5 (0.02)	0.5 (0.02)
Hatch Coamings including Stays		1.0 (0.04)	1.0 (0.04)	1.0 (0.04)
Hatch Cover		1.0 (0.04)	1.0 (0.04)	1.0 (0.04)
Fuel Oil Tank Top		1.0 (0.04)	1.5 (0.06)	1.5 (0.06)
Strut	In Double Bottom Tank	--	2.0 (0.08) **	
	In Side Tank	--	1.0 (0.04) *	

* 2.0 mm (0.08 in.) for non-vertical members (also see **)

** May be reduced to 1.5 mm (0.06 in.) if located inside fuel oil tank

*** May be reduced to 1.0 mm (0.04 in.) if located between dry and tank spaces, or between fuel oil tanks

Notes: 1 In splash zone (1.5 meters down from 2nd deck), use uniform corrosion value of 2.0 mm (0.08 in.) for all internal members within this zone. Boundary plating of tank is considered according to the above table.

2 It is recognized that corrosion depends on many factors including coating properties, cargo and temperature of carriage and that actual wastage rates observed may be appreciably different from those given here.

3 Pitting and grooving are regarded as localized phenomena and are not covered in this table.

Fig. 3.14 Nominal design corrosion values for container ships (ABS rules, 2013)

From the previous studies, the corrosion wastages are recognized as many factors including the coating properties, cargo and temperature of carriages but are complex to identify with ages. Some of time-dependent corrosion wastages models considered the durability coating which can provide the longer protection to prevent corrosion as the Fig. 3.14. Nevertheless, there is only the strict requirement for seawater ballast tank that is called PSPC (Performance Standard for Protective Coatings) which is based on the SOLAS (International Convention for the Safety

of Life at Sea) II-1/3-2. Accordingly, only the ballast tank area will be considered with coating life in the later on analysis.

From the research of “A time-dependent corrosion wastage model for seawater ballast tank structures of ships” (Paik, 2003) as the Fig. 3.15 performed different corrosion wastage models for researchers to consider the nonlinear corrosion wastage model which corresponds to the specific situation of corrosion with time.

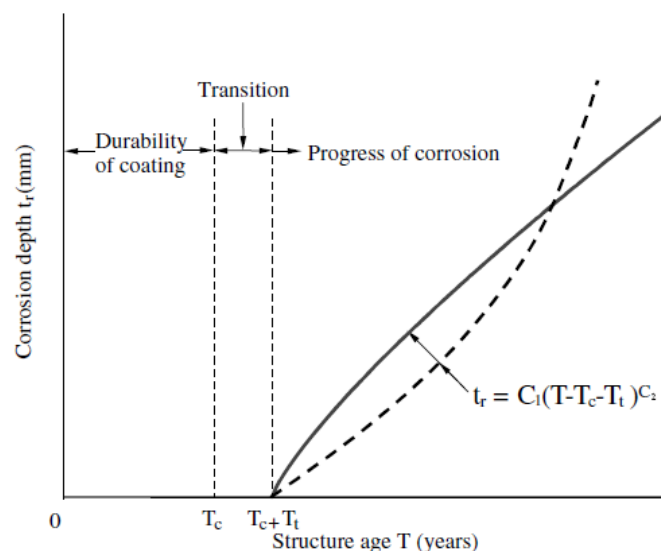


Fig. 3.15 Schematic of the corrosion process for marine structures (Paik, 2003)

✓ Pipe duct area/ void space

For the pipe duct area, there are particular rules as PSPC for coatings. To simplify the consideration of aged plates that we use the 20 years design life time from ABS rules to calculate the corrosion ratio of container ship structures.

✓ Seawater ballast area

PSPC is the standard of coating requirements of seawater ballast tank for all kinds of ships which intend to provide a target useful coating life of 15 years considered to be the time period from initial application over which the coating system is intended to remain in “GOOD” condition. On the other hand, the “GOOD” condition in PSPC that means the corrosion percentage under 3% of breakdown of coating or area rust, and under 20% of the local breakdown of coating or rust on edges or weld lines by regular examinations.

Contrast with the consideration of coating life 15 years of PSPC that we use the reference formula from the study “The corrosion wastage consideration is based on the A time-dependent corrosion wastage model for seawater ballast tank structures of ships” to estimate the suitable coating life time for the analysis model as Fig. 3.16. It represented the comparison of annualized

corrosion rate formulations, and the first three formulas refer to the average trend with 5 to 10 years coating life. In addition, the No.4 to No.6 formulas are the severe trend of 95% and above band with 5 to 10 years of coating life.

In the formula 1 to 3 that t_{r1} , t_{r2} , t_{r3} with the consideration of coating life 5 years, 7.5 years and 10 years individually.

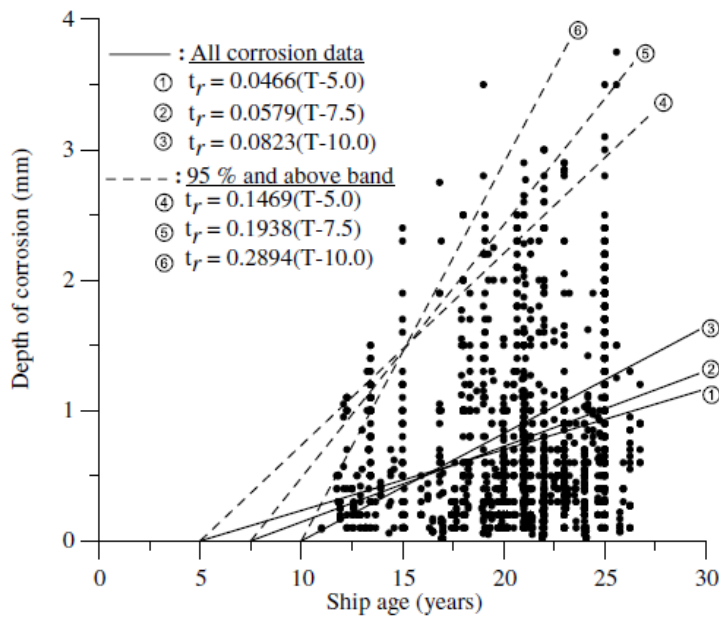


Fig. 3.16 Comparison of annualized corrosion rate formulas, together with the measured corrosion data for seawater ballast tanks (Paik, 2004)

When followed the design life T as 20 years from ABS Safehull software that we can found out the calculation results of each formula as follows:

$$t_{r1} = 0.0466 (T-5.0) = 0.699 \text{ mm} \quad (1)$$

$$t_{r2} = 0.0579 (T-7.5) = 0.724 \text{ mm} \quad (2)$$

$$t_{r3} = 0.0823 (T-10.0) = 0.823 \text{ mm} \quad (3)$$

$$t_{r4} = 0.1469 (T-5.0) = 2.204 \text{ mm} \quad (4)$$

$$t_{r5} = 0.1938 (T-7.5) = 2.422 \text{ mm} \quad (5)$$

$$t_{r6} = 0.2894 (T-10.0) = 2.894 \text{ mm} \quad (6)$$

From the ABS rules of steel vessels (PART 5C-5 for container ship) that the nominal design corrosion margin for coated seawater ballast tank plates needs to be in the range of 1.5 to 2.0 mm for a 20 year service life time which is similar with the result of t_{r4} .

In summary, the time variant aged plate model has been accomplished with 5 years coating life consideration in ballast tank area and average ratio for later on 15 years which is available to be obtained in the Table 3.7 and Fig. 3.17 for the present study.

Table 3.7 Corrosion ratios of ballast tank and void space according to plate ages

Ages of plates	5 years	10 years	15 years	20 years	25 years
Ratio of corrosion wastage (ballast tank area)	0.00	0.33	0.67	1.00	1.33
Ratio of corrosion wastage (pipe duct space/ void area)	0.25	0.50	0.75	1.00	1.25

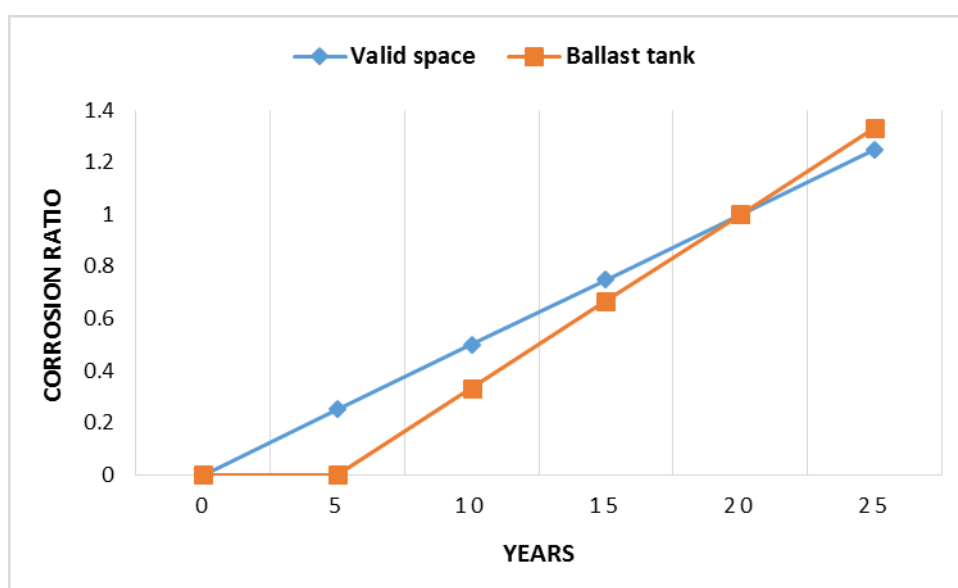


Fig. 3.17 Assumption of corrosion ratio with consideration of age plates for two different area

3.5 INITIAL DEFLECTIONS

The plates are subject to biaxial compressive loads and there are no welding residual stresses to be considered. However we ignored the welding effect, the initial deflection of plates and stiffeners are still exist, which corresponds to the plate buckling as follows. In software ULSAP that the initial maximum deflection of plates and stiffeners need to be considered as the ISO formula below, and the detailed calculation results for each case under consideration of temperature effect for yielding stress and aged plates for corrosion wastage deduction are show in the appendix.

Fig. 3.18 and Fig. 3.19 represent the example of deformed models for both plate and stiffener, and the formulas for calculating the exact initial deflection of plates and stiffeners according to the local deformation from plate and stiffeners respectively.

Furthermore, the estimation formulas for calculating maximum initial deflection of plates and stiffeners also have been introduced here.

- Initial maximum deflection of plates w_{opl} , where t_p is the plate thickness, and $\beta = \frac{b}{t_p} \sqrt{\frac{\sigma_{yp}}{E}}$

$$w_{opl} = 0.1\beta^2 t_p \tag{7}$$

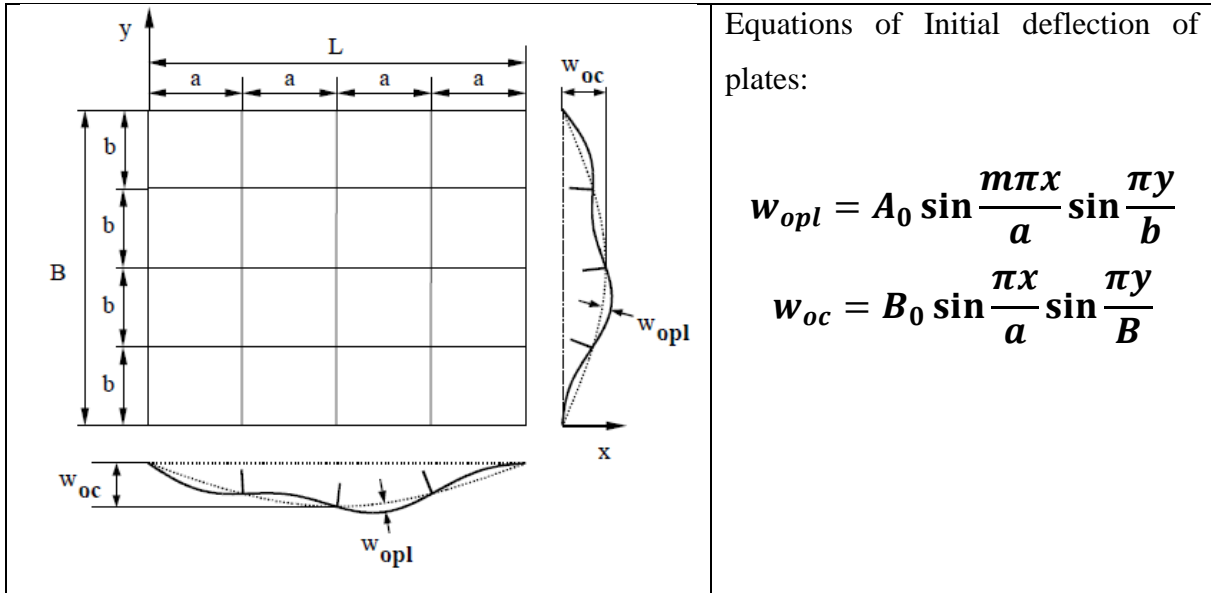


Fig. 3.18 Schematic of initial deflection on plates

- Initial maximum deflection of stiffeners w_{os} , where a is the plate length.

$$w_{os} = 0.0015a \tag{8}$$

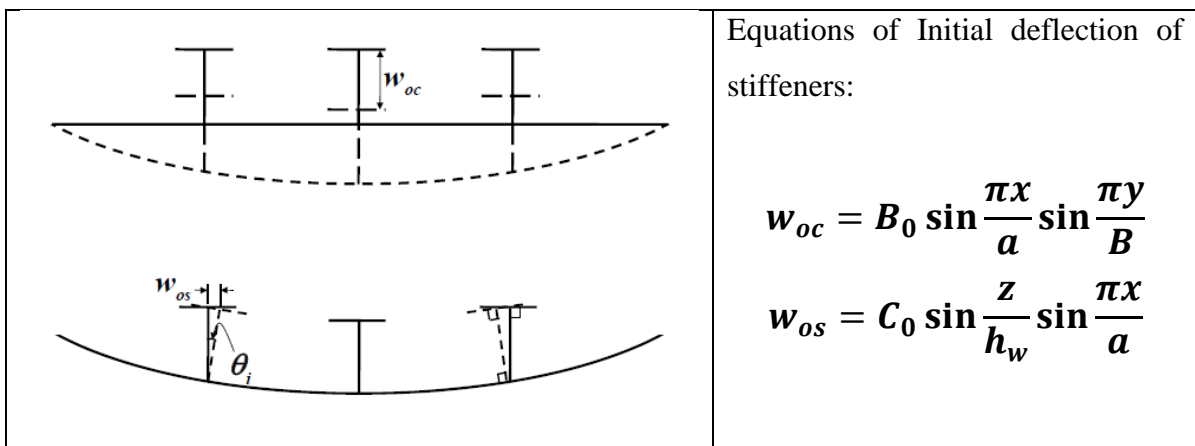


Fig. 3.19 Schematic of initial deflection on stiffeners

The initial maximum deflection of stiffeners for each analysis cases will be the same based on the same plate length, 4210 mm. From the formula (8), all the initial maximum deflection of stiffeners are 6.315 mm.

4. ULTIMATE STRENGTH CALCULATIONS

By the two parts of calculation of ultimate strength to comprehend the strength behaviour from the effect of low temperatures and connected with the concept with material property changing as an foundation for further research or design reference which are:

1. Stiffened plate with corrosion wastage by aged and consideration of low temperature effect to the yielding stress
2. Hull girder ultimate strength calculation applied on a 13,000 TEU container ship without iced classification under both consideration for low temperature and aged corrossions.

4.1 ULTIMATE STRENGTH OF STIFFENER PANELS

For stiffened panels that we choose the most critical part of local panels on container ship which will occur the maximum bending moment position with different compartment: upper deck, inner bottom plate and bottom plate.

4.1.1 ANALYSIS RESULTS FOR STIFFENER PANELS

Here we have the seven cases results which represent in the Fig. 4.1 to Fig. 4.21.

Where:

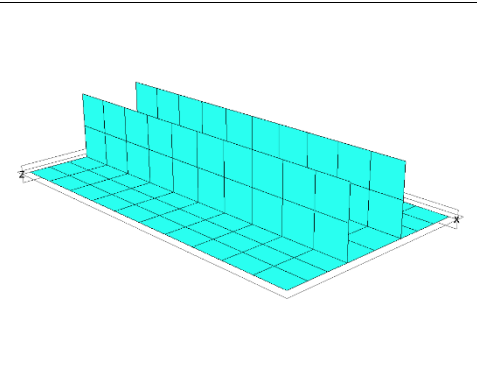
σ_y equ. is equal to σ_y (yielding stress) at temperature 20°C which is used in all results.

σ_{yu} is the ultimate stress under y direction compression loads.

σ_{xu} is the ultimate stress under x direction compression loads.

Fig. 4.1, Fig. 4.4, Fig. 4.7, Fig. 4.10, Fig. 4.13, Fig. 4.16, Fig. 4.19 show the ISUM models for each case and detailed input data for calculating the ultimate strength of stiffened panels.

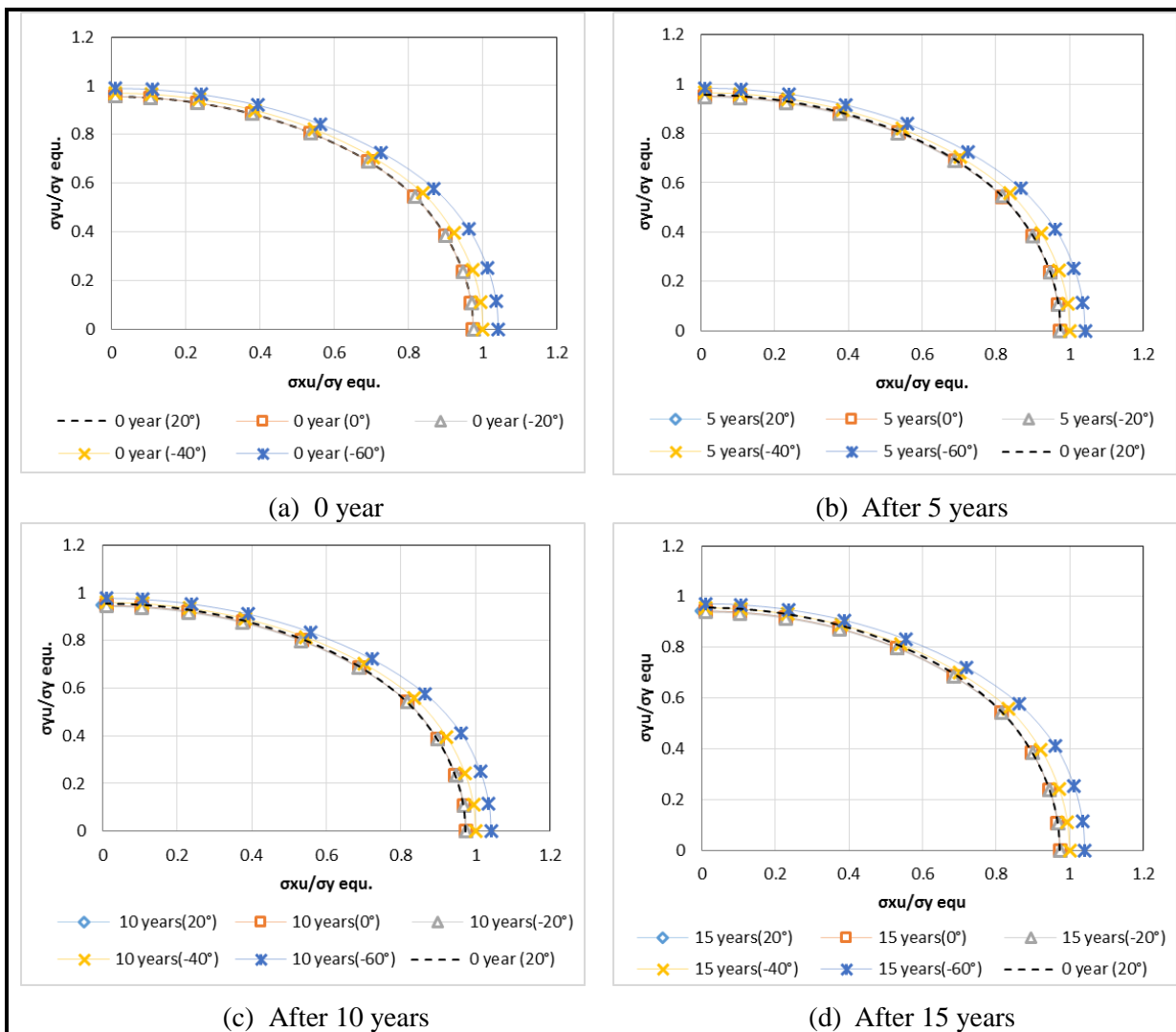
Case 1: Upper deck (which is not considering the coating life)

 <p data-bbox="268 1861 815 1926">Fig. 4.1 Schematic of stiffener panel of upper deck</p>	<p data-bbox="863 1507 1203 1541">Panel length, a : 4210 mm</p> <p data-bbox="863 1561 1222 1594">Panel breadth, B : 2400 mm</p> <p data-bbox="863 1615 1246 1648">Stiffener spacing, b : 800 mm</p> <p data-bbox="863 1668 1214 1702">Plate thickness, tp : 78 mm</p> <p data-bbox="863 1722 1289 1756">Stiffener scantling: 800x78 (FB)</p> <p data-bbox="863 1776 1390 1809">Corrosion wastage from rules: 1.5 mm</p> <p data-bbox="863 1830 1066 1863">Material: AH36</p>
--	---

a) Same aged plate under different temperatures

The Fig. 4.2 represents the differences of ultimate strength ratio between temperature and aged considerations. It could be found out the results are similar of room temperature, 0°C and -20°C in the same aged plates, but the clear discrepancy of results for -40°C and -60°C.

In this case, when the biaxial compressive load applied on the stiffened panel, the ultimate strength were similar on both axial, but a bit higher on x-axis. Further, in the same year that the ultimate strength on x axis increased with the temperature decreasing.



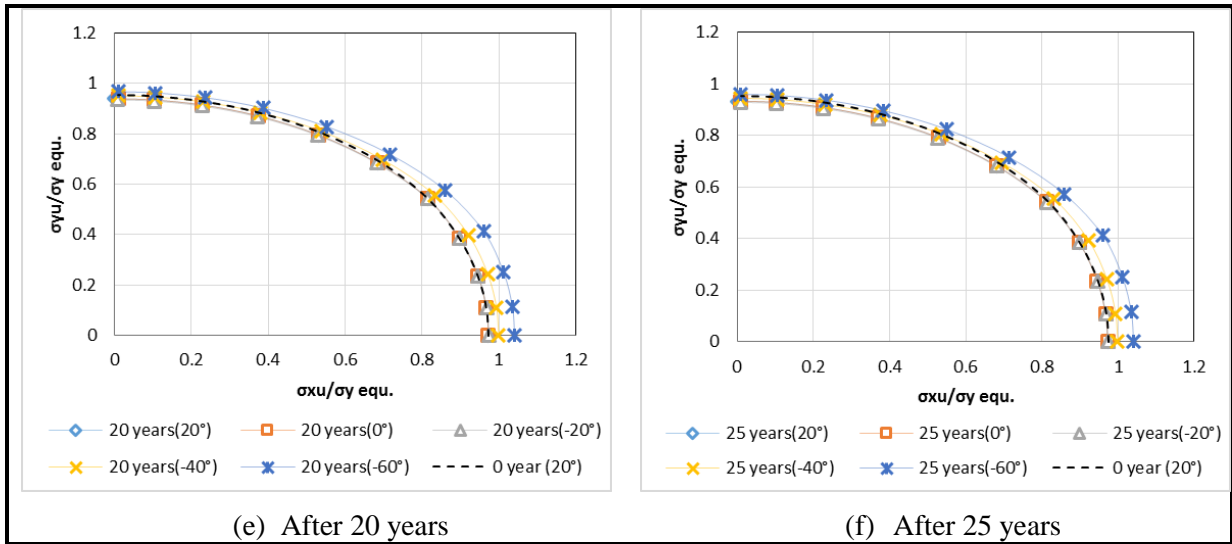
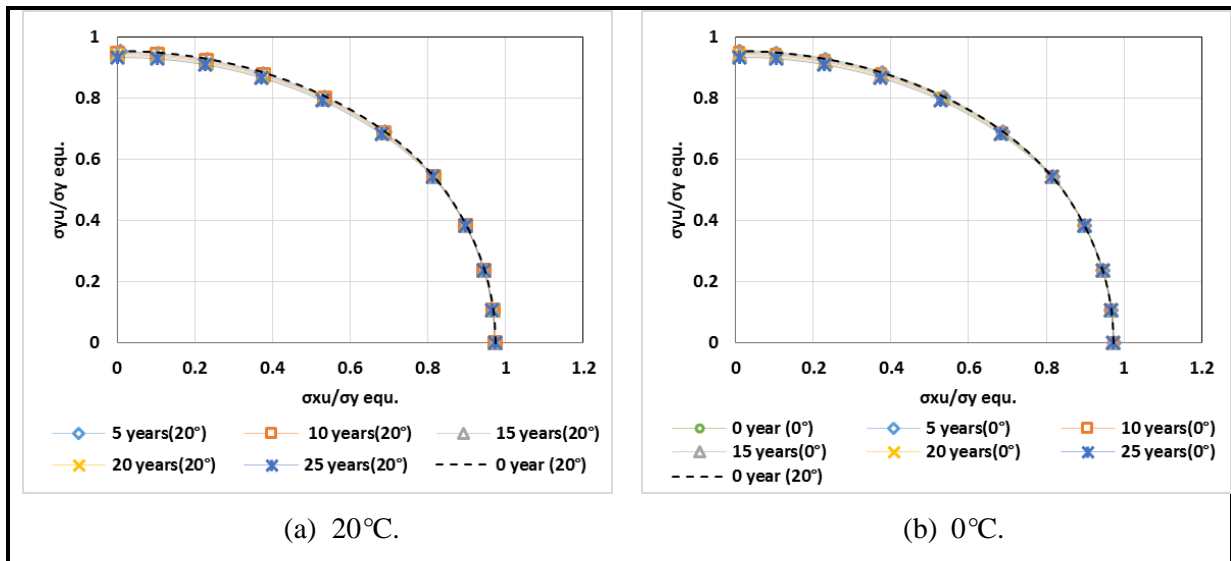


Fig. 4.2 Ratios of ultimate strength for different aged upper deck plates under low temperatures

b) Same temperature consideration for different aged plates

From the result Fig. 4.3 from (a) to (c) that indicated the minor participation of corrosion wastage compared with yielding increasing under low temperature. Alternatively, after considering the temperature lower to -40°C , it showed the ultimate strength ratio is higher than intact condition which means the majority of effecting the result is temperature.

Especially in Fig. 4.3 (e), it shows the gap between intact condition and other 6 cases under -60°C . By comparing the intact condition with 25 years old plates under -60°C , although the corrosion wastage need to consider 1.25 times, we could conclude the effect from temperature differences are more influential.



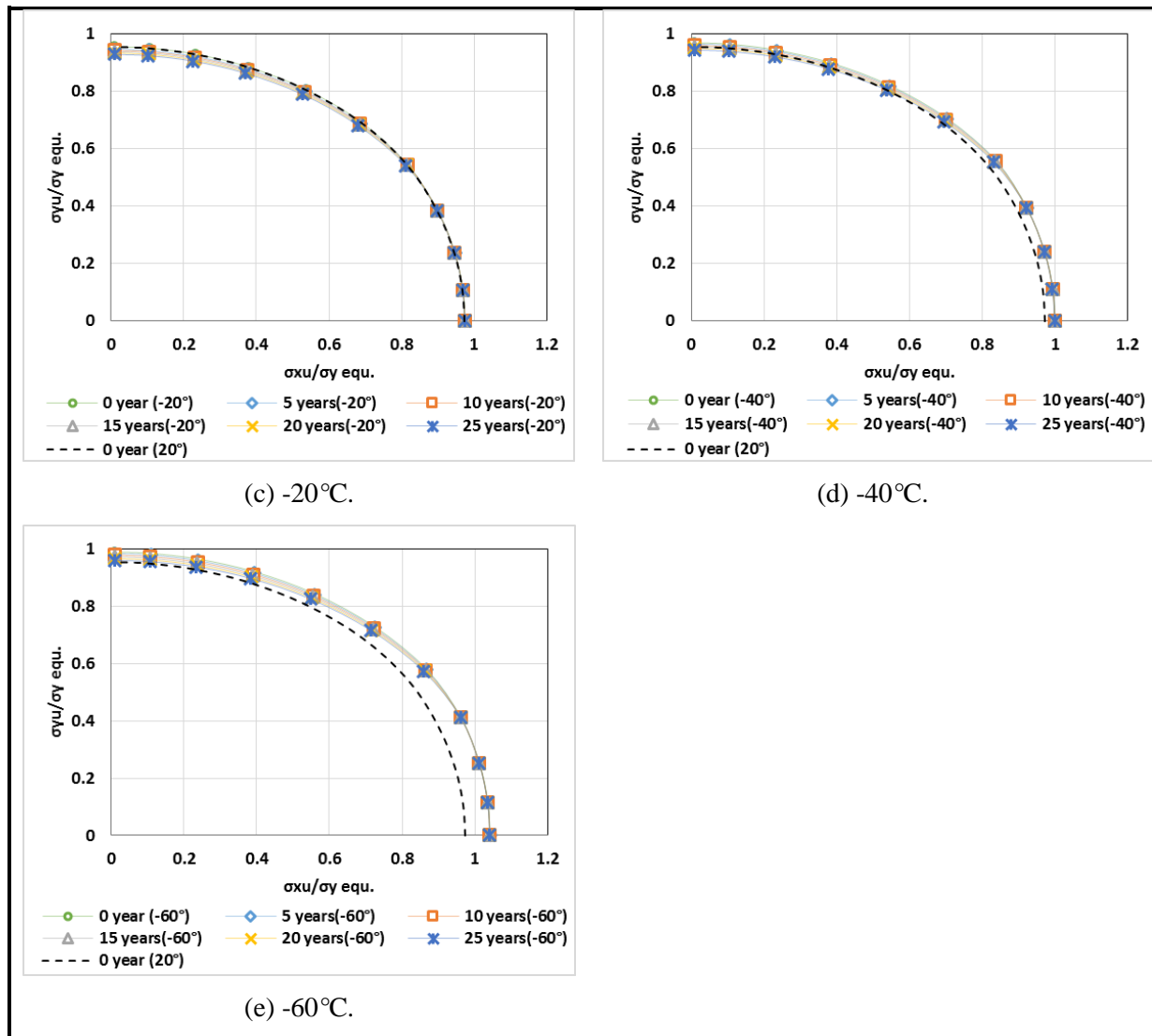
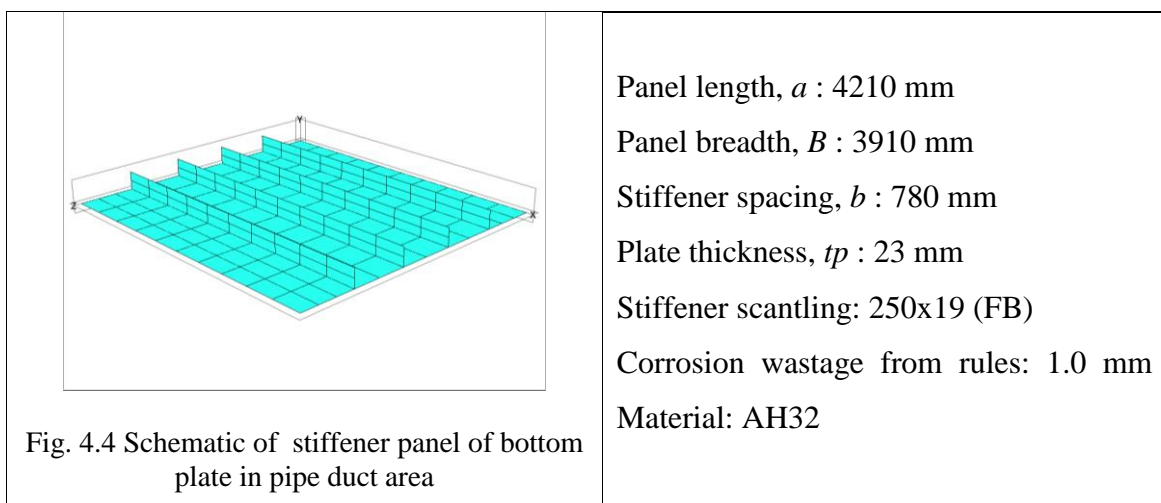


Fig. 4.3 Ratios of ultimate strength for upper deck plates with same temperature consideration according to ages

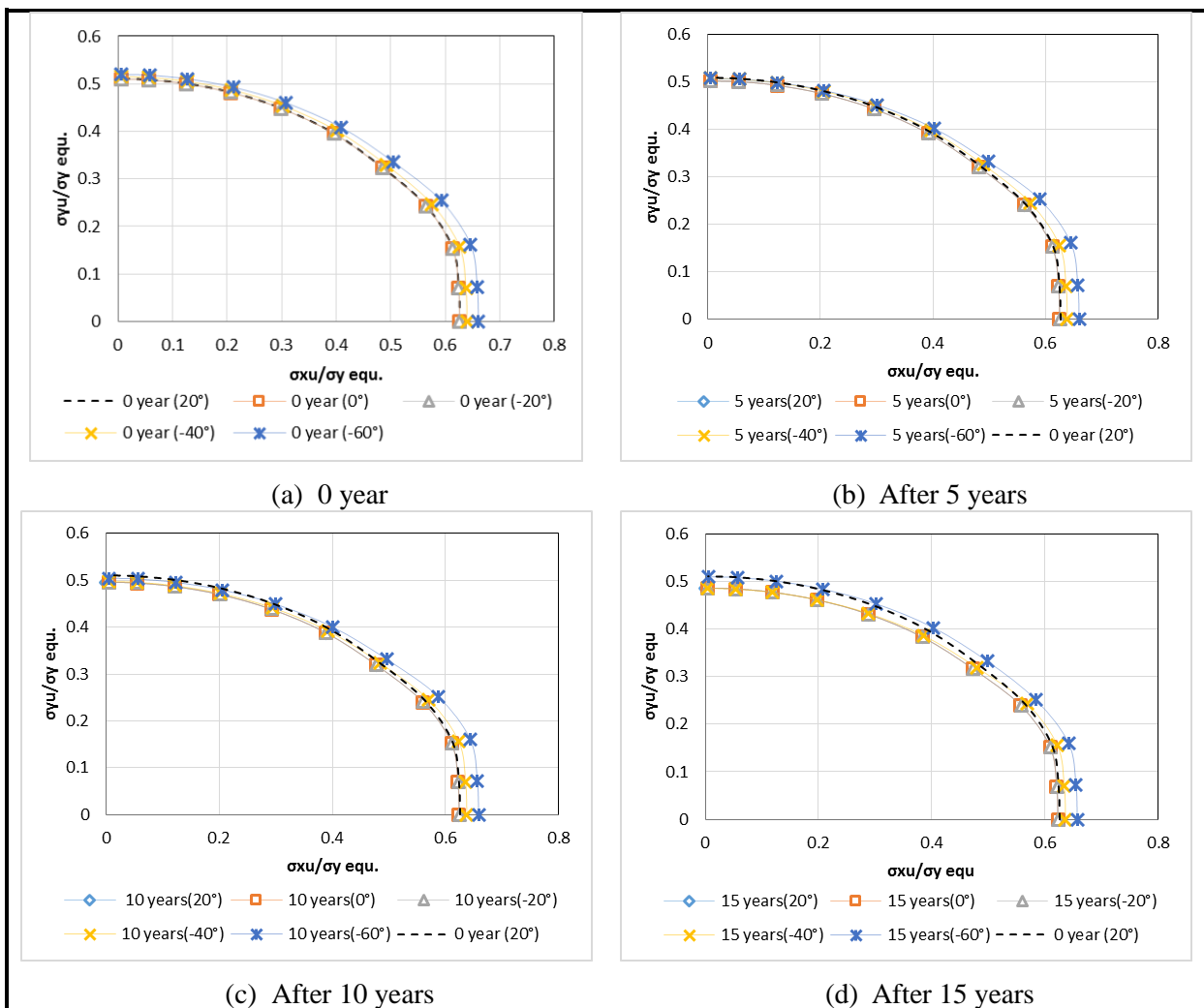
Case 2: Bottom plate (pipe duct area which is not considering the coating life)



a) Same aged plate under different temperatures

The result of case 2 is similar with case 1, which represent the differences of ultimate strength ratio between temperature and aged considerations. It could be found out the results are similar of room temperature, 0°C and -20°C in the same aged plates, but the clear discrepancy of results for -40°C and -60°C.

The ratio of ultimate yielding stress in y axis reached around 0.5 in each case, but the ratio are over 0.6 in y axis where we can see the difference of load capacity of structure arrangement. In Fig. 4.5 (f) that could not find the clear relations between the corrosion wastage and temperatures because the intact condition has the higher value of ratio in y direction, but not also in x direction.



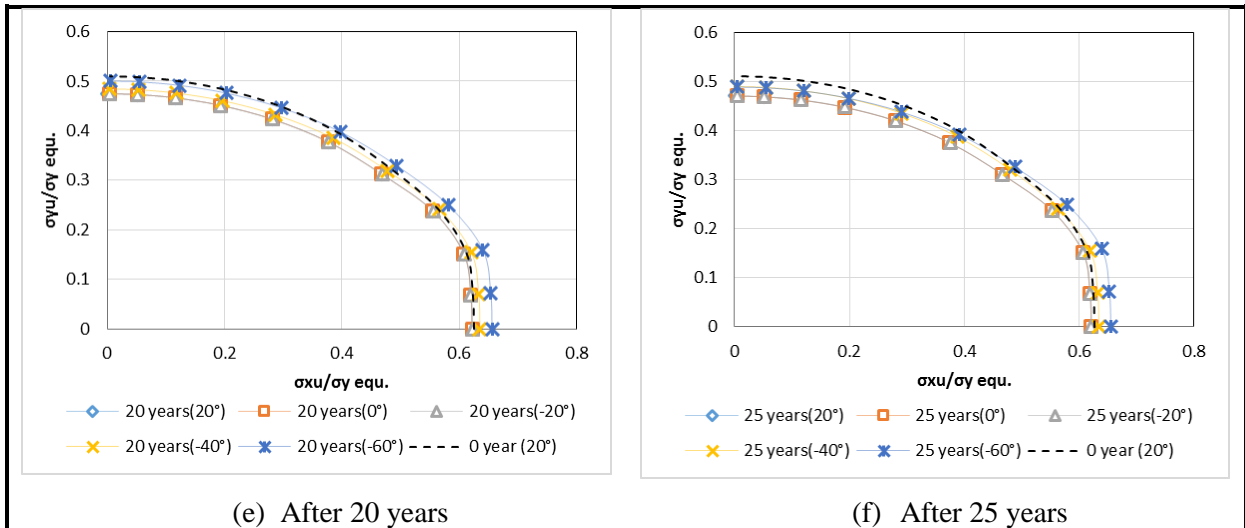
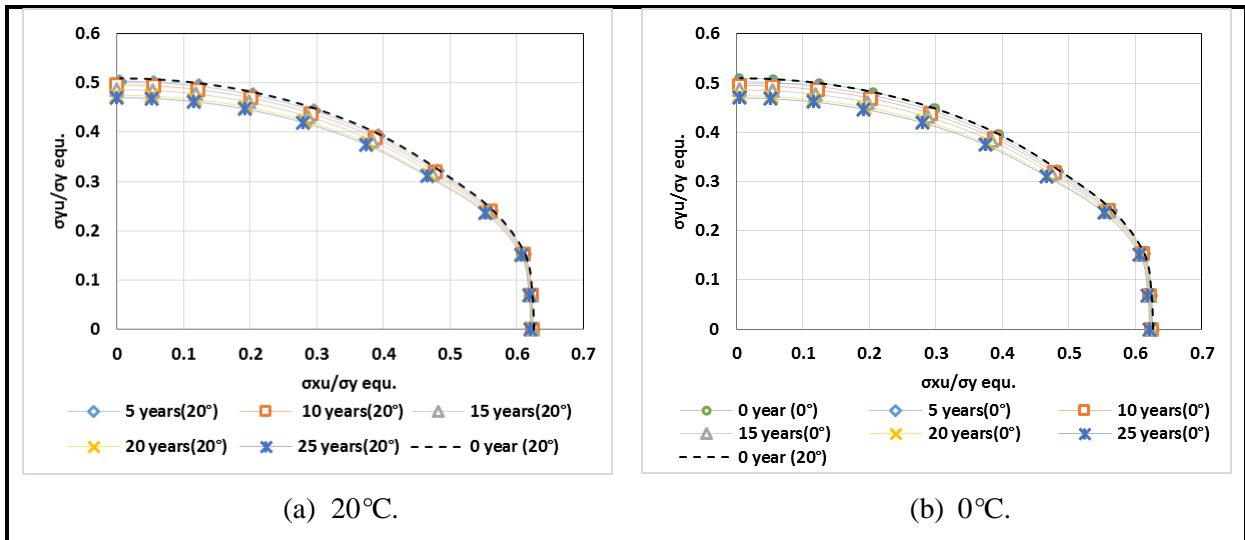


Fig. 4.5 Ratios of ultimate strength for different aged bottom plates (in pipe duct area) under low temperatures

b) Same temperature consideration for different aged plates

In case 2 that we could find out the intact condition is showing the highest value of ratio in sub figure (a) to (c) in Fig.4.6. With the temperature decreasing, the intact condition loss its advantage that is replaced with the -40°C and -60°C cases by increasing yielding stress which rises up the load capacity. Especially we can find out this situation that the ratio of intact condition is around 0.5 which is between 0 year and 25 years in y axis, but less than all other cases in x axis in subfigure (e).



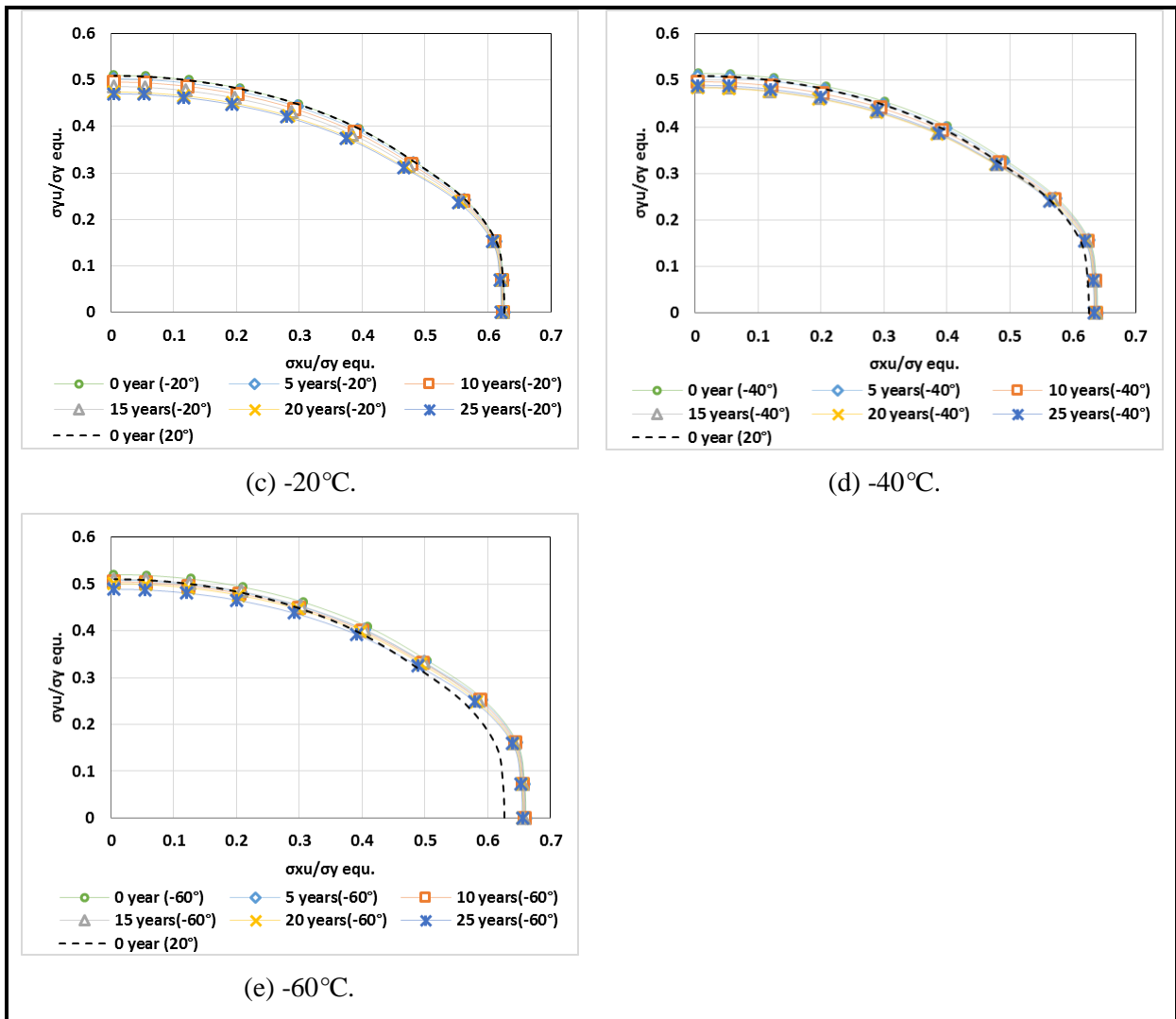
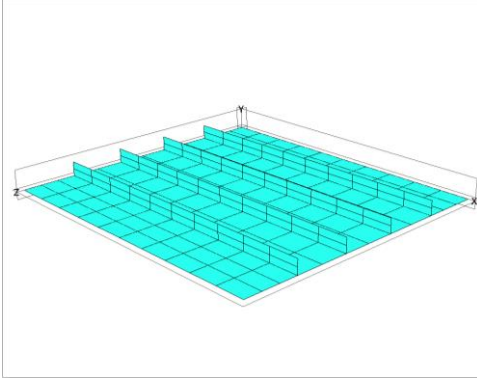


Fig. 4.6 Ratios of ultimate strength for bottom plates (in pipe duct area) with same temperature consideration according to ages

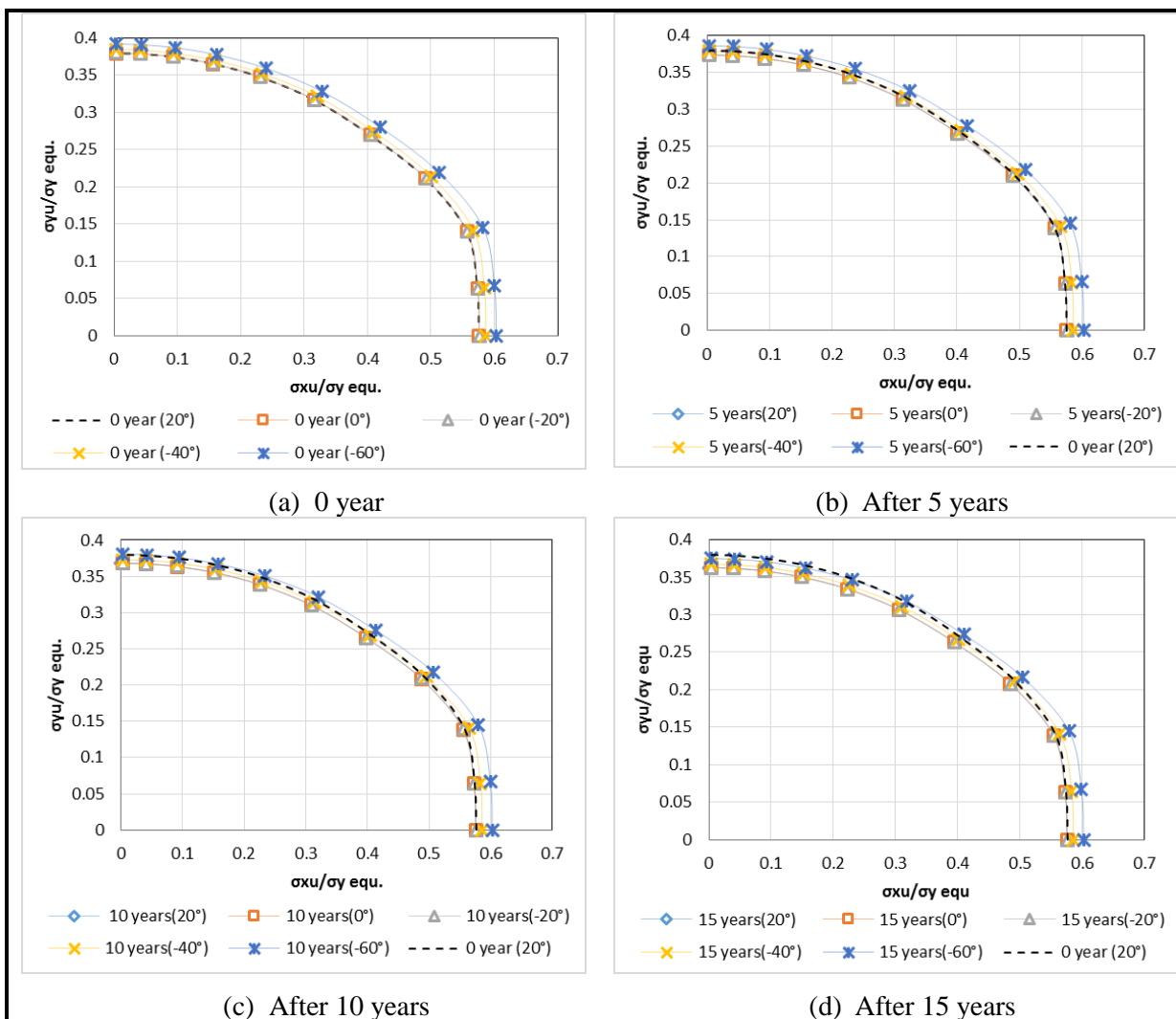
Case 3: Inner bottom plate (pipe duct area which is not considering the coating life)

 <p>Fig. 4.7 Schematic of stiffener panel of inner bottom plate in pipe duct area</p>	<p>Panel length, a : 4210 mm</p> <p>Panel breadth, B : 3910 mm</p> <p>Stiffener spacing, b : 780 mm</p> <p>Plate thickness, tp : 18 mm</p> <p>Stiffener scantling: 200x25 (FB)</p> <p>Corrosion wastage from rules: 1.0 mm</p> <p>Material: AH32</p>
--	--

a) Same aged plate under different temperatures

The Fig. 4.8 represents the differences of ultimate strength ratio between temperature and aged considerations. In subfigure (a) to (c) that we can find out when structure were just established, the lower temperature is a plus for ultimate strength, but within the time passing by structure ages the ultimate strength ratio start to decrease by the corrosion deductions

The result of case 3 is similar with case 2, the same tendency of curve can be found out of 20°C, 0°C, and -20°C for each case in Fig. 4.8. Compared with the case 2 (bottom plate), case 3 is inner bottom plate which have less plate thickness and stiffer strength that cause the ratio difference in y axis which lower than 0.4.



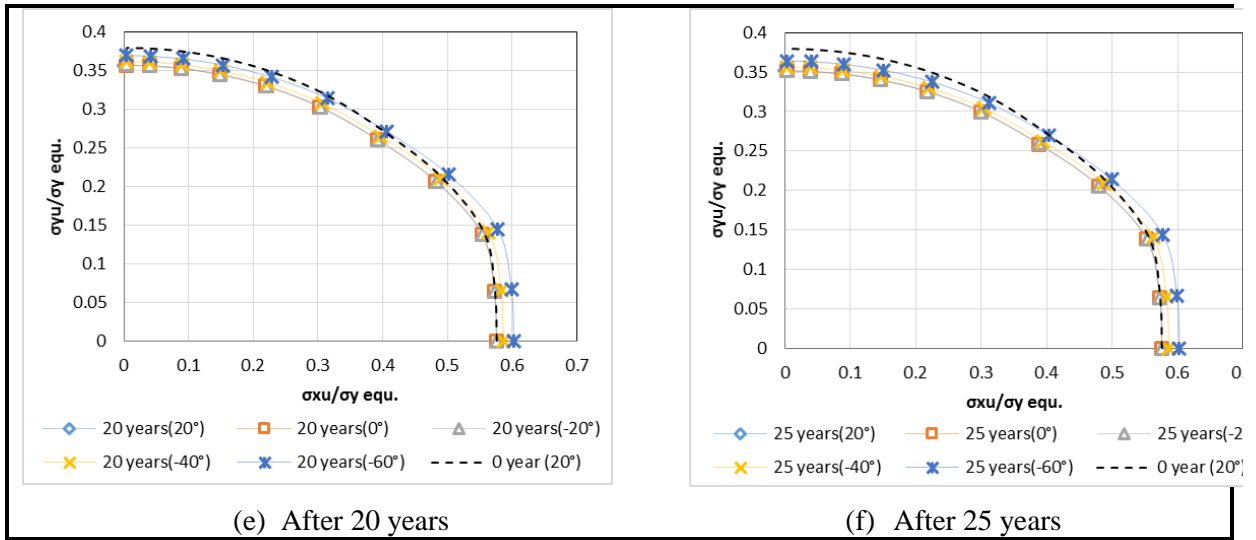
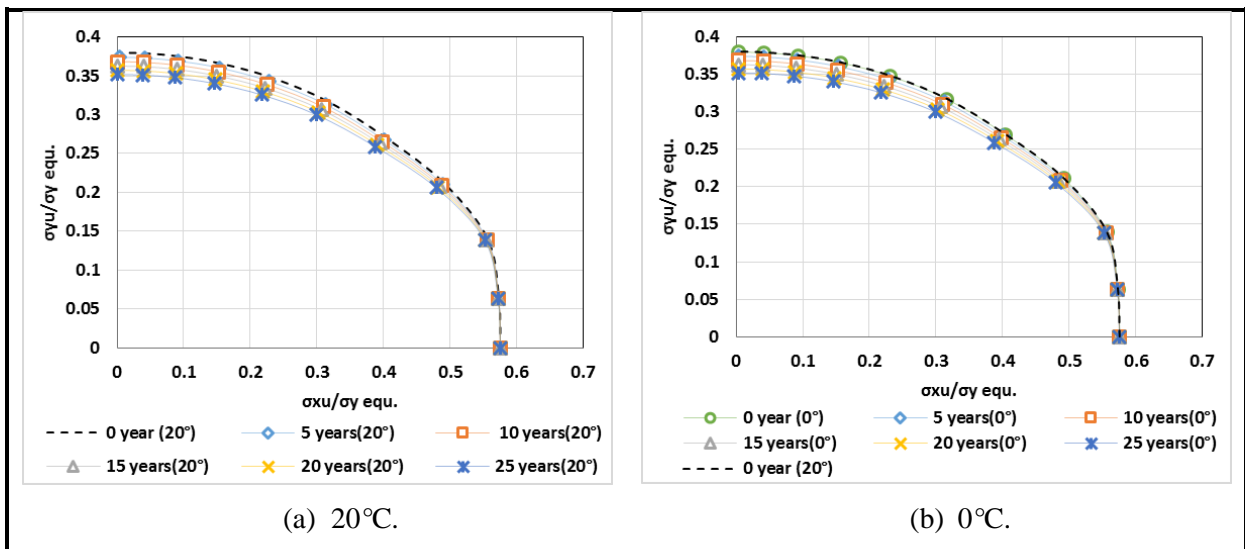


Fig. 4.8 Ratios of ultimate strength for different aged inner bottom plates (in pipe duct area) under low temperatures

b) Same aged plate under different temperatures

In Fig. 4.9 that represent the differences of ultimate strength ratio in the same temperature with various ages. From subfigure (a) to (c) that show the same value of ultimate strength ratio in x direction which is around 0.58. That means the influence from corrosion wastage is quiet smaller for strength in x direction, but the differences in y direction can be find out.

Similar tendency of the curve with case 1 and case 2, which are using the flat bar as the supporting stiffeners.



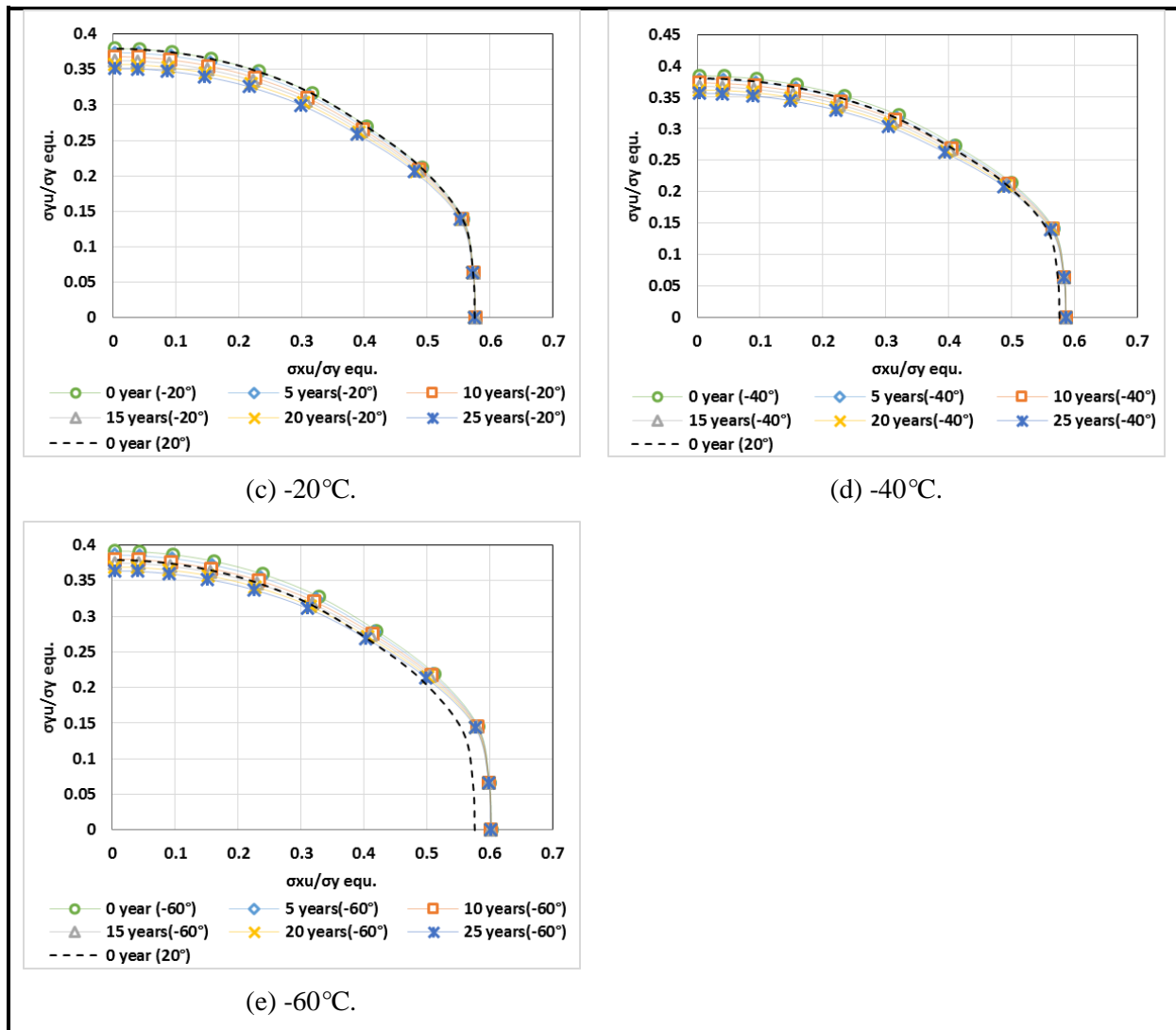
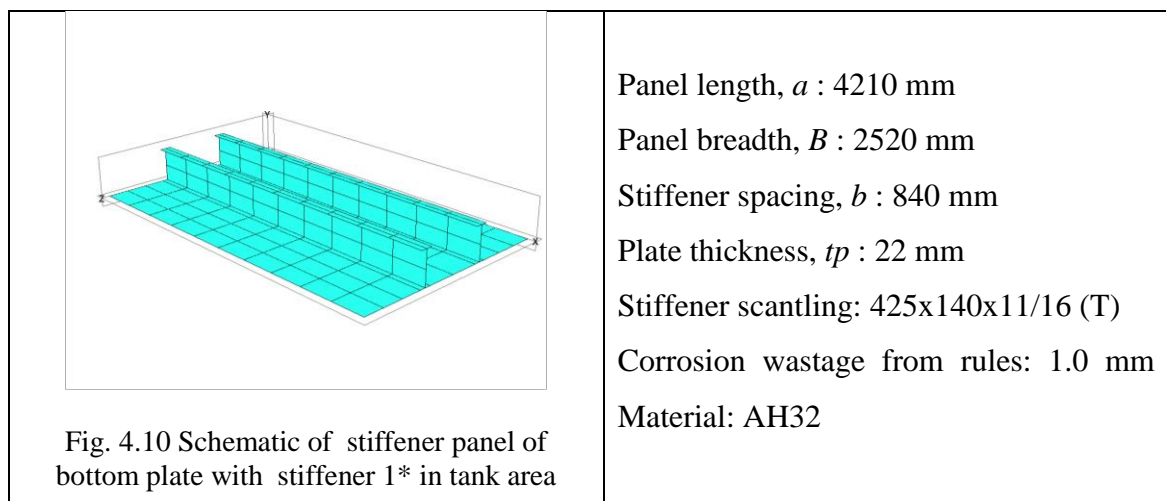


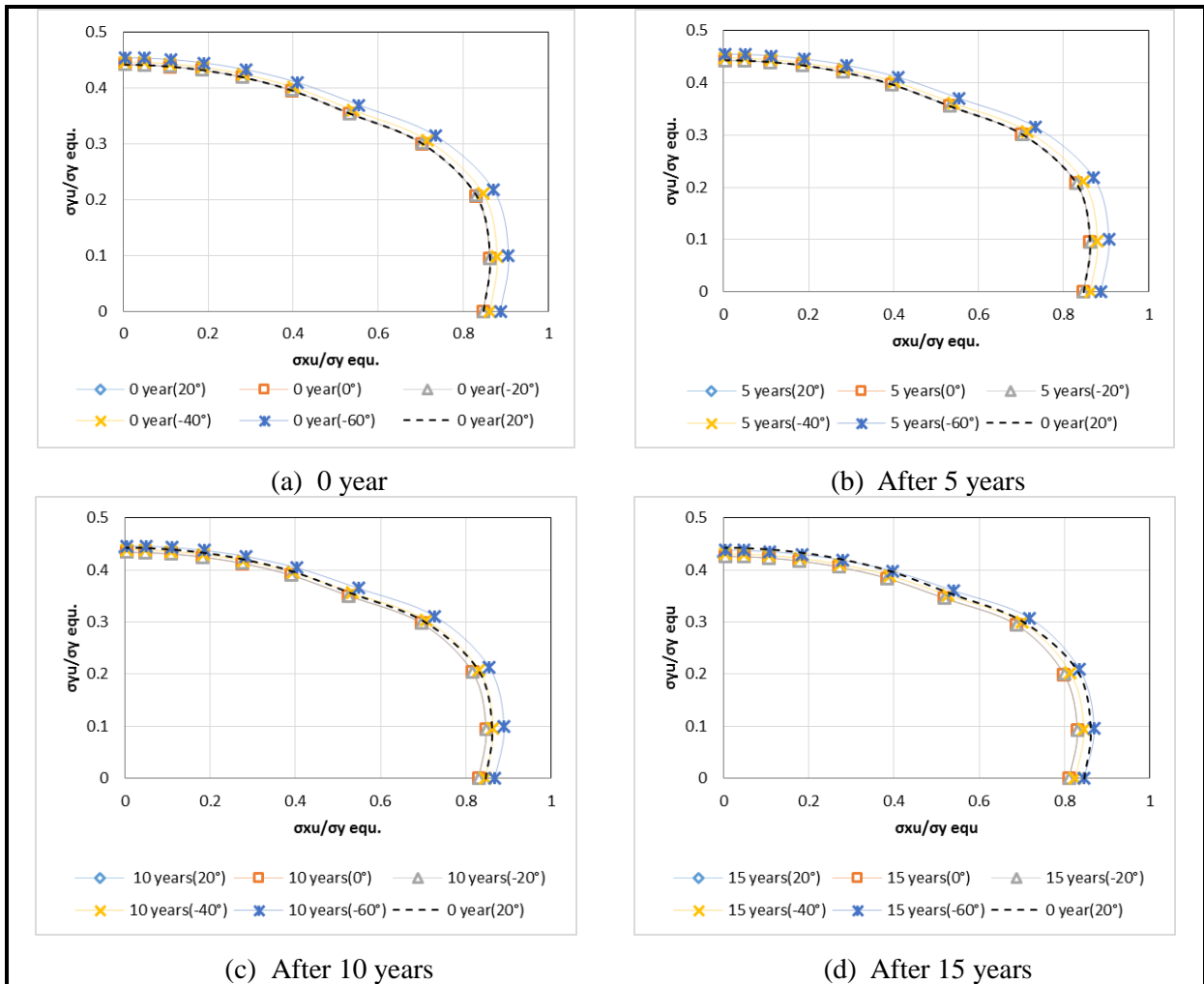
Fig. 4.9 Ratios of ultimate strength for inner bottom plates (in pipe duct area) with same temperature consideration according to ages

Case 4: Bottom plate with stiffener 1* (ballast tank area)



a) Same aged plate under different temperatures

Evaluate the ultimate strength of bottom stiffened panel that we can have the following results which show the ultimate strength ratio in both x and y directions in Fig. 4.11. We can find out the ratio in x axis is two times rather than in y axis, and show almost the same curve (overlap) for 20°C, 0°C and -20°C in all sub figures, only -40°C and -60°C these two cases can be distinguished.



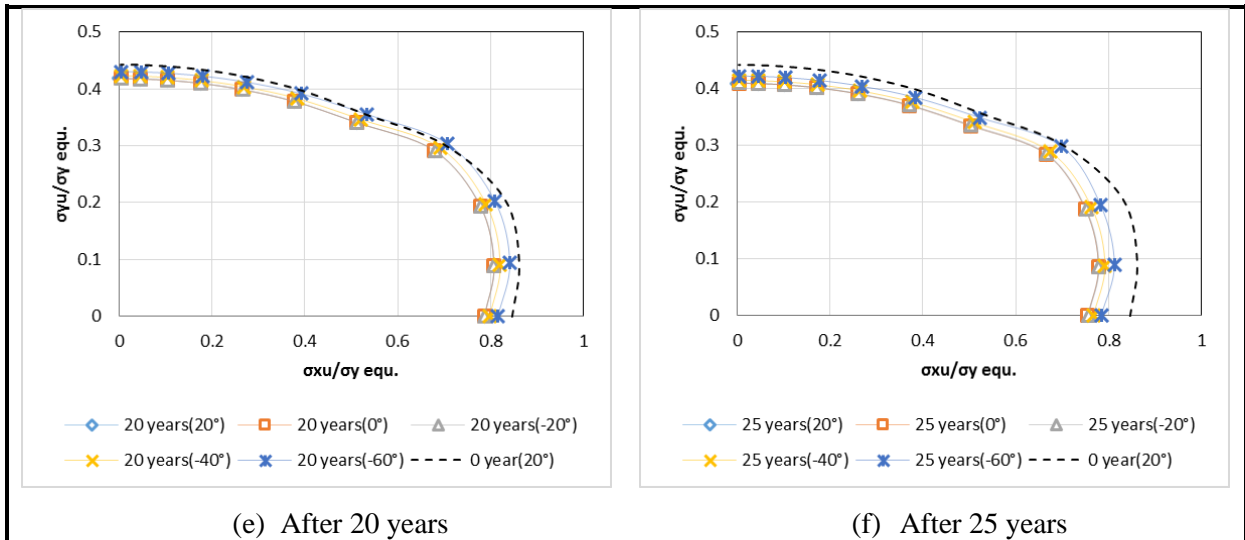
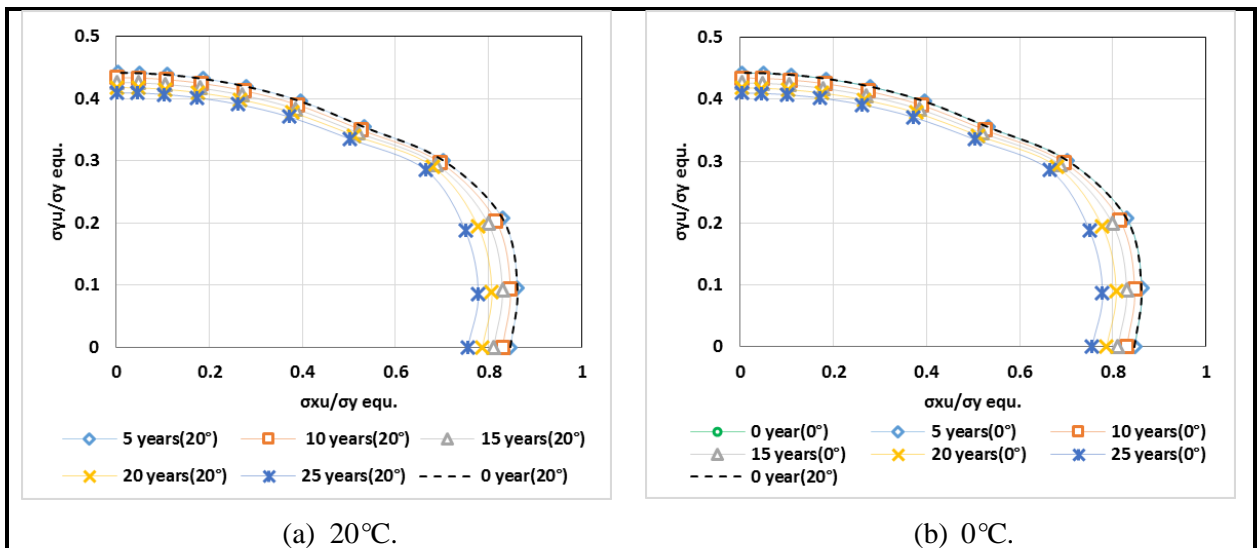


Fig. 4.11 Ratios of ultimate strength for different aged bottom plates with stiffener*1 (in ballast tank area) under low temperatures

b) Same temperature consideration for different aged plates

Different with previous three cases with flat bar as stiffener, T-bar is used as supporting stiffener in case 4. Therefore, we could find out the difference clearly in each sub figure in Fig. 4.12. The difference between each curve represent the effect from corrosion wastage, which is a liner parameter according to rules. Difference between the ratio in x and y axis that the spacing of each curve is smaller in y axis rather in x axis in Fig. 4.12 (e).



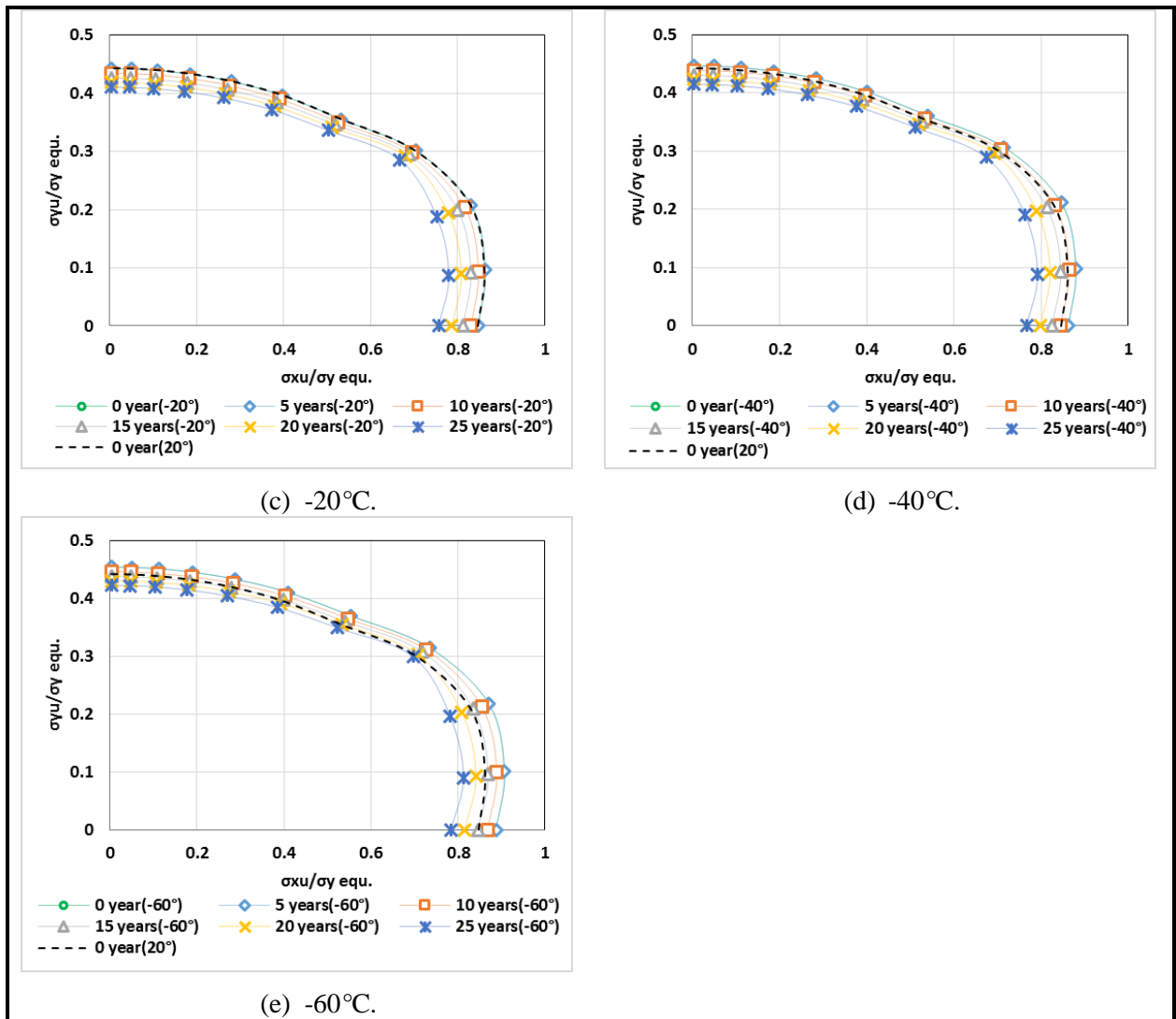
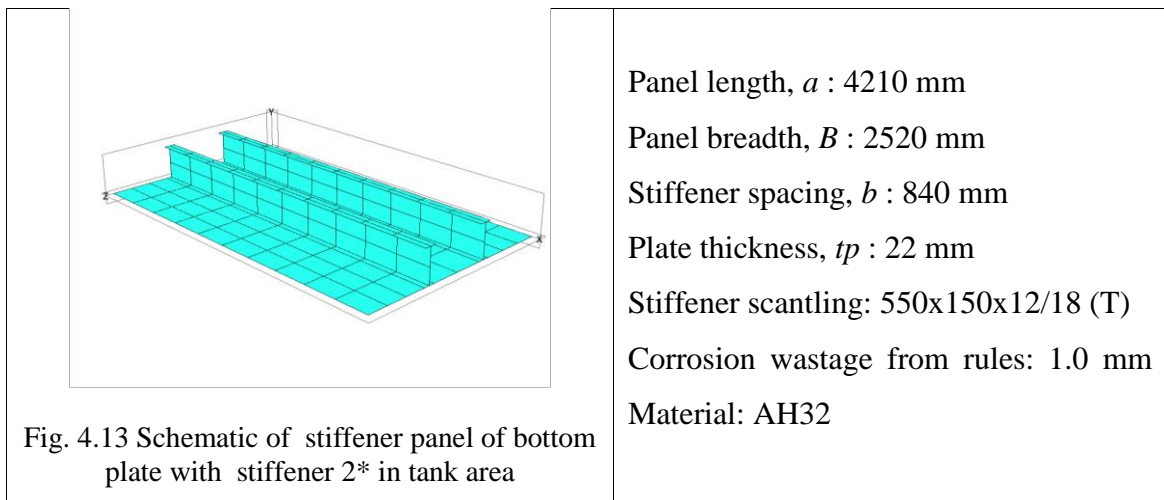


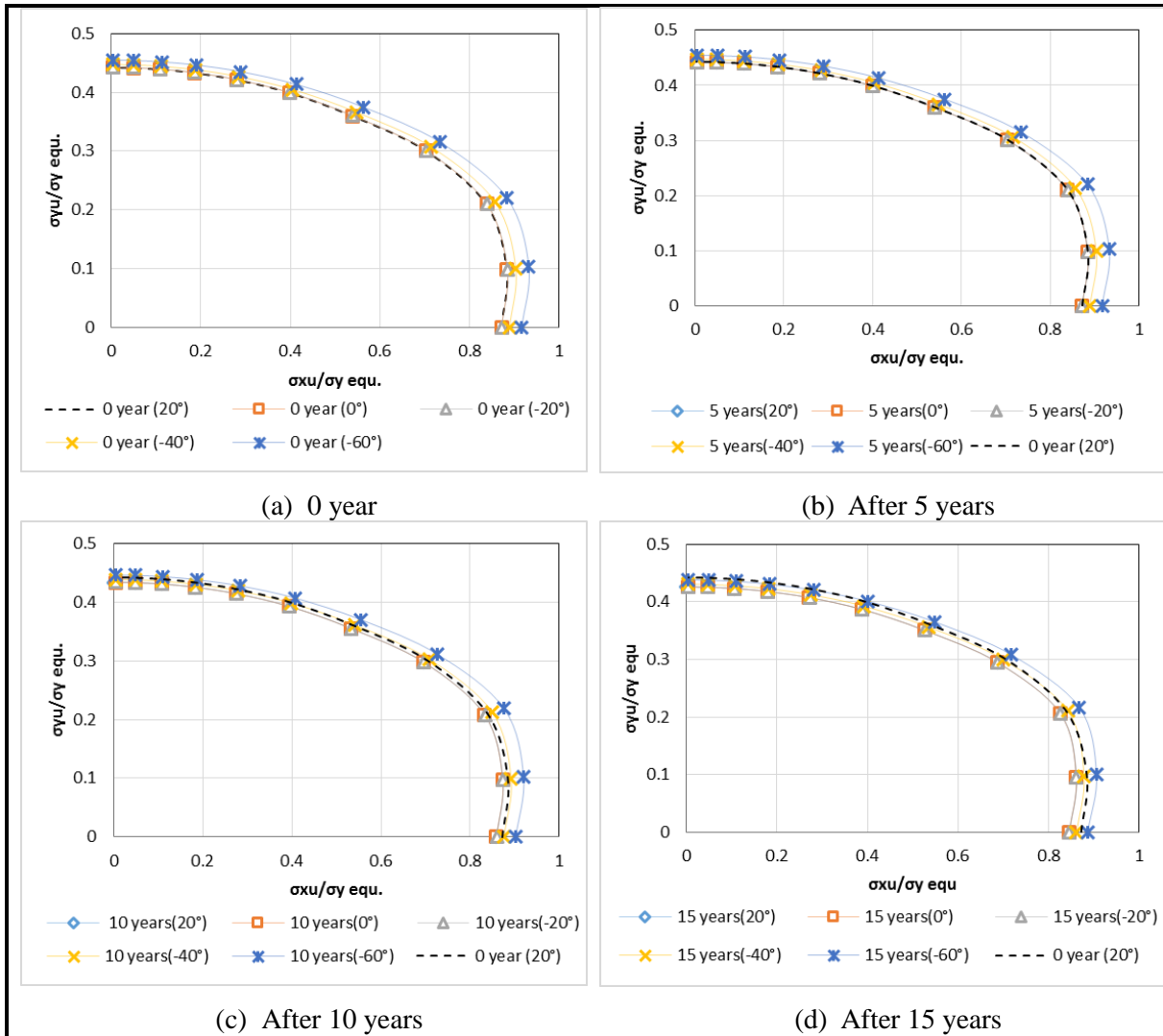
Fig. 4.12 Ratios of ultimate strength for bottom plates with stiffener*1 (ballast tank area) with same temperature consideration according to ages

Case 5: Bottom plate with stiffener 2* (ballast tank area)



a) Same aged plate under different temperatures

Here we could compare with case 4 which keep the same plate thickness, but increase the supporting stiffener from 425x140x11/16 to 550x150x12/18 that the almost same tendency of curve we can see in Fig. 4.14. However, the concept with increasing structure scantlings should cause the higher ultimate strength, the ratio of ultimate strength only increase in x axis obviously in Fig. 4.14 (f). In case 4 that ratio reached just under 0.8, but in case 5 that increased up to 0.8 in 25 years condition.



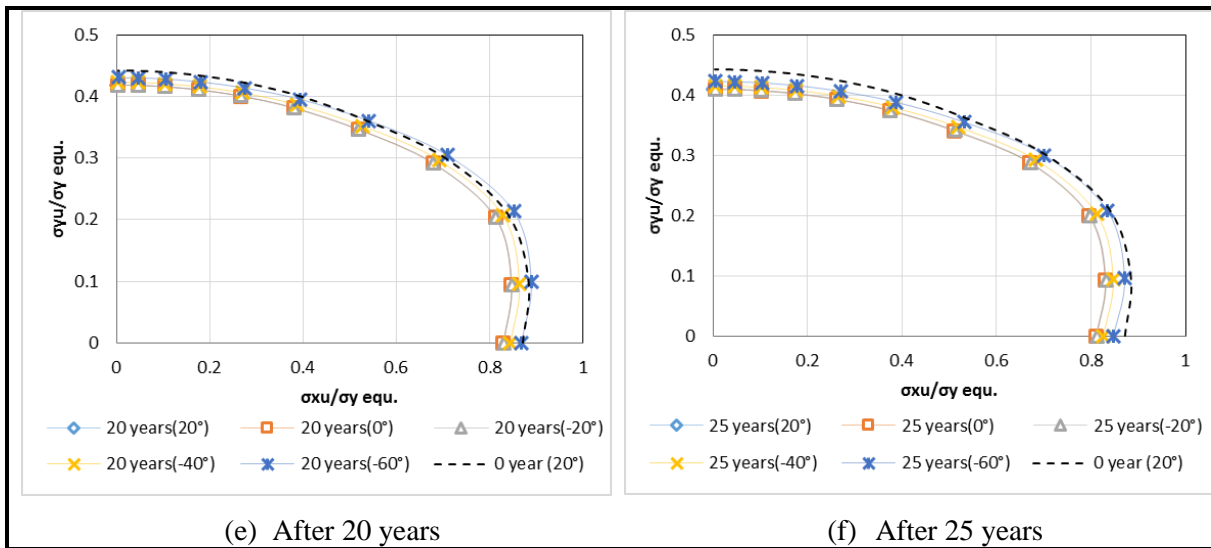
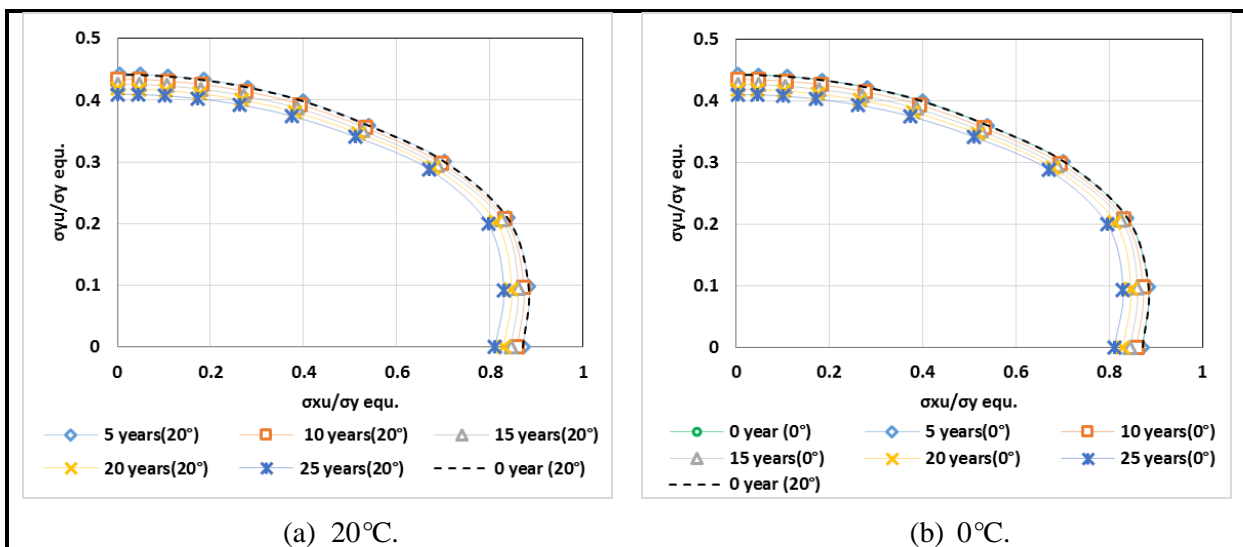


Fig. 4.14 Ratios of ultimate strength for different aged bottom plates with stiffener*2 (in ballast tank area) under low temperatures

b) Same temperature consideration for different aged plates

Compared with case 4, we can see the smooth curve in each case that have the same spacing between different ages considerations in Fig. 4.15.

In Fig. 4.15 (e) shows the ultimate strength ratio of 25 years condition is smaller than intact condition in x axis only, but it less than 10 years condition in y axis. That means the comparison of influence between ages and temperatures are different for x and y axis. Under -60°C that can compete with 20 years corrosion wastage in x axis, but only can provide the advantage of 15 years corrosion consideration in y axis.



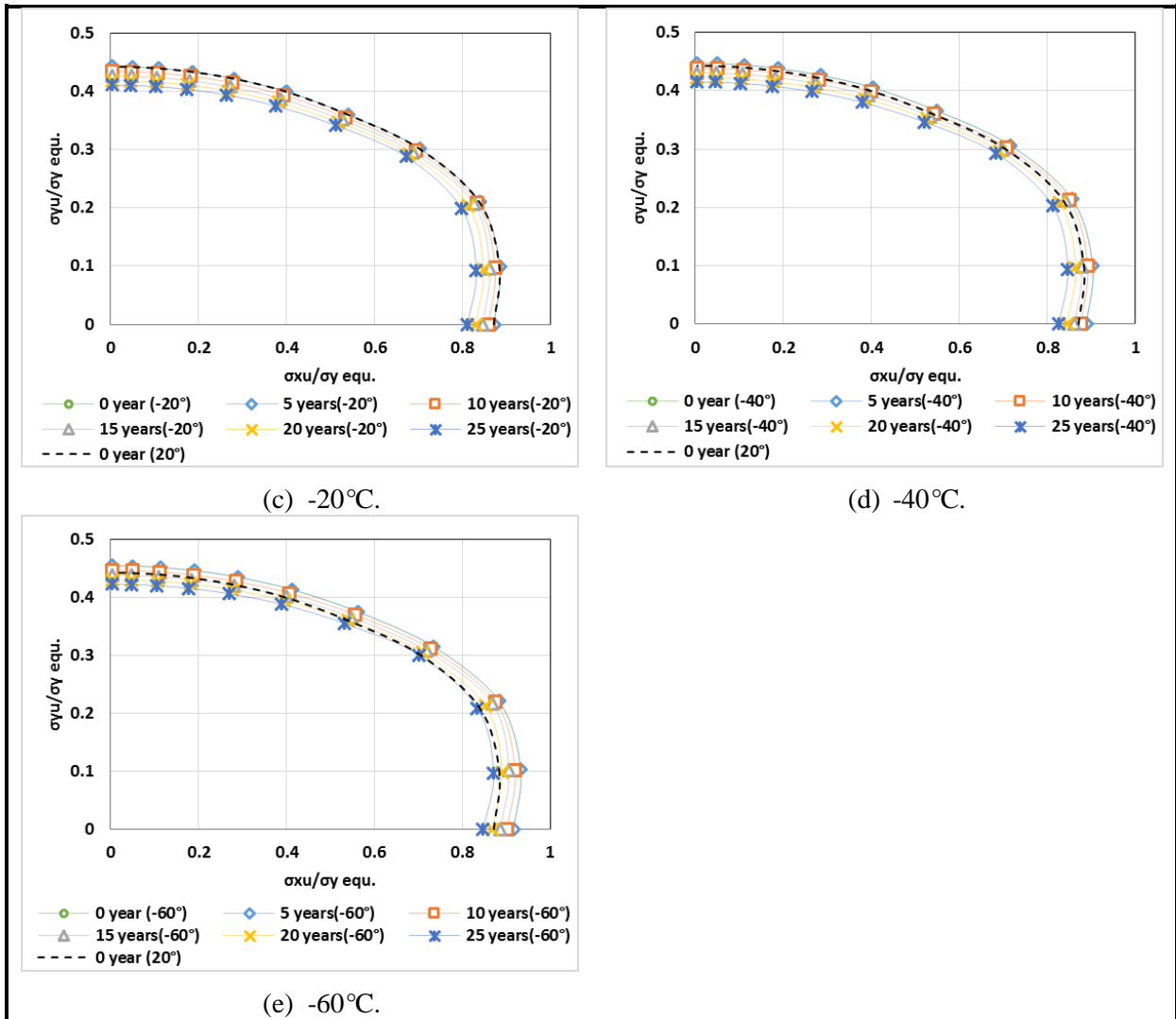
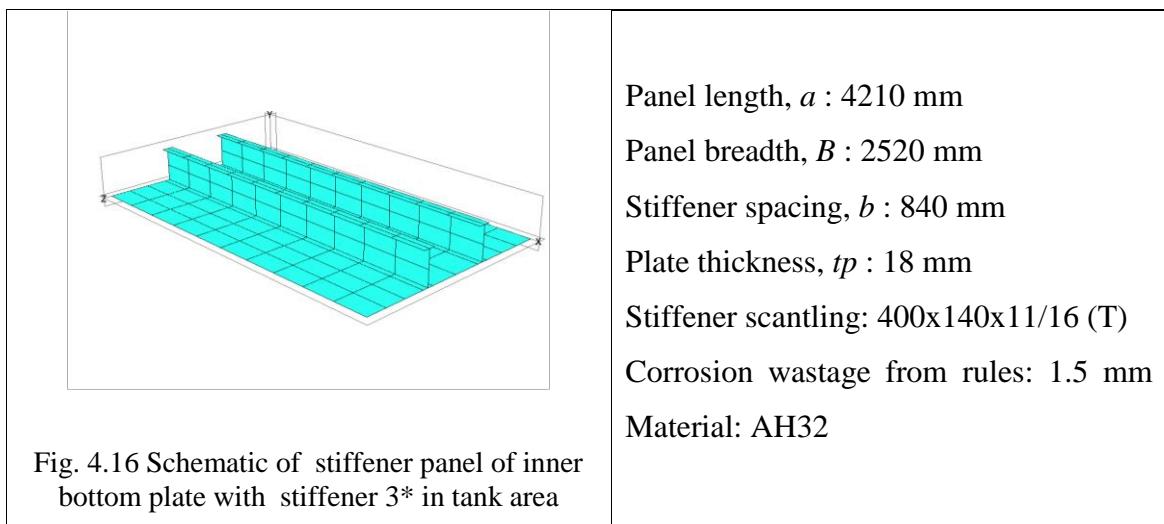


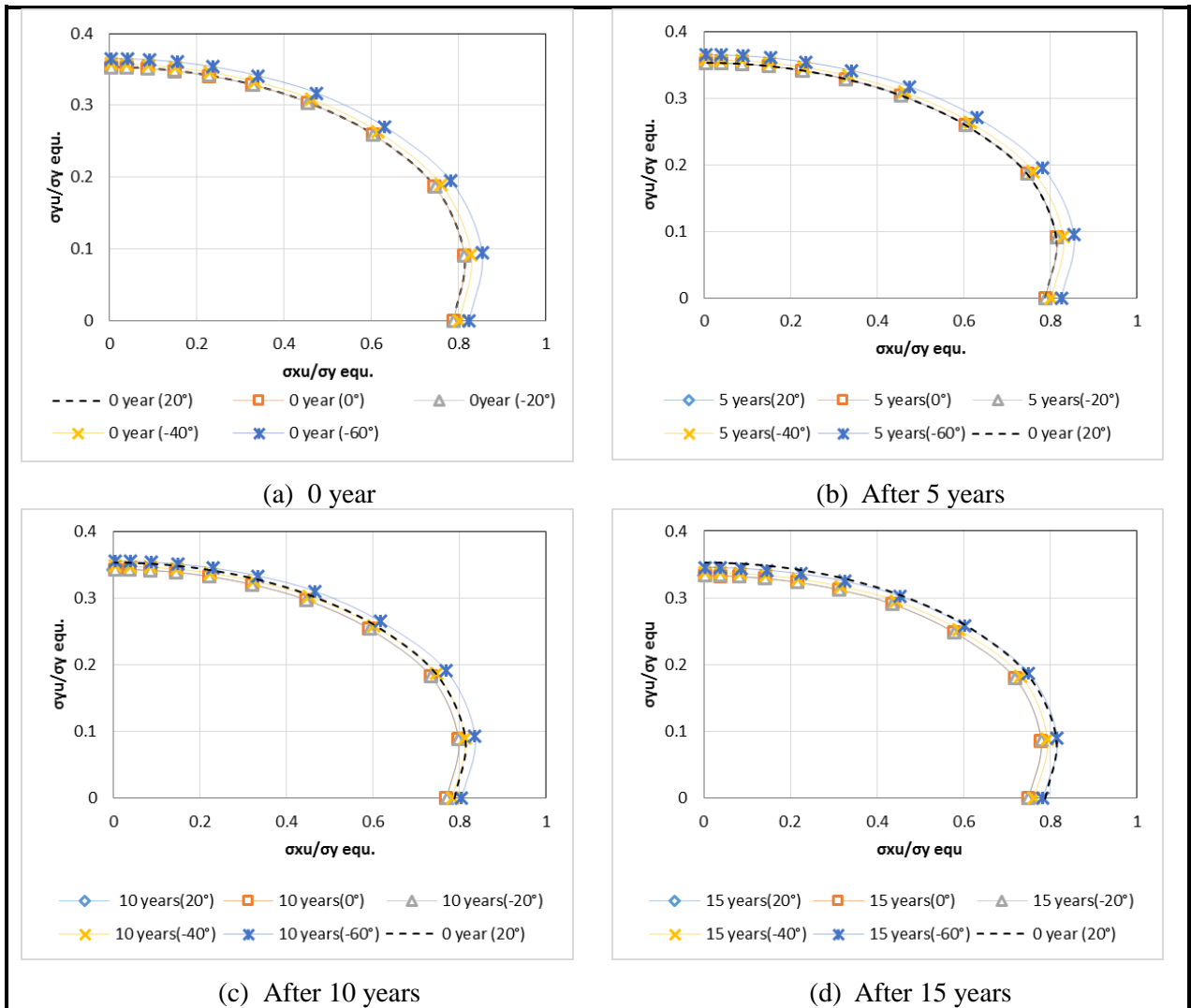
Fig. 4.15 Ratios of ultimate strength for bottom plates with stiffener*2 (ballast tank area) with same temperature consideration according to ages

Case 6: Inner bottom plate with stiffener 3* (ballast tank area)



a) Same aged plate under different temperatures

Similar with case 4 and case 5 but consider in inner bottom plate for case 6. From Fig. 4.17 (a) to (f), we can see the changes between temperature and corrosion wastage consideration by ages. In Fig. 4.17 (a) that intact performed the same tendency with 0°C and -20°C, but along with the ages increasing, the advantage provide by lower temperature is no longer exist. Until the Fig. 4.17 (f) that shows intact condition has higher ultimate strength than other cases which means the influence from corrosion wastage is much higher than temperature for inner bottom plate.



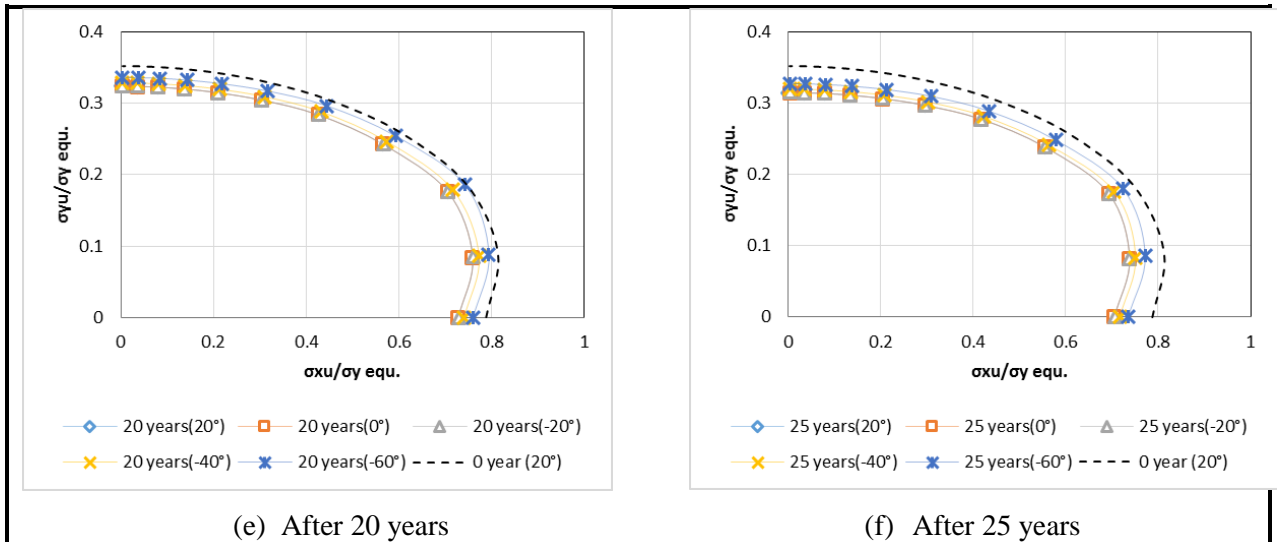
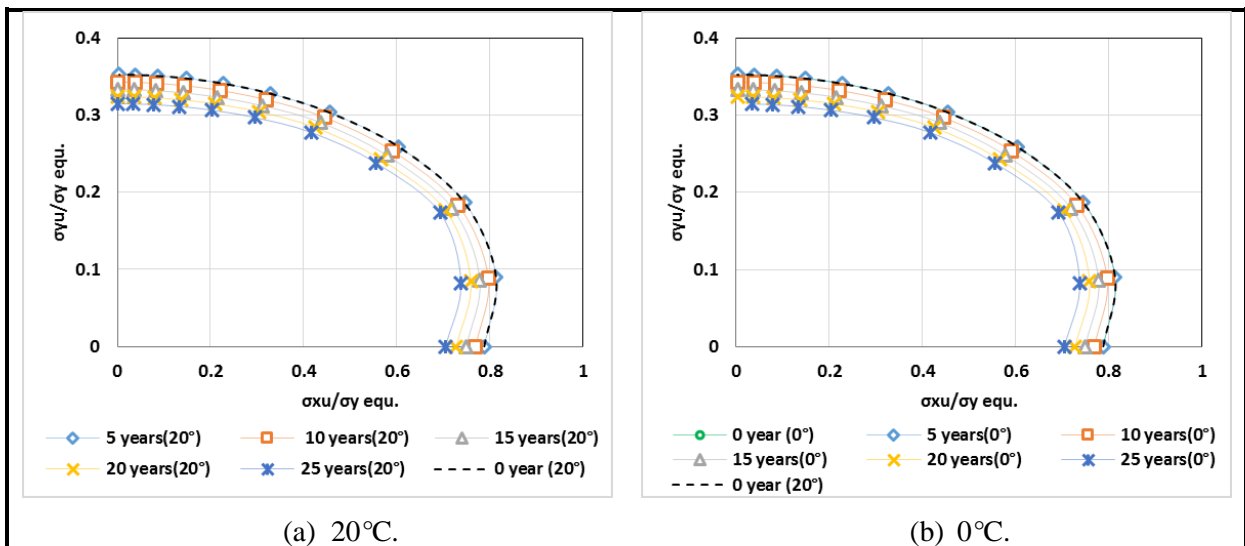


Fig. 4.17 Ratios of ultimate strength for different aged inner bottom plates with stiffener*3 (in ballast tank area) under low temperatures

b) Same temperature consideration for different aged plates

Fig. 4.18 represents the ultimate strength of inner bottom plate according to the changes of structure ages under same temperature consideration. From subfigure (a) to (c) that we can see the effect from corrosion wastage of each 5 years, and it cause the reducing ultimate strength of ratio in both x and y axis. From subfigure (d) to (e) that we can see the effect from temperatures which is effecting the ratio by increasing the yielding stress.



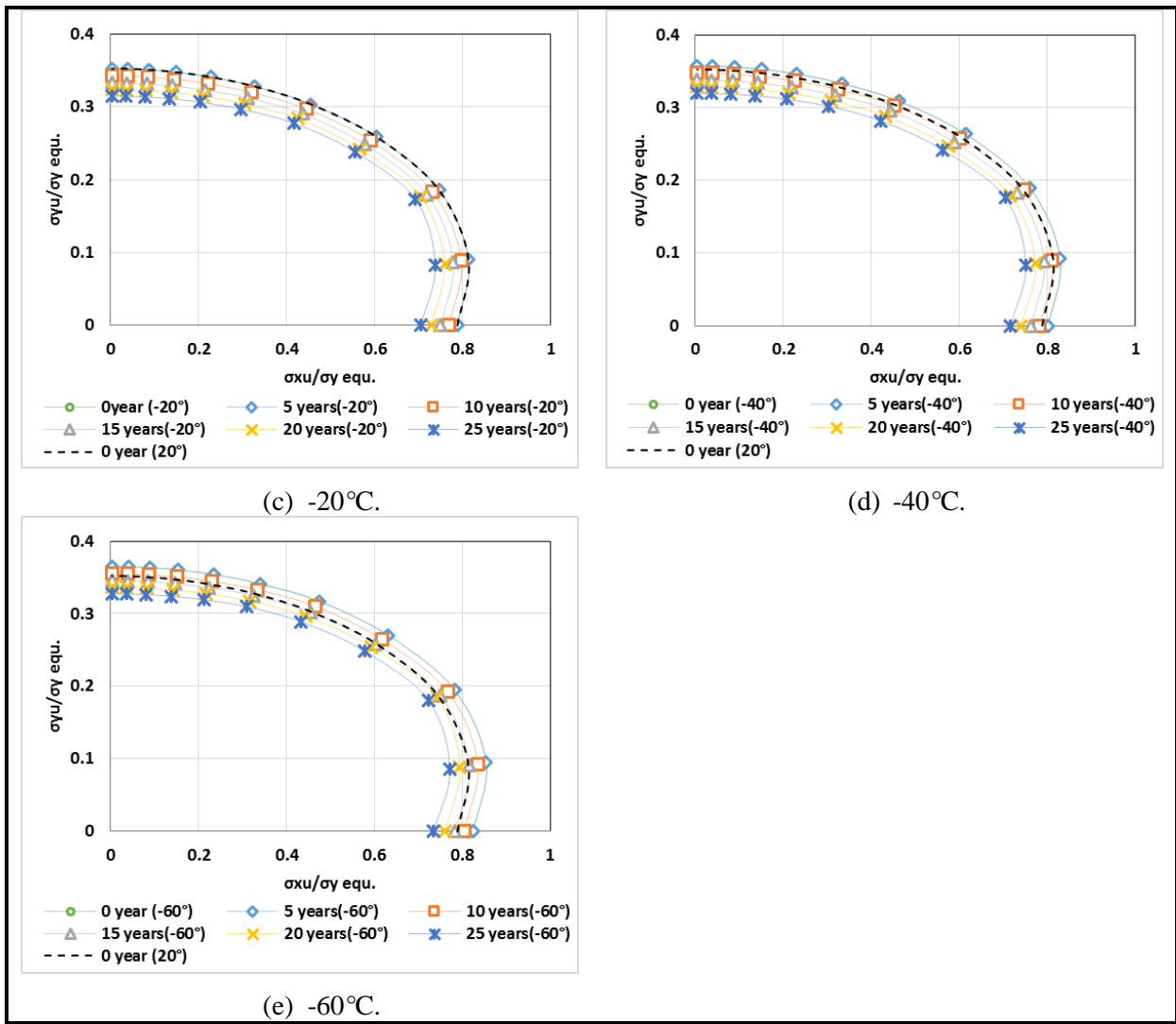
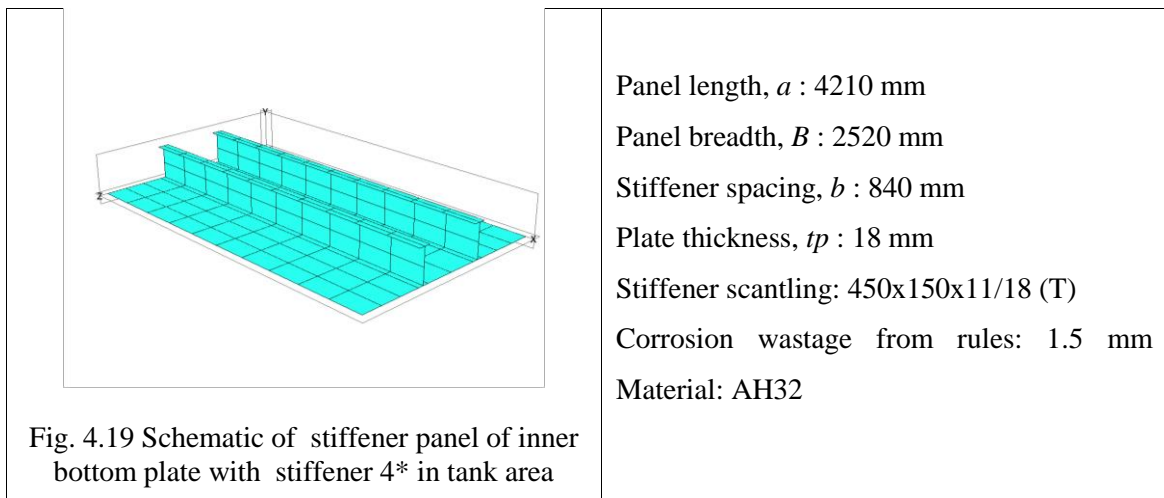


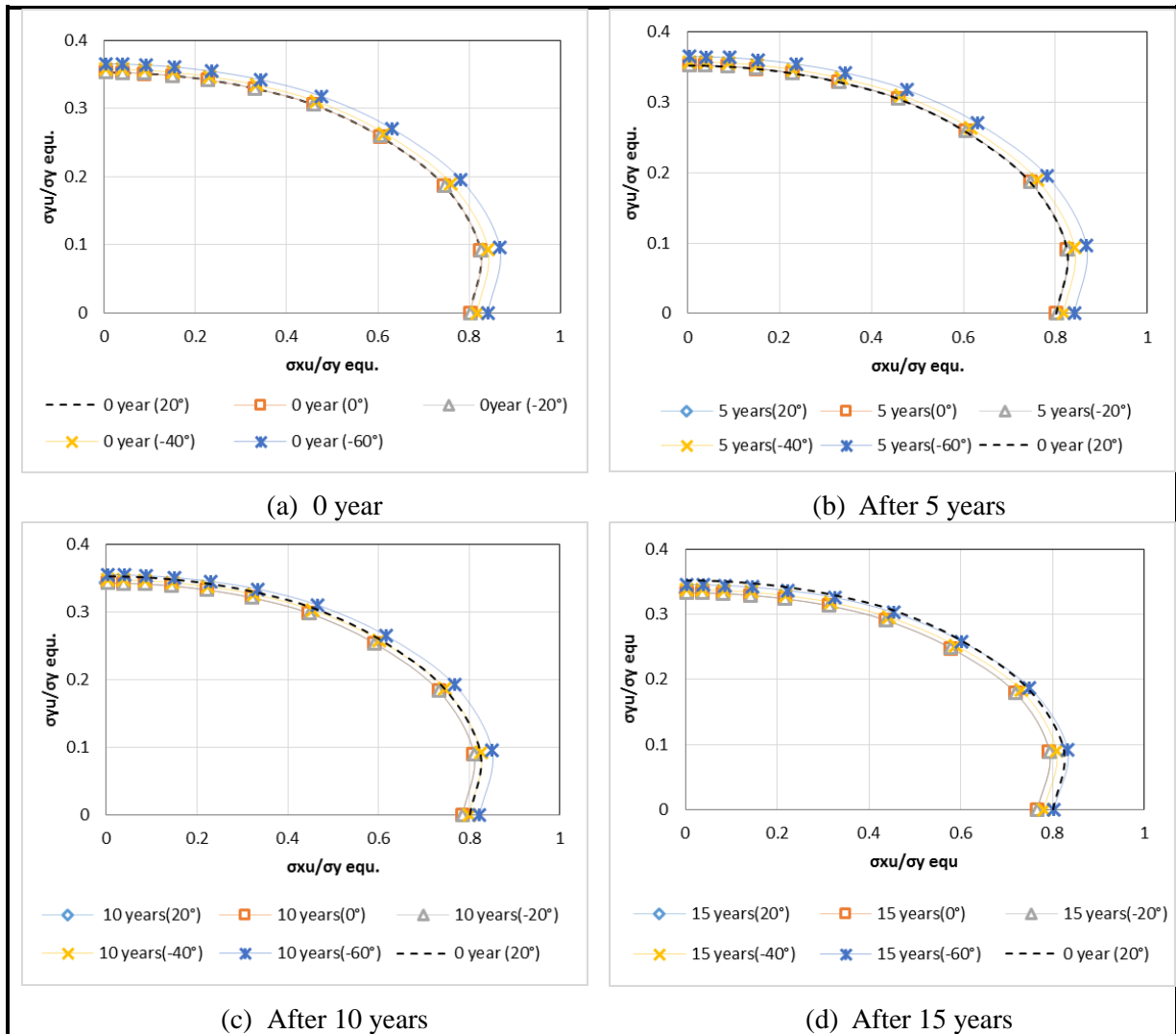
Fig. 4.18 Ratios of ultimate strength for inner bottom plates with stiffener*3 (ballast tank area) with same temperature consideration according to ages

Case 7: Inner bottom plate with stiffener 4* (ballast tank area)



a) Same aged plate under different temperatures

Similar result with case 6, we can see the tiny differences of the ultimate strength ratio increased in x axis in Fig. 4.20, and same tendency with all conditions of structure ages and temperatures with case 6. In Fig. 4.20 (d) that the curves of intact condition overlap with 15 years under -60 °C, but the ultimate strength decreased with the structure ages increased. Finally in sub figure (f), all the conditions curves are under intact one.



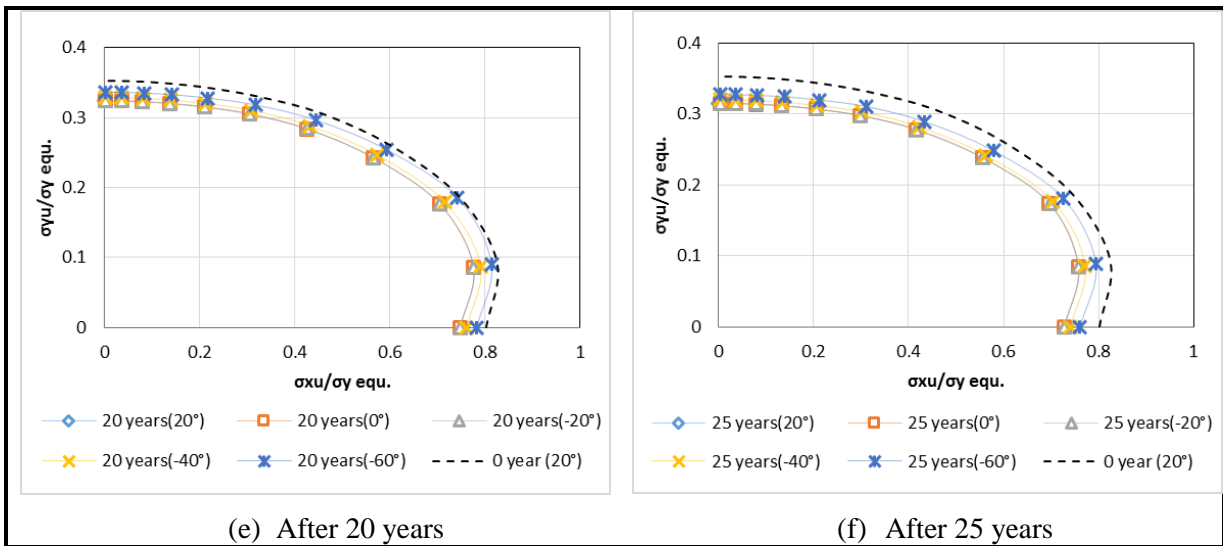
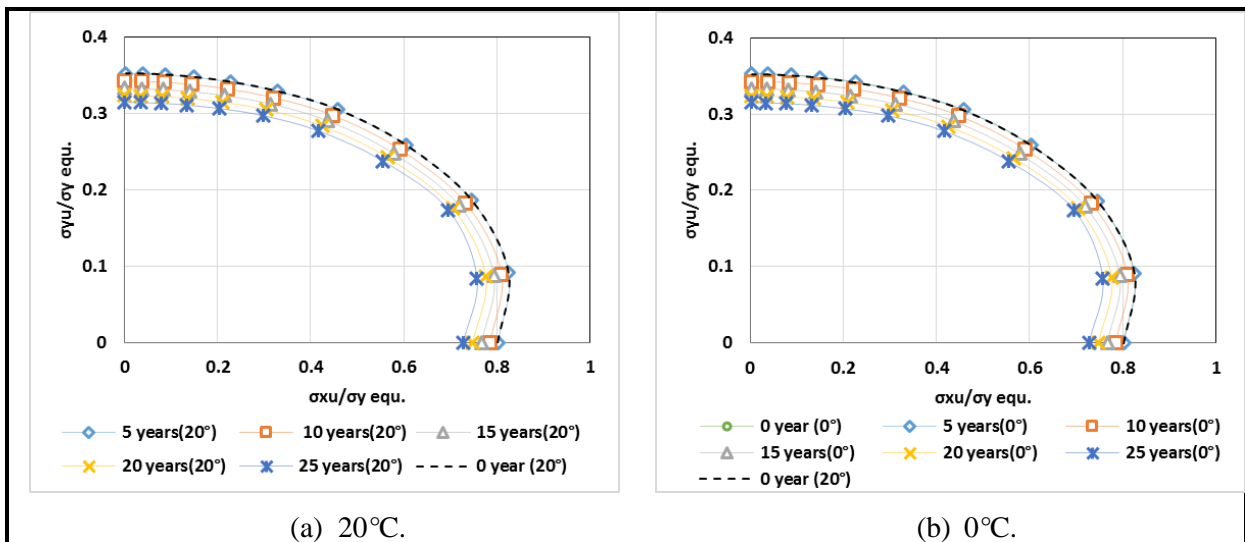


Fig. 4.20 Ratios of ultimate strength for different aged inner bottom plates with stiffener*4 (in ballast tank area) under low temperatures

b) Same temperature consideration for different aged plates

Fig. 4.21 shows the ratios of ultimate strength with same temperature consideration according to ages, and it could be found out the overlap curve of intact condition with 5 years under 20°C, 0°C, and -20°C conditions. In Fig. 4.21 (e) that the intact condition shows similar with 15 years with -60°C, that we could conclude the ultimate strength ratio have been effected more form ages.



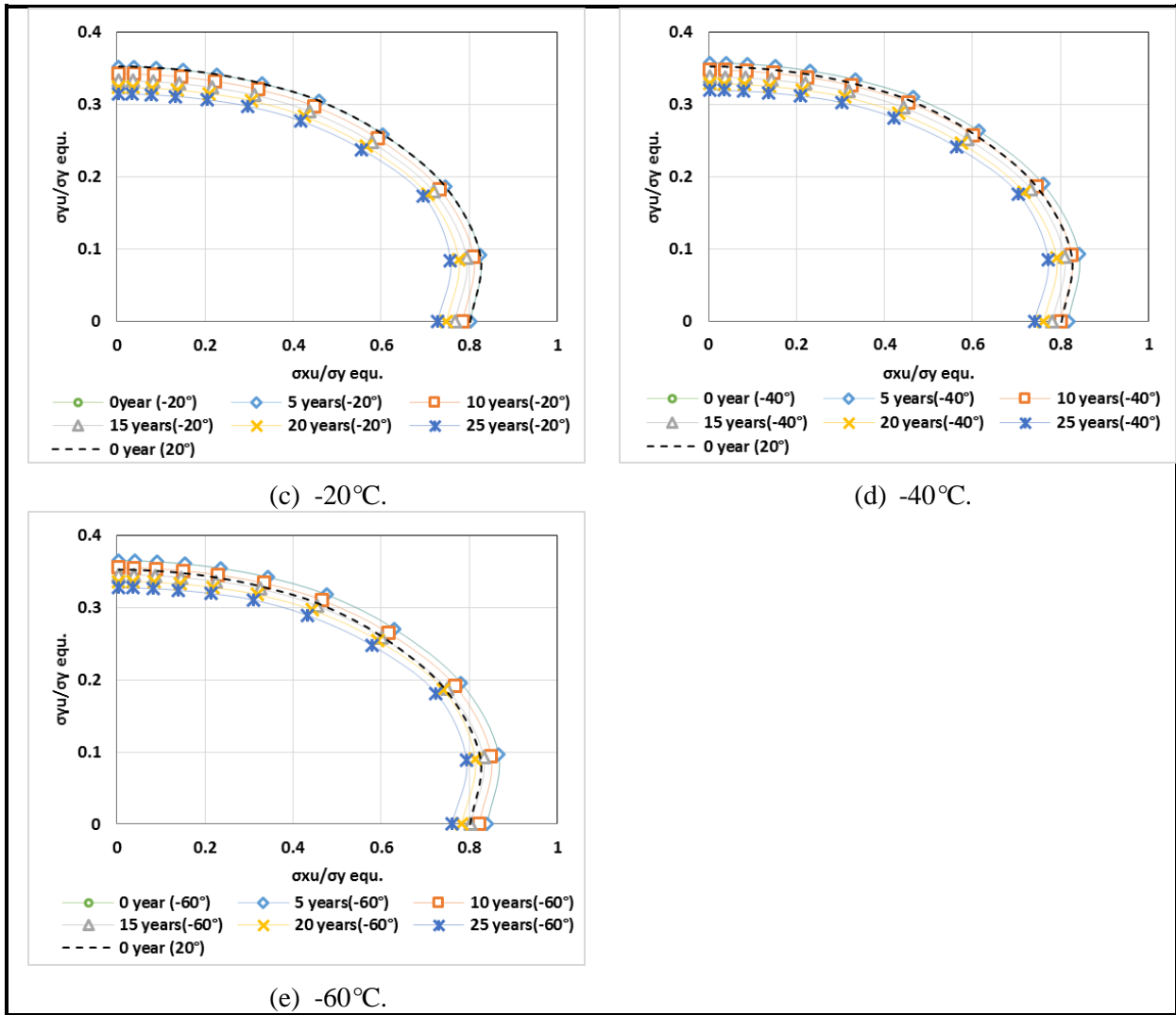


Fig. 4.21 Ratios of ultimate strength for inner bottom plates with stiffener*4 (ballast tank area) with same temperature consideration according to ages

4.1.2 DISCUSSION THE RESULTS FOR STIFFENER PANEL ANALYSIS

For each cases that we use the as-built condition with temperature 20°C which consider as the intact condition to compare with others. Form the result in 4.1.1 that we can see the tendency of the ratios from bending moment with the effect of both temperature and corrosion wastage effects. Therefore, we could separate the results into two parts which the stiffener is flat bar in first three cases and T bar stiffener in the last four cases.

It’s interesting to find out the different structure arrangement will have different results of ultimate strength. Such as case 1 that consider the upper deck which have the higher effect of ultimate strength than corrosion wastage. We could check the Fig. 4.3 (e) under -60°C that for all aged structures have higher ultimate ratio in both x and y axis than intact condition.

Besides, we thought case 2 and case 3 will have the similar results, but it's not. We find out the ultimate strength ratio will be higher in x axis according to the temperature decreasing; but in y axis it effect between temperature and corrosion. Therefore the ultimate strength ratio is similar with 15 years condition under -60°C .

For case 4 and case 5 that consider the same position with similar plate thickness but different supporting stiffener scantlings, which we can see in Fig. 4.12 (e) represent the overlap curve with 15years under -60°C in both x and y axis. Different from case 4, in Fig. 4.15 (e) shows the same value in y axis, but higher value in x axis. That means the increasing scantling did not help a lot in supporting y axial loads.

Different form case 4 and case 5, compared with Fig. 4.18 (e) and Fig. 4.21 (e) that show the similar value in x and y axis in both figures which represents the structure behaviour after loaded will not be the same due to the arrangement of plate thickness and stiffener scantlings.

For most of cases in this analysis results, we could simply conclude the temperature can bring higher ultimate strength, but when also considering the corrosion wastage after 15 years, the advantage provide by low temperature is less than the effect from corrosion deduction.

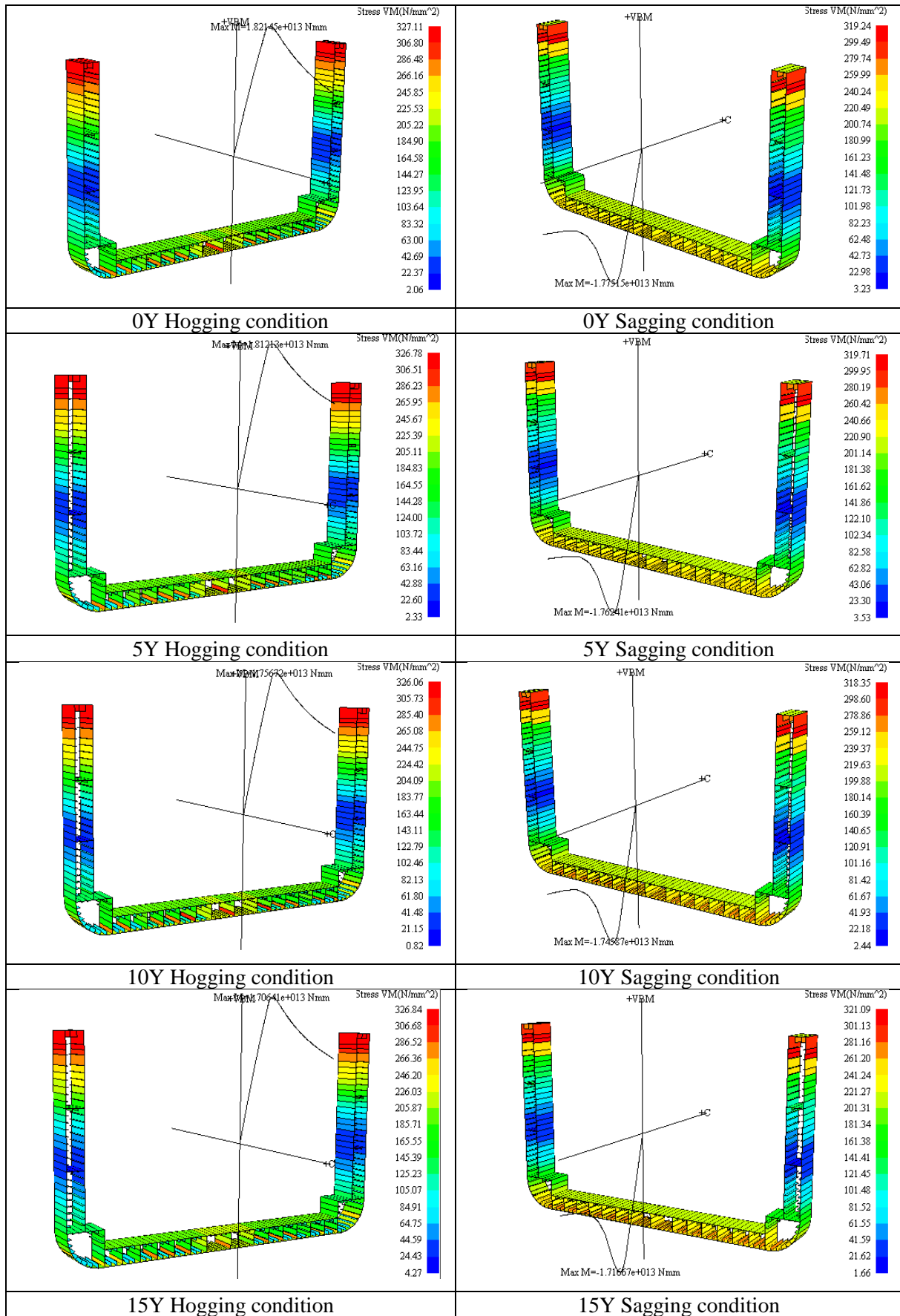
Therefore, the main issue of the effect of ultimate strength can be divided into two parts which are considering the ultimate strength effect under low temperature with corrosion wastage less than 15 years; other will be over 15 years. These results could be considered as the foundation for engineer to design the ship structure under low temperatures.

4.2 ULTIMATE STRENGTH OF HULL GIRDERS

In this section that we will evaluate the ultimate hull girder bending moment, and represent the Von Mises stresses distribution under hogging and sagging loads which can be discussed with the stiffened panel results, and observe the conclusion of the influence relation between the temperature and corrosion wastage.

4.2.1 ANALYSIS RESULTS FOR HULL GIRDERS

From the following Fig. 4.22 to Fig. 4.26 that we could find out the maximum value of vertical bending moment and Von Mises stress for both hogging and sagging conditions under aged consideration and low temperatures. It also represents the distribution of Von Mises stresses of hull structures.



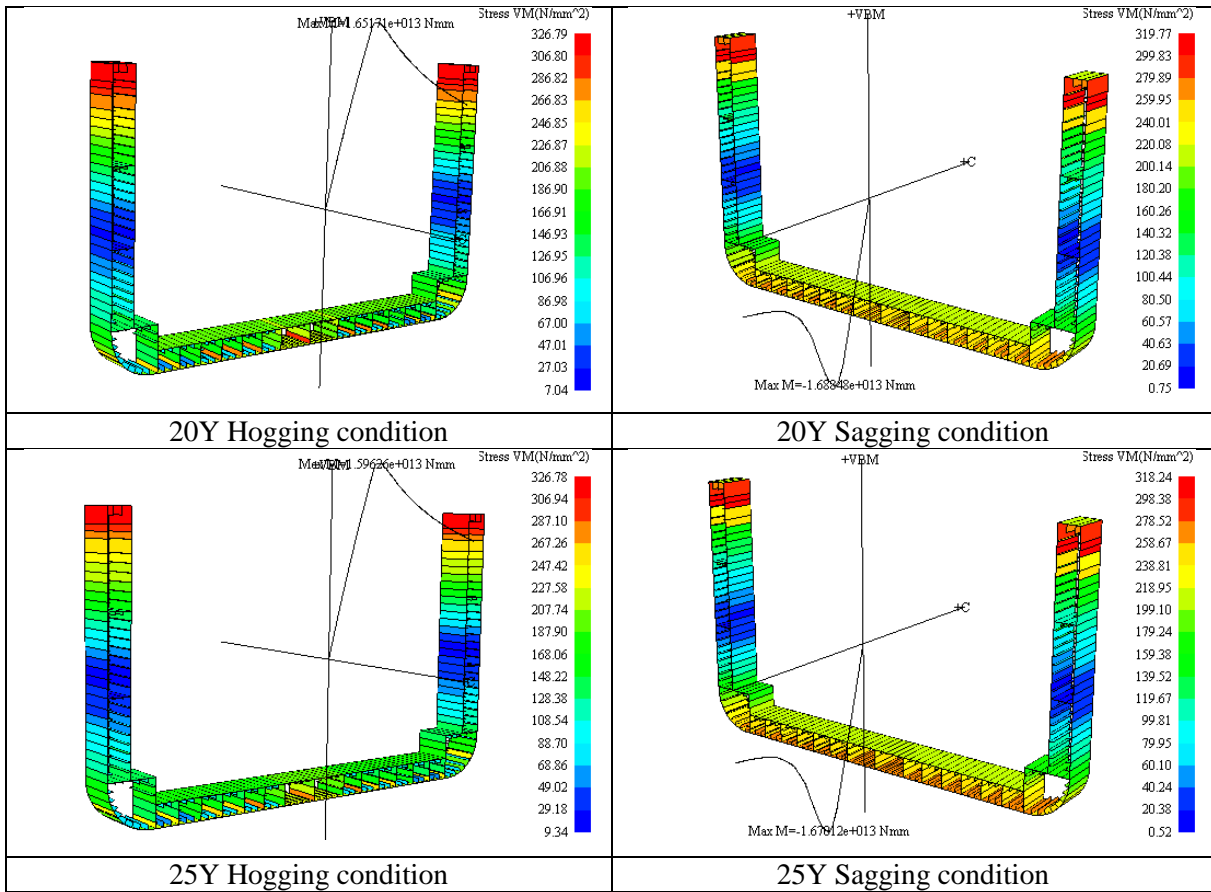
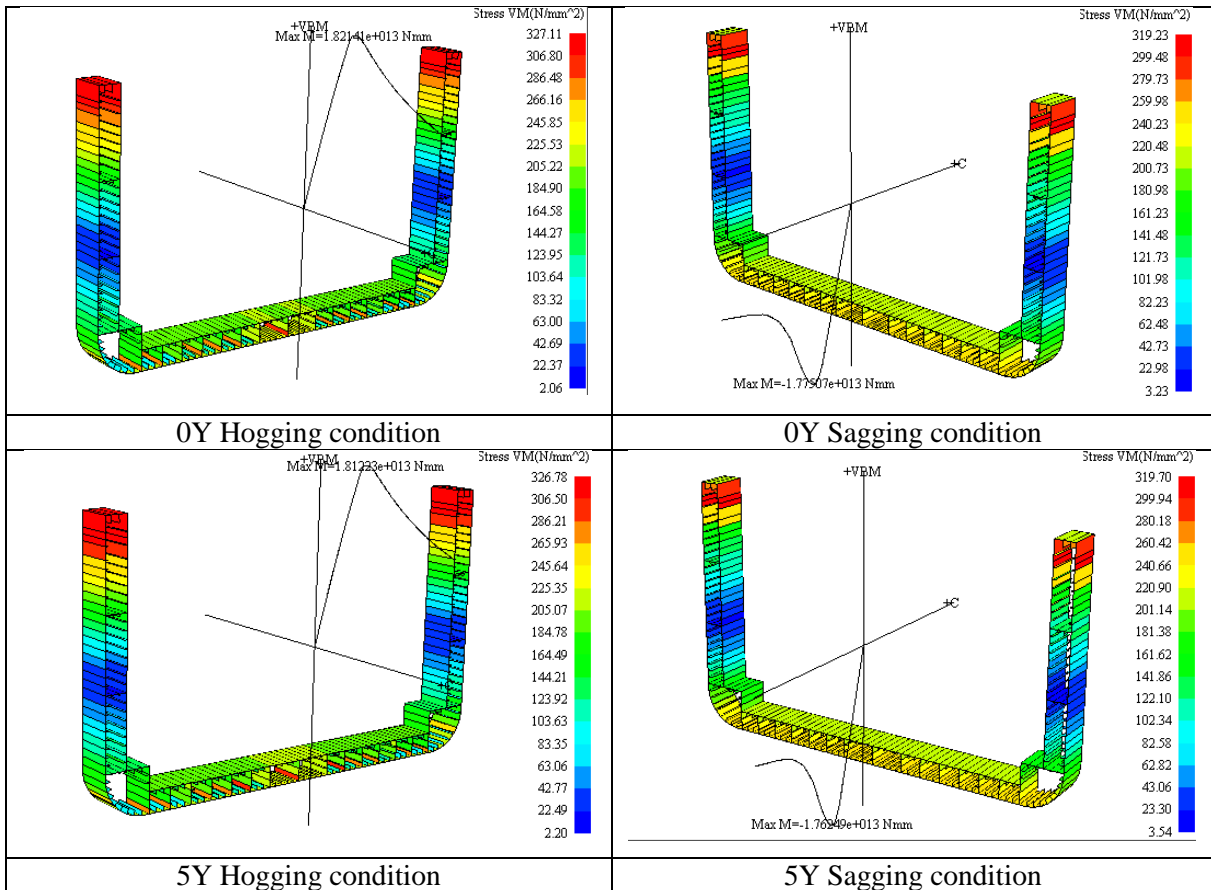


Fig. 4.22 Distribution of Von Mises stress for hogging and sagging conditions in each age consideration (20°C)



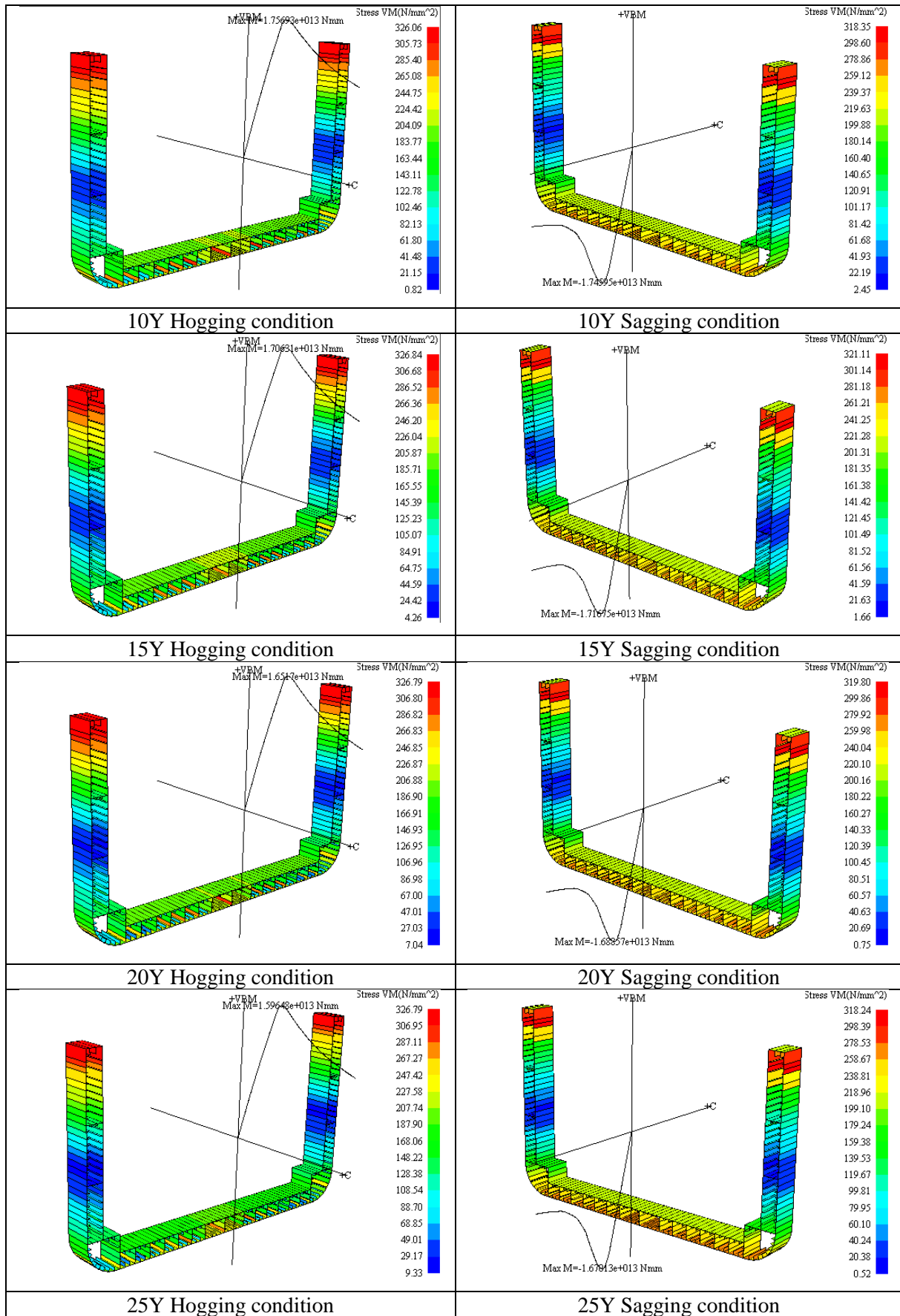
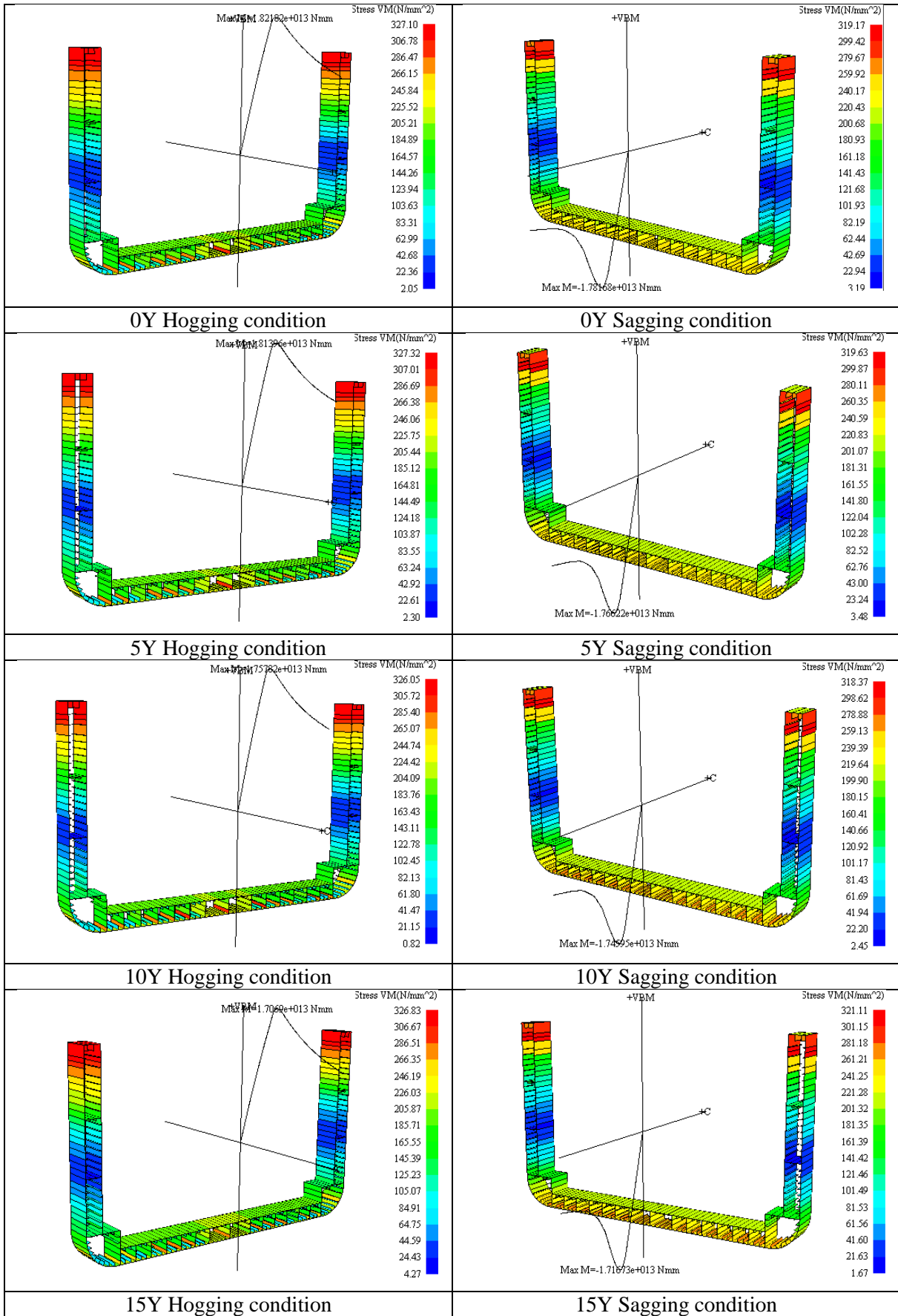


Fig. 4.23 Distribution of Von Mises stress for hogging and sagging conditions in each age consideration (0°C)



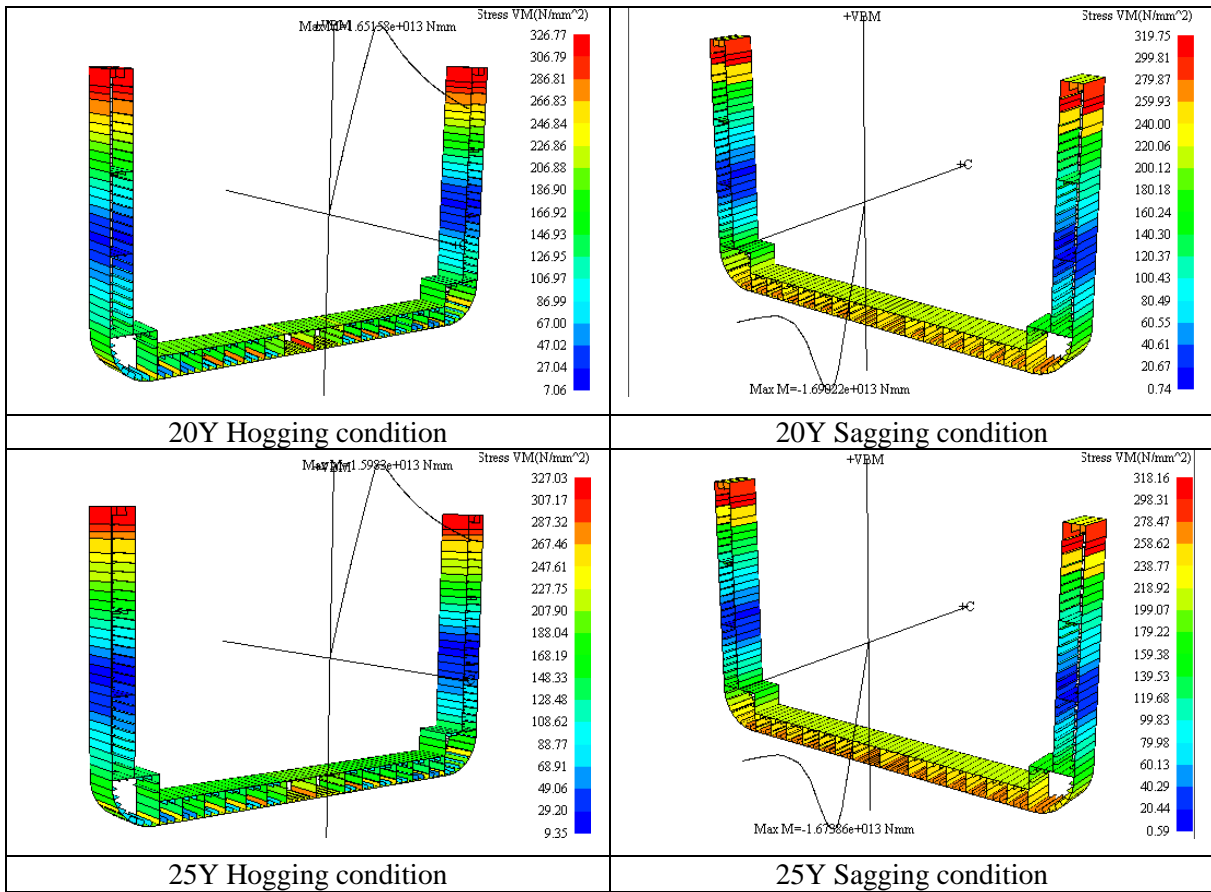
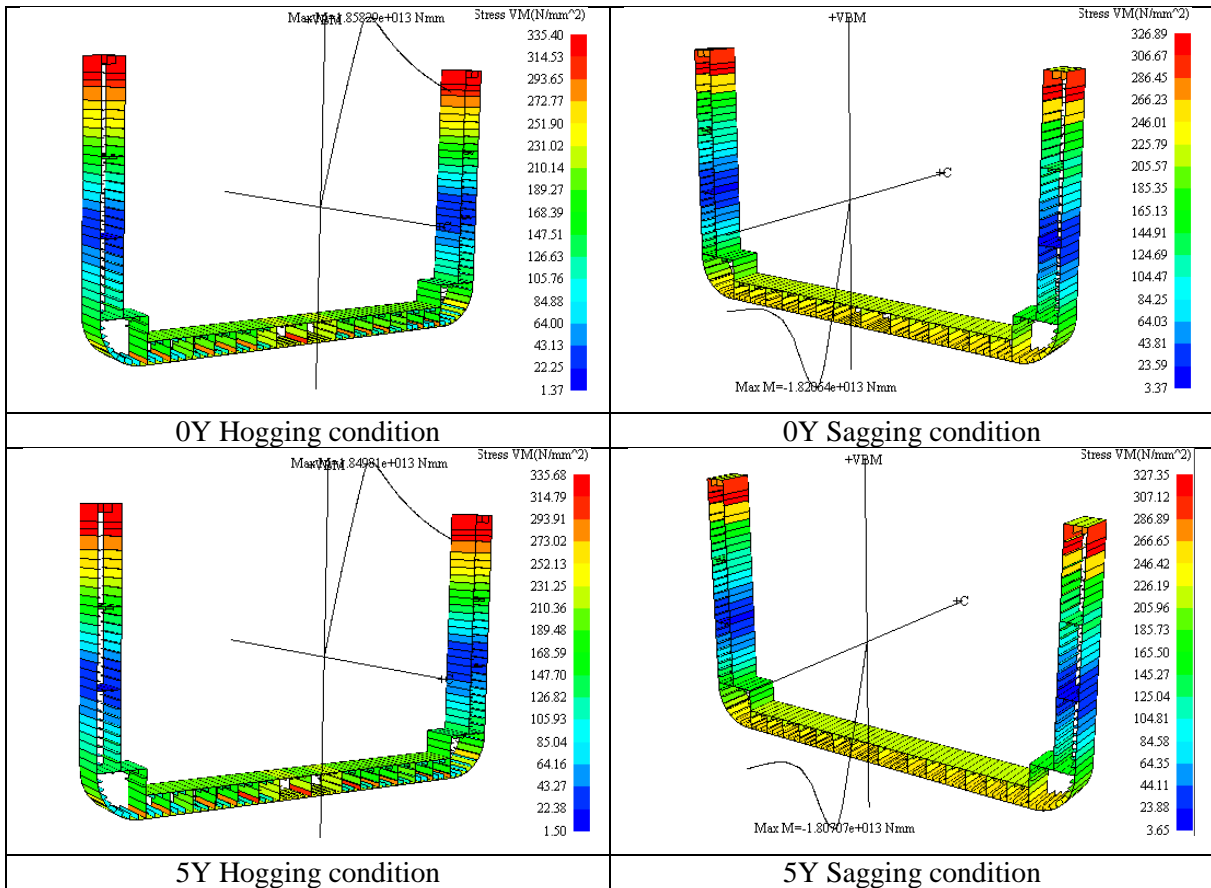


Fig. 4.24 Distribution of Von Mises stress for hogging and sagging conditions in each age consideration (-20°C)



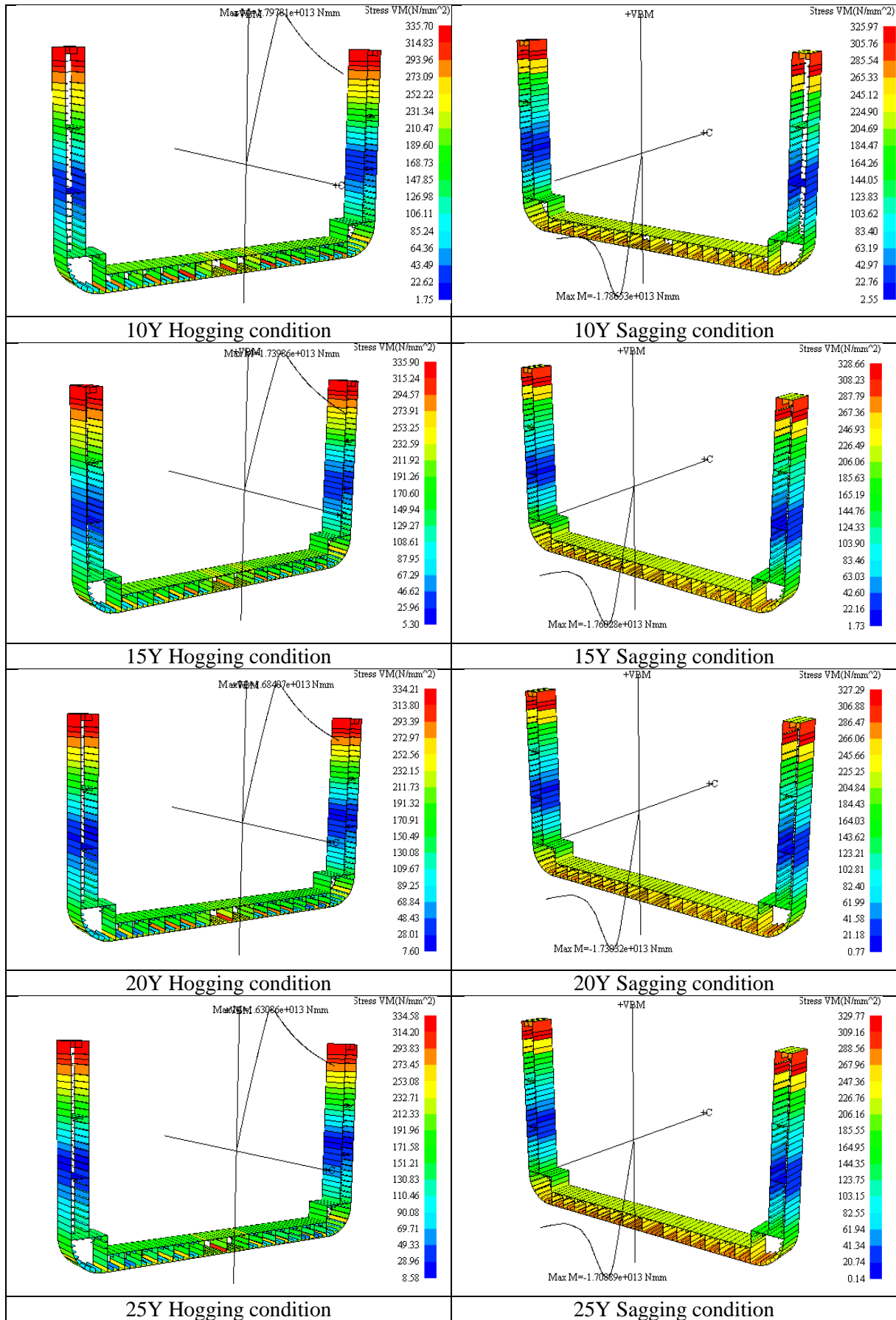
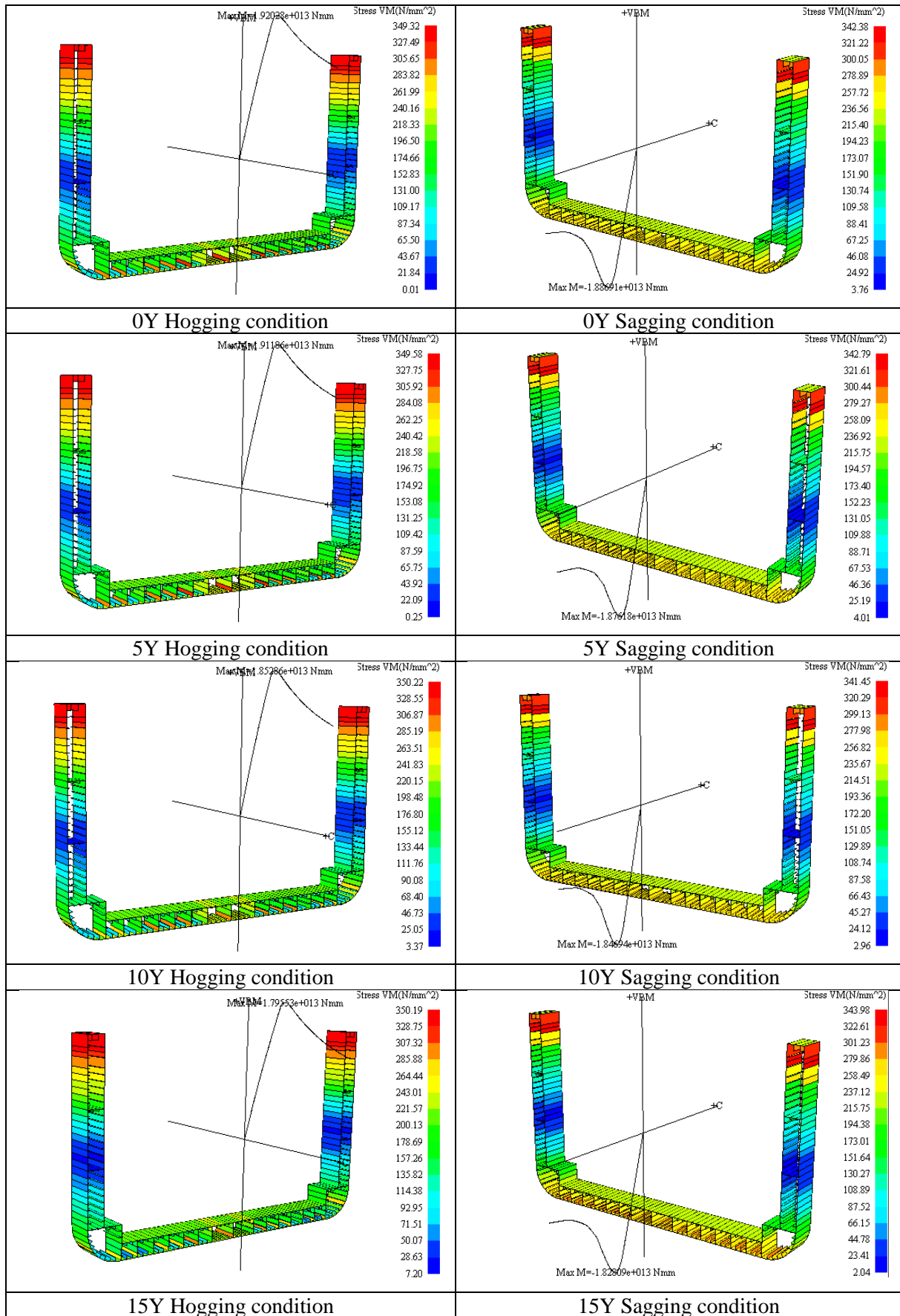


Fig. 4.25 Distribution of Von Mises stress for hogging and sagging conditions in each age consideration (-40°C)



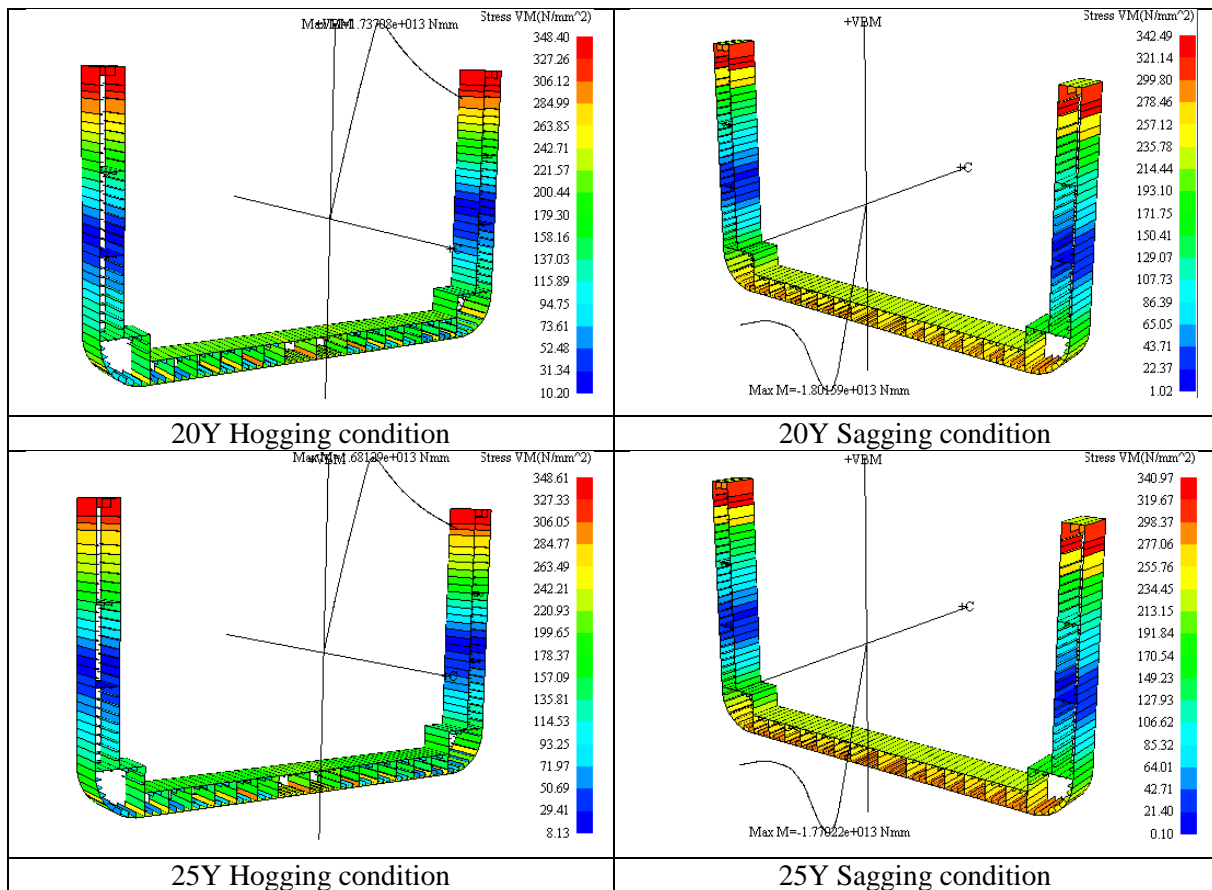
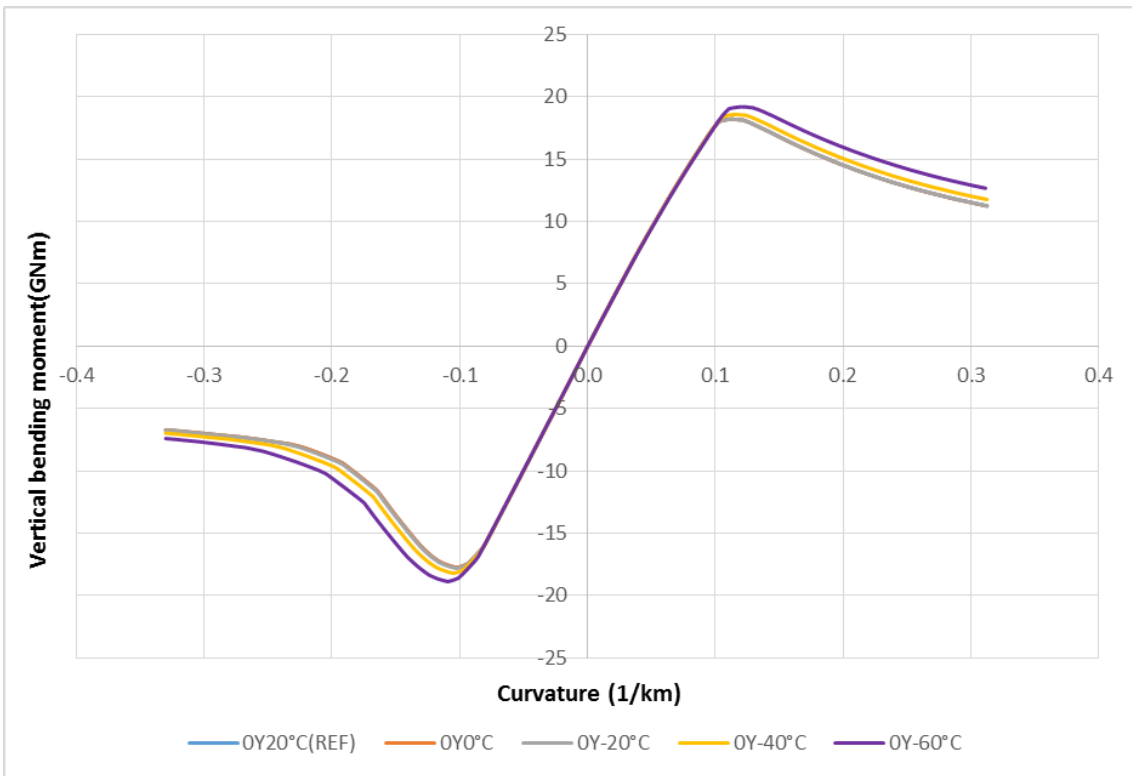


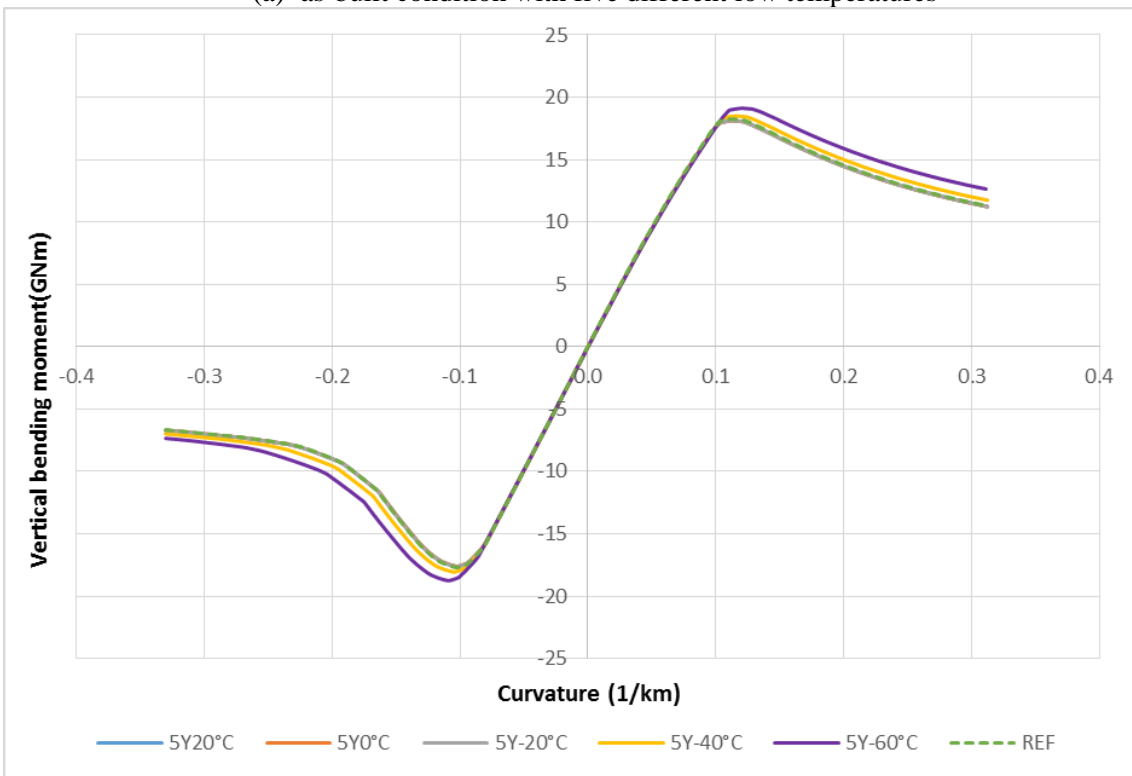
Fig. 4.26 Distribution of Von Mises stress for hogging and sagging conditions in each age consideration (-60°C)

The Fig. 4.27 represents the relations of analysis results between the curvature and vertical bending moments for 6 different age consideration under low temperatures, and the “ref” data is the condition of new established structures in room temperature 20°C which means without any corrosion deduction consideration. Fig. 4.27 (a) shows the only three lines with the overlap curve of 0Y20°C, 0Y0°C, and 0Y-20°C which similar in Fig. 4.27 (b) to (f).

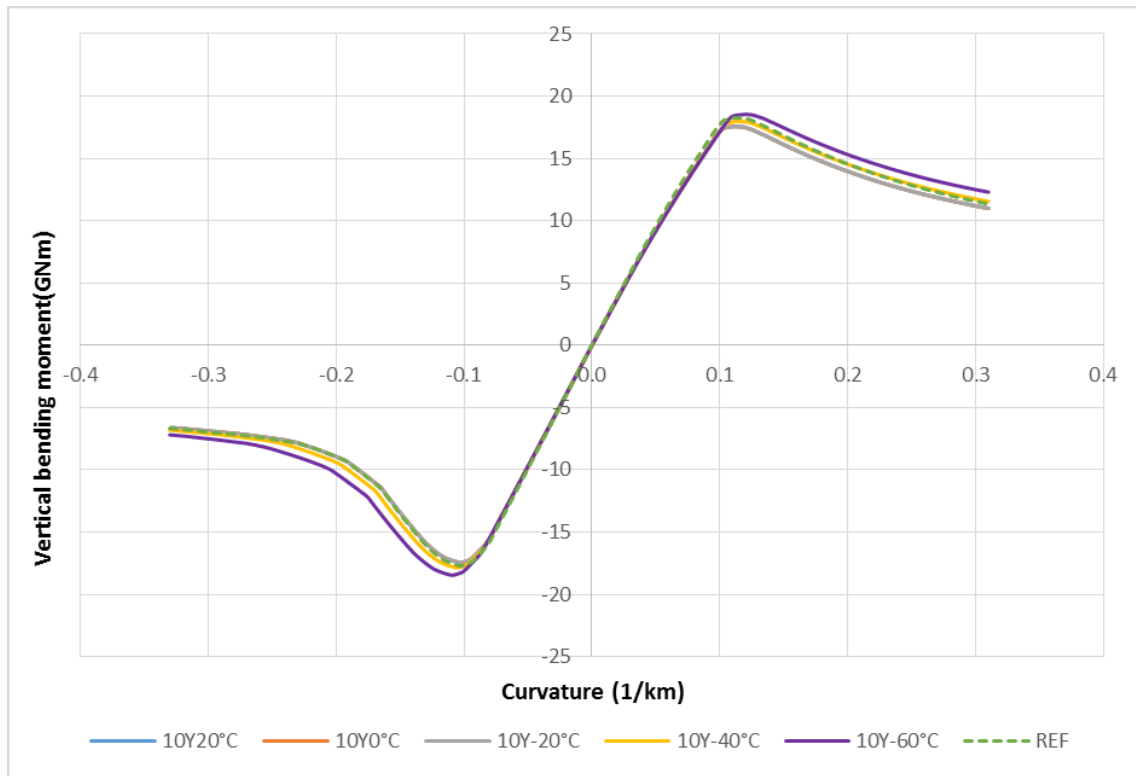
Generally, all the aged conditions that represent the same tendency when the temperature in 0°C, 20°C (RT), and -20°C. On the other hand, the difference can be found between -40°C and -60°C clearly, and the lowest temperature has the highest vertical bending moment as expected. When looking up the Fig. 4.27 (d) which is 15 years aged structures that the curvature of -60°C is not the highest one compared to intact condition of as-built structures with room temperature 20°C. In other words, the majority of ultimate strength effect changes from the yielding stress of material (low temperature) to corrosion deductions after 15 years.



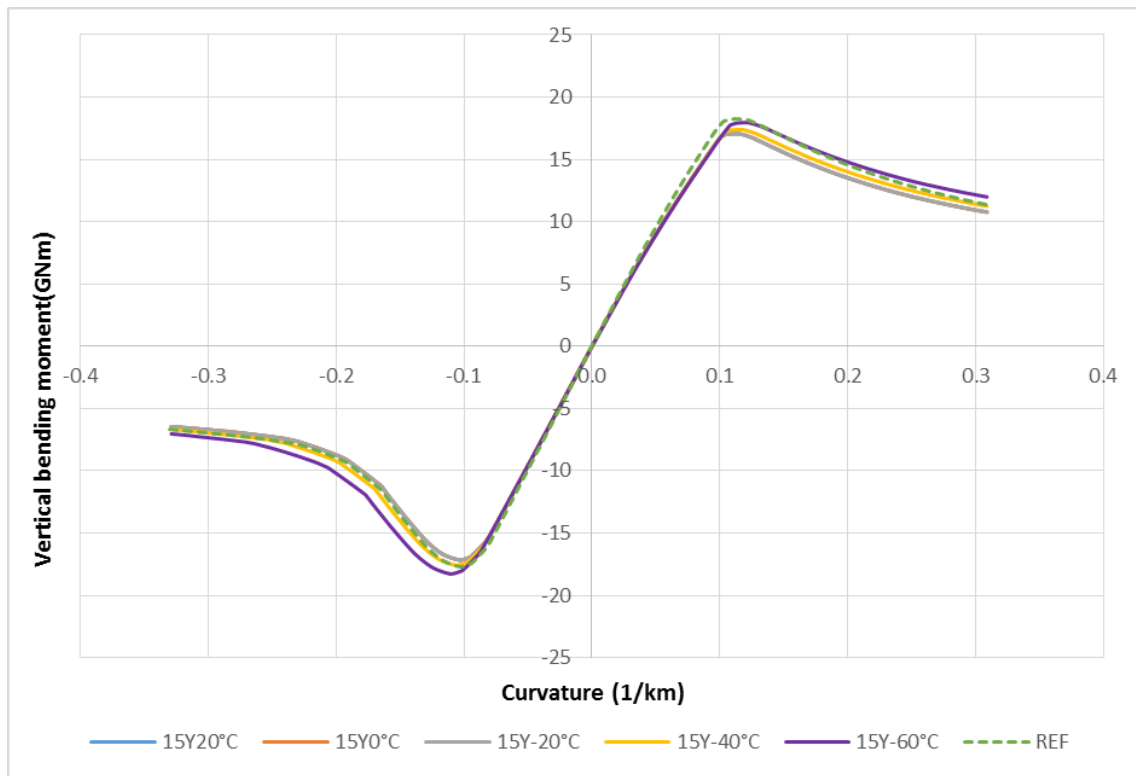
(a) as-built condition with five different low temperatures



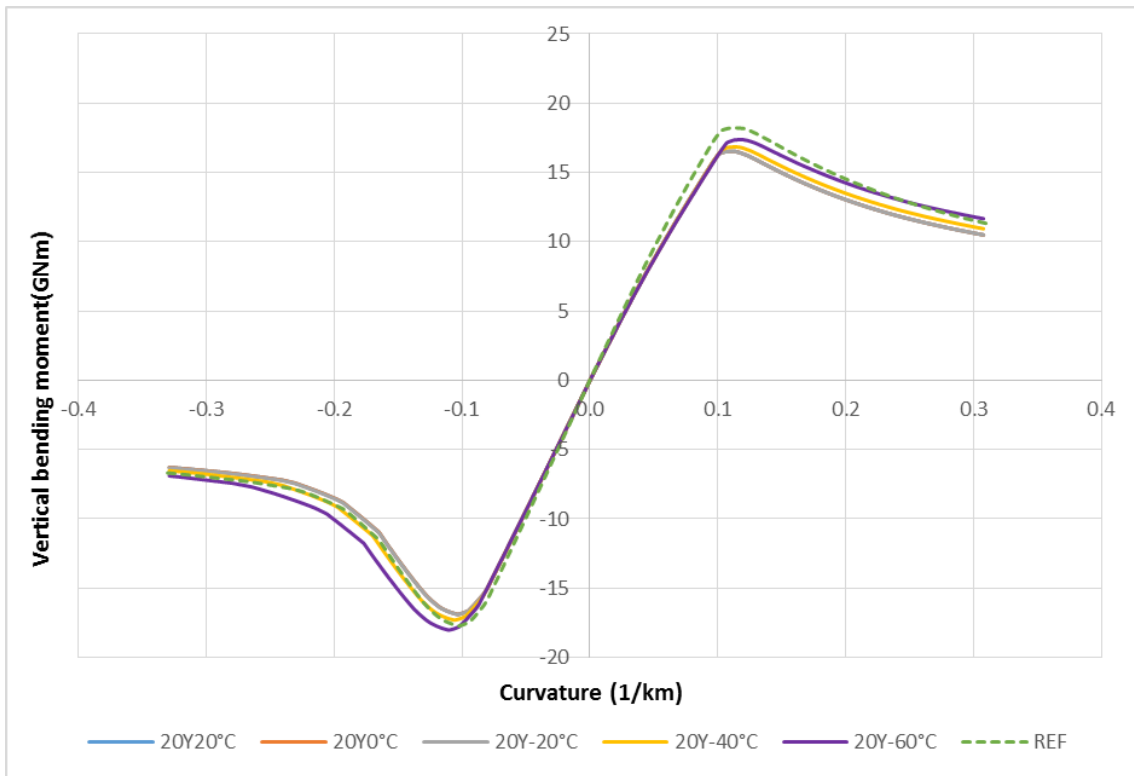
(b) 5 years condition with five different low temperatures



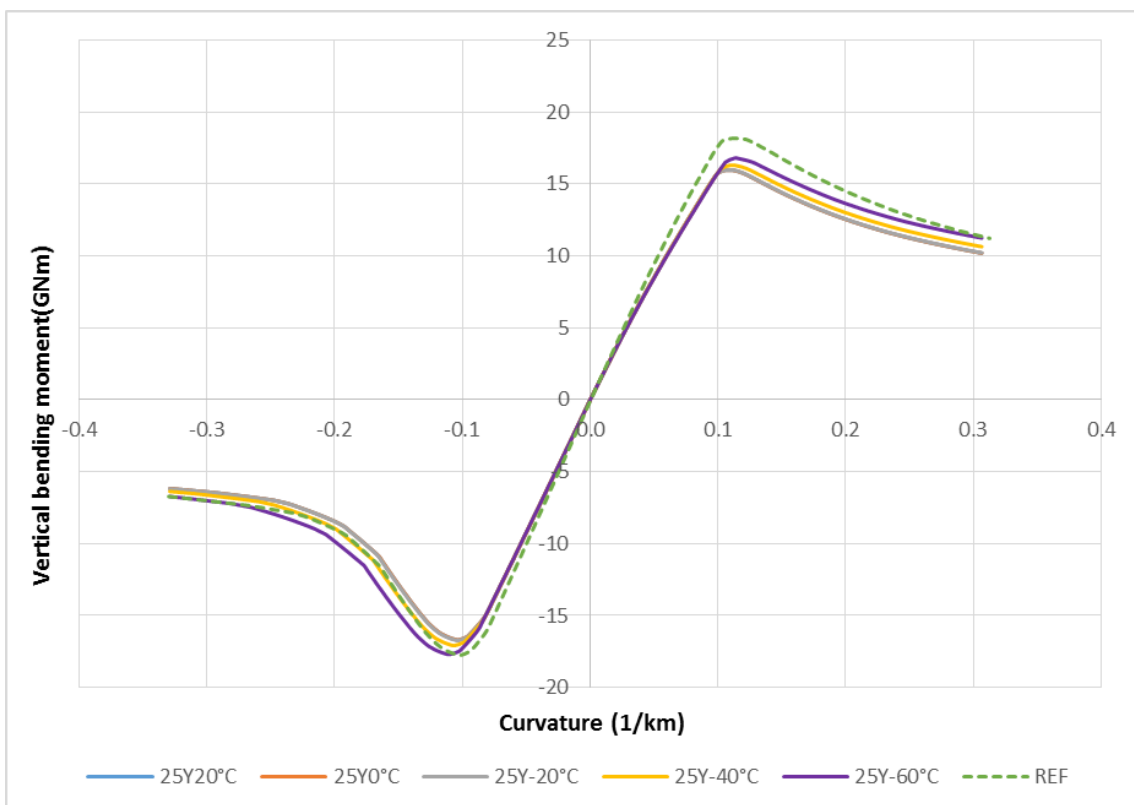
(c) 10 years condition with five different low temperatures



(d) 15 years condition with five different low temperatures



(e) 20 years condition with five different low temperatures



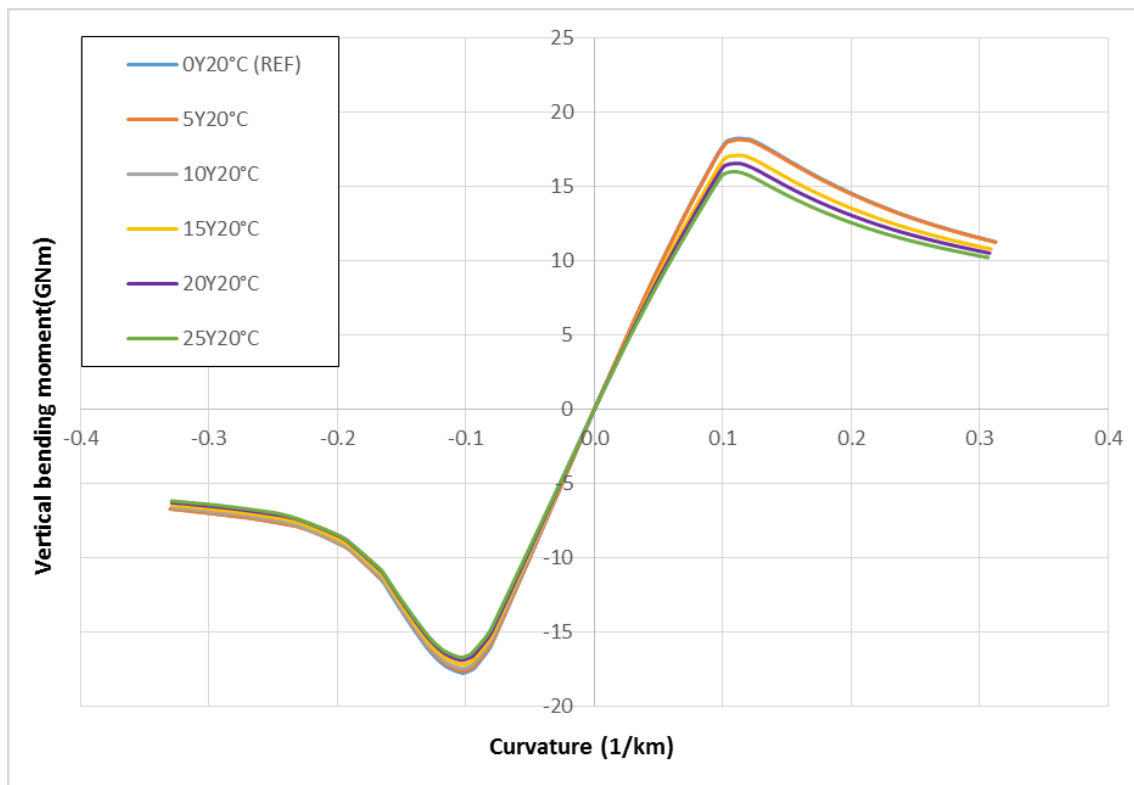
(f) 25 years condition with five different low temperatures

Fig. 4.27 Ultimate hull girder longitudinal strength with different low temperatures and same age consideration under vertical bending moment

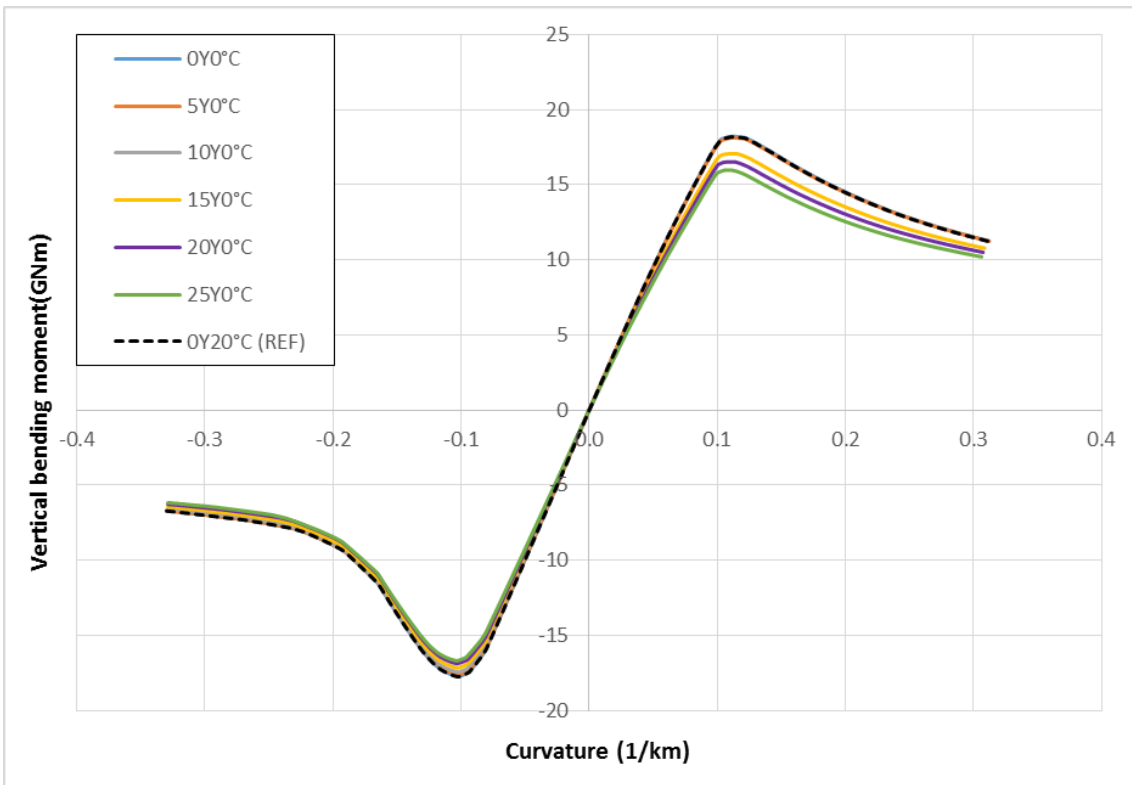
From Fig. 4.28 (a) to Fig. 4.28 (f) that show the overlap lines of 0Y, 5Y, and 10Y cases.

In subfigure (a) that we can find out the 0Y, 5Y, and 10Y case almost in the same line with intact condition, and then are 15Y, 20Y, and 25Y in order. We could see the same tendency in Fig. 4.28 (b) and (c).

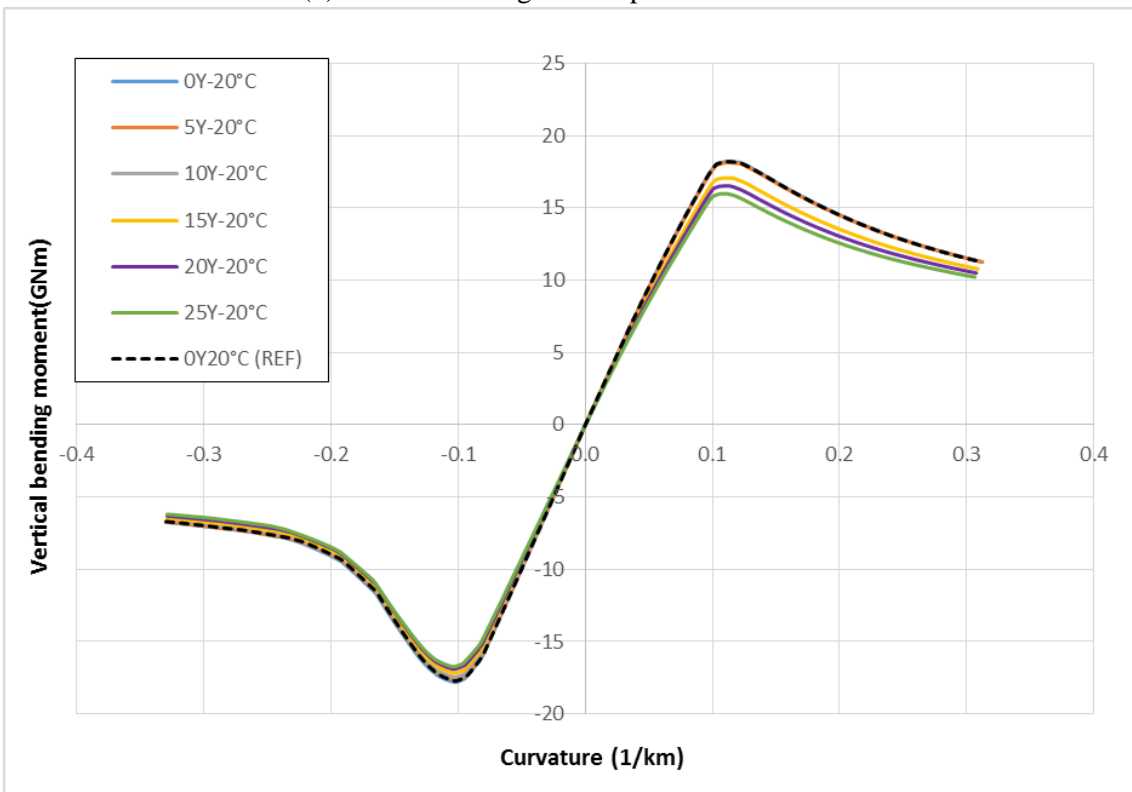
When the temperature decreasing, we could find out all the cases in Fig. 4.28 (d) and (e) increasing compared with intact condition. Which means the majority of ultimate strength for hull girder structures is from corrosion deductions not the yielding stress of material (low temperature).



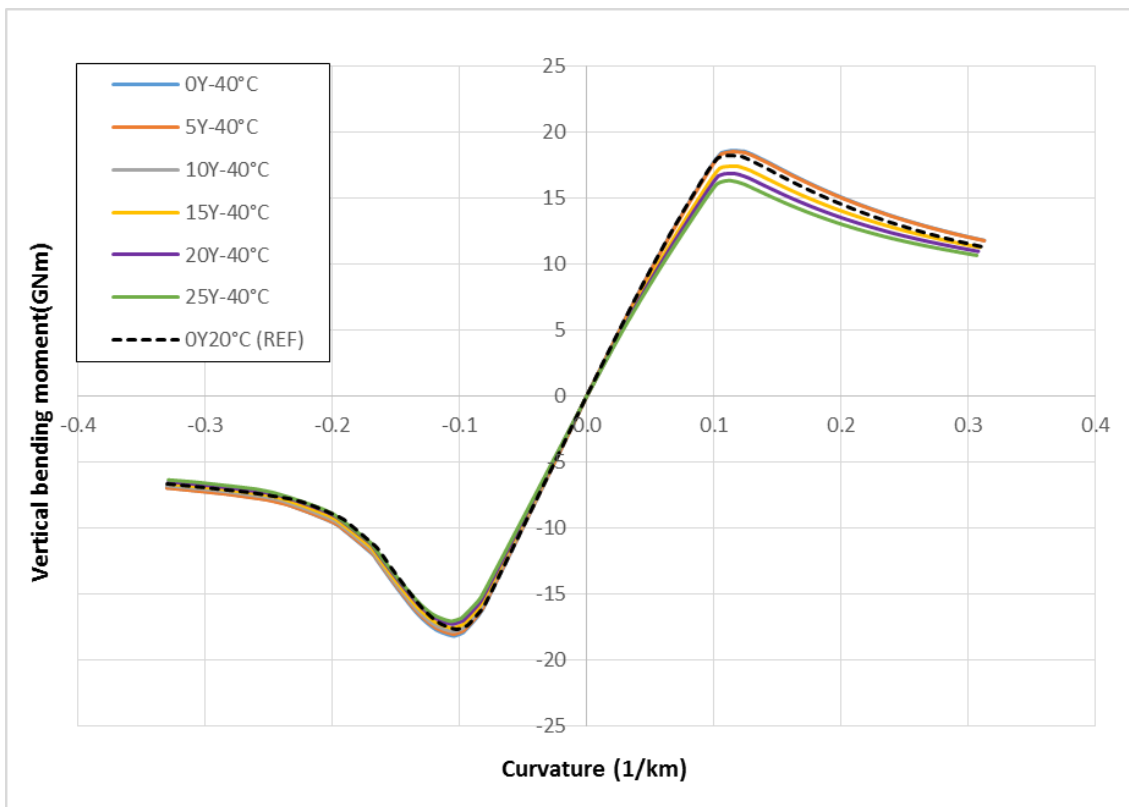
(a) Six different ages of ship structures under room temperature (20°C)



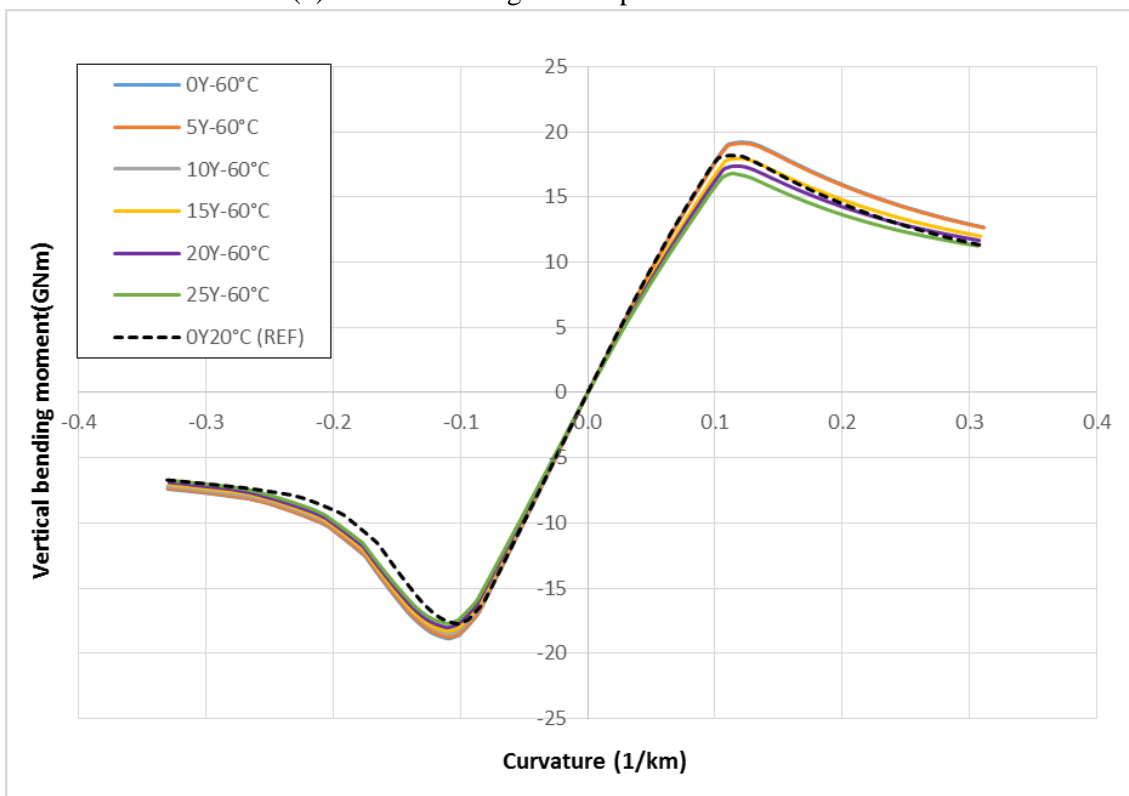
(b) Six different ages of ship structures under 0°C



(c) Six different ages of ship structures under -20°C



(d) Six different ages of ship structures under -40°C



(e) Six different ages of ship structures under -60°C

Fig. 4.28 Ultimate hull girder longitudinal strength with different structure ages with same temperature consideration under vertical bending moment

4.2.2 DISCUSSION THE RESULTS FOR HULL GIRDERS ANALYSIS

The ratio in the figures from Fig. 4.29 to Fig. 4.30 which are the bending moment ratio of each case/ the intact condition as equation below. To put it more simply, in the equation (9) that M_u is the vertical bending moment of ultimate strength for each case and the numerator is the intact condition which is as-built structures with room temperature 20°C.

$$Ratio = \frac{M_u}{M_{uo(as-built)}} \tag{9}$$

The Fig. 4.29 and Fig. 4.30 present the differences of bending moment ratio of both hogging and sagging conditions under different temperatures. In temperature 20°C, 0°C and -20°C for hogging conditions that show the similar value of bending moment ratio. The alternative is the cases of -40°C and -60°C which can be found out the diversity easily.

As the same results in sagging conditions, there are minor differences between temperature 20°C, 0°C and -20°C but -40°C and -60°C cases that we can see it alternatively.

To summarize, it compared the interaction between corrosion wastage and increase of yielding stress. Which the result of bending moment ratio show the linear trend related to the assumption of corrosion wastage and the differences between temperatures are in the same trend of yielding ratios. The detailed of the minor differences can be checked in the table of summary. In that case, it can be known the hypothesis of material and corrosion wastage are related to obtain the different results.

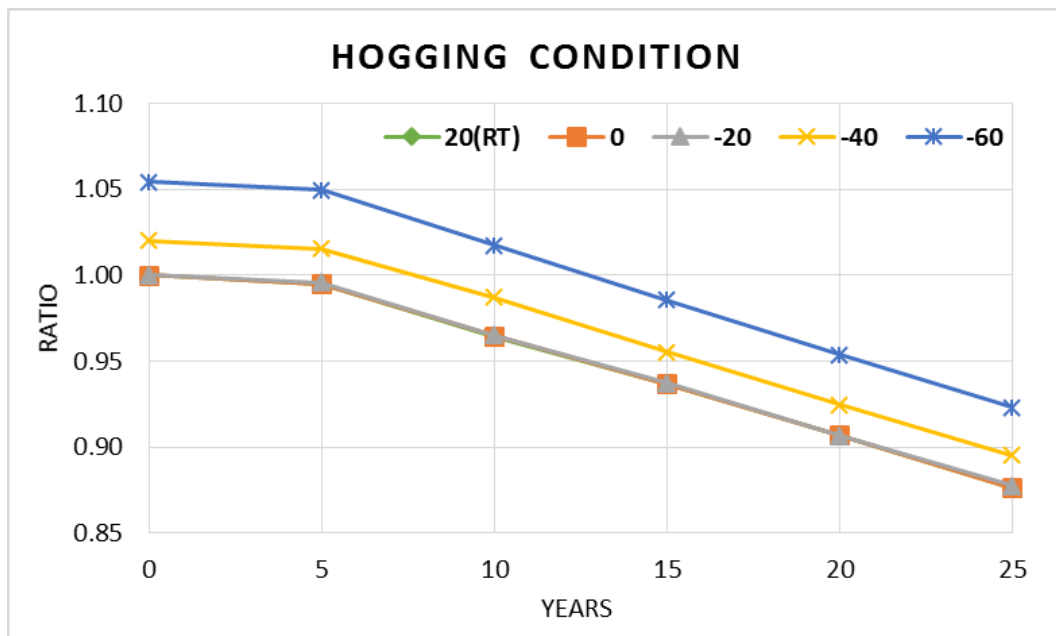


Fig. 4.29 Summary of the bending moment of ultimate strength under temperature and aged plates effect (hogging condition)

From the calculation results of hogging condition that we can observe these equations for calculating the vertical bending moment ratio of the range from as-built condition to 25 years old structures which have two slopes of line to apply. The detailed formula shows in the Table 4.1.

Table 4.1 Formulas for calculating the ultimate vertical bending moment ratio (Hogging condition)

	$(0 \leq T \leq 5)$	$(5 \leq T \leq 25)$
20°C	$R = -0.001T + 1$	$R = -0.0059T + 1.0243$
0°C	$R = -0.001T + 1$	$R = -0.0059T + 1.0243$
-20°C	$R = -0.0009T + 1.0002$	$R = -0.0059T + 1.025$
-40°C	$R = -0.0009T + 1.0203$	$R = -0.0061T + 1.0464$
-60°C	$R = -0.0009T + 1.0543$	$R = -0.0063T + 1.0809$

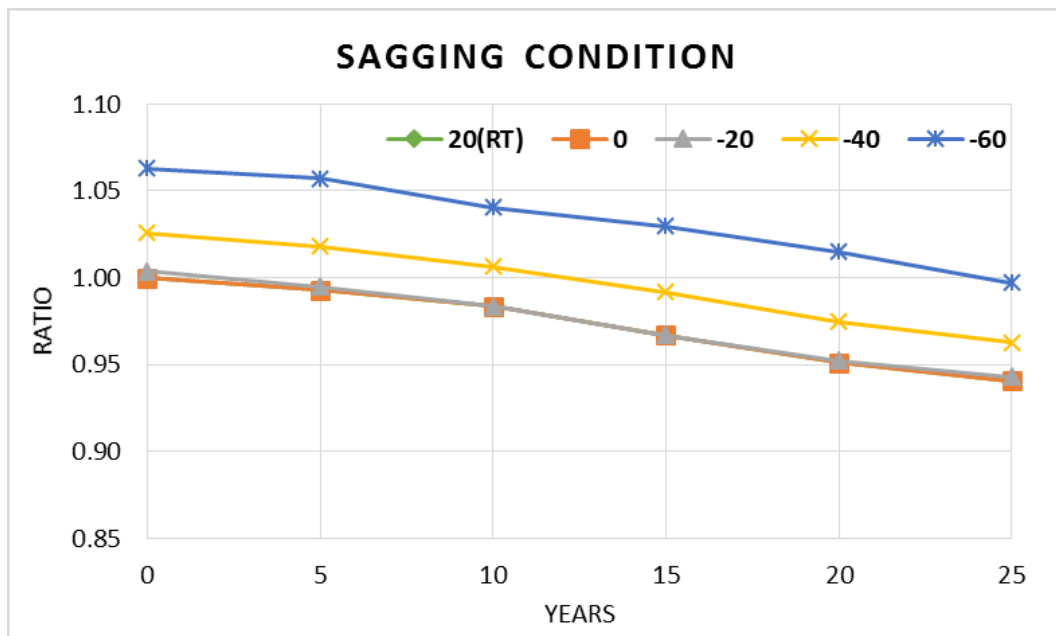


Fig. 4.30 Summary of the bending moment of ultimate strength under temperature and aged plates effect (sagging condition)

Further, the formulas for sagging conditions under each low temperature have been illustrated in Table 4.2.

Table 4.2 Formulas for calculating the ultimate vertical bending moment ratio (Sagging condition)

	$(5 \leq T \leq 25)$
20°C	$R = -0.0025T + 1.0038$
0°C	$R = -0.0025T + 1.0038$
-20°C	$R = -0.0026T + 1.0061$
-40°C	$R = -0.0026T + 1.0293$
-60°C	$R = -0.0027T + 1.067$

From Fig. 4.31 and Fig. 4.32 where we can see the relation between concerning structure ages of corrosion wastage with the variety low temperatures. In hogging condition that represents the similar spacing between each age that we can refer to the assumption of corrosion wastage was according to the liner relation of design ages. To summarize the phenomenon of results that we can conclude the both of hogging and sagging condition that tendency of ratio with the similar tendency of corrosion wastage deduction. Furthermore, the corrosion wastage effect the hogging bending moment more than the sagging one which we can check on the value of both 25 years old structures, the ratio of hogging condition in room temperature is 0.875, but 0.94 in sagging condition. In other words, we could say the effect of corrosion wastage will be sensitive reflect in hogging condition.

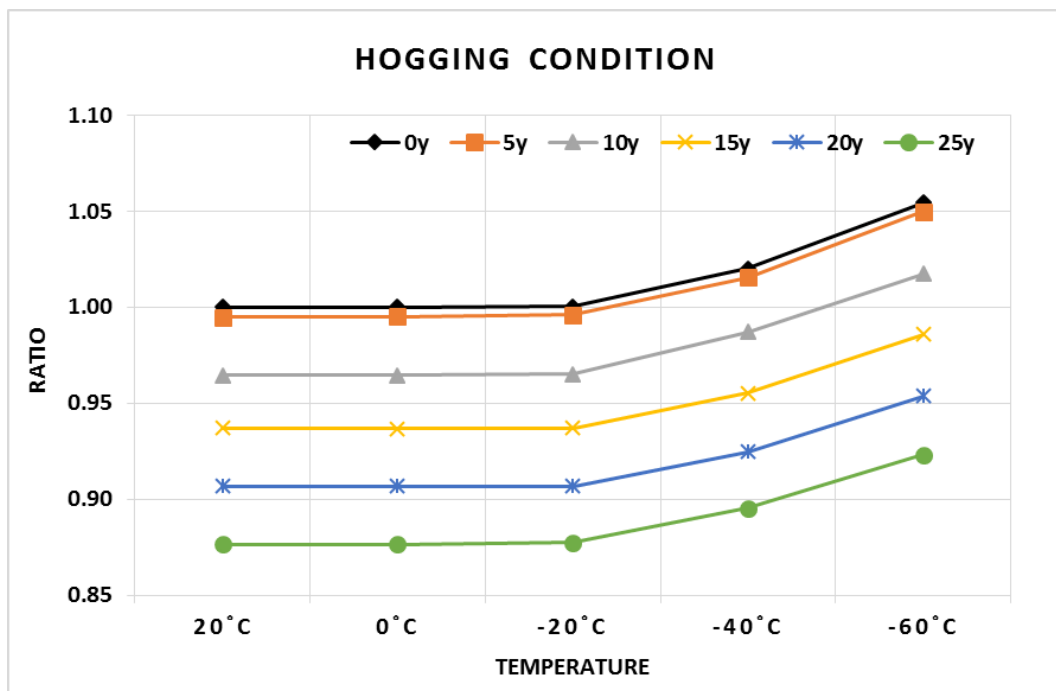


Fig. 4.31 Summary of the ultimate bending moment under temperature and aged plates effect (hogging condition)

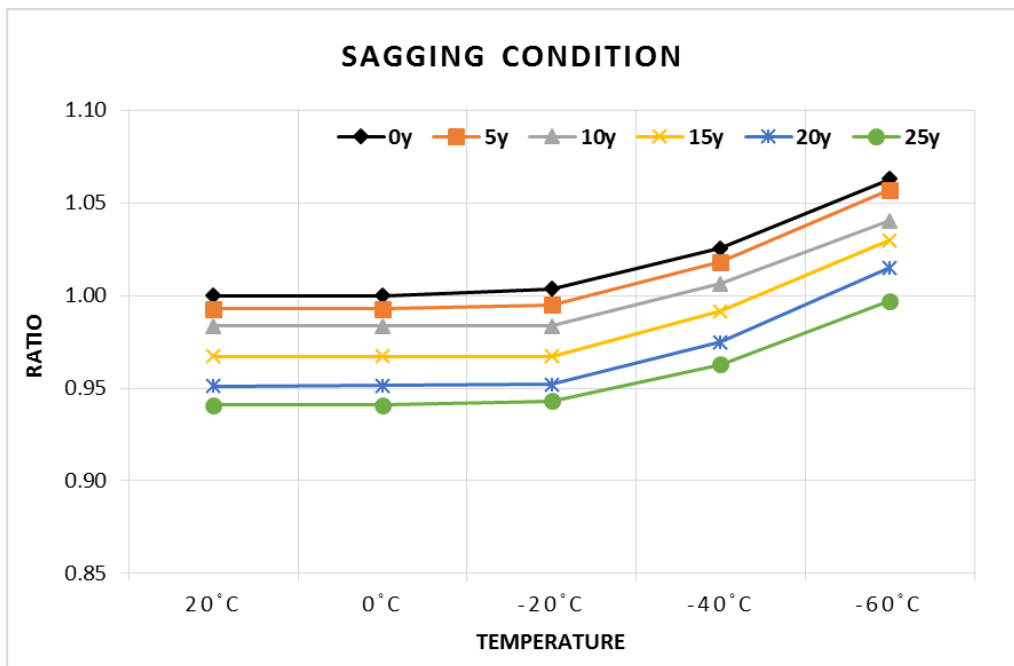


Fig. 4.32 Summary of the ultimate bending moment under temperature and aged plates effect (sagging condition)

Table 4.3 Summary ratio of vertical bending moment with room temperature for hogging and sagging conditions

Temperature/ Years	Hogging conditions					Sagging conditions				
	20°C (RT)	0°C	-20°C	-40°C	-60°C	20°C (RT)	0°C	-20°C	-40°C	-60°C
0y	1.000	1.000	1.000	1.020	1.054	1.000	1.000	1.004	1.026	1.063
5y	0.995	0.995	0.996	1.016	1.050	0.993	0.993	0.995	1.018	1.057
10y	0.964	0.965	0.965	0.987	1.017	0.984	0.984	0.984	1.006	1.040
15y	0.937	0.937	0.937	0.955	0.986	0.967	0.967	0.967	0.992	1.030
20y	0.907	0.907	0.907	0.925	0.954	0.951	0.951	0.952	0.975	1.015
25y	0.876	0.877	0.878	0.895	0.923	0.941	0.941	0.943	0.963	0.997

We can find out the increase of vertical bending moment under temperature from room temperature to -60°C is around 5% which is on the basis of the increasing yielding stress, but the variation for corrosion wastage can be obtain 12% which means the main effect between temperature and corrosion which corrosion wastage has higher influences.

Investigate with the assumption of both corrosion wastage and yielding increasing by decreased temperature, the combination of hull structures have the majority of ultimate strength effect from corrosion wastage in hogging conditions, but another possibility would be almost identical effect for sagging conditions. The future work could be more efficient which is according to the tendency of real corrosion deduction to have the inference associated with bending moment ratios.

5. COLLISION ANALYSIS

After Minorsky (1959) provided the simplified method of estimating the absorb energy by the damage volume of ship structures, this method had been applied to assess the total energy in ship collision or grounding cases. Generally, the failure mode of ship structures can distinguish as plate or stiffener buckling, tearing of plates, and folding of plates, but it might be more complicated with several failure modes of real damage situations.

When ship collision or grounding happened, we should not only focus the interaction between structures, but also ship hull with the external fluid. To solve and understand this kind of complex problem sufficiently that the researchers set a system to describe the structure behaviour of mechanics which are external dynamics and internal mechanics as Fig. 5.1.

The distinguishment established by Minorsky (1959) base on the research of collision problems. The external dynamics assumed the ship as a rigid body which study the impact force, the pressure of fluid and the interaction with ship structures with its activities. The pressure from fluid can be calculated as an added mass. Also, the buoyancy force, weight, viscous flow and wave force need to be considered as well.

On the other hand, the internal mechanic studies the energy dissipation and absorption by structure deformation, damage, and friction on ship structures. From Fig. 5.1 below that we can understand the external and internal mechanics in a grounding problem easily.

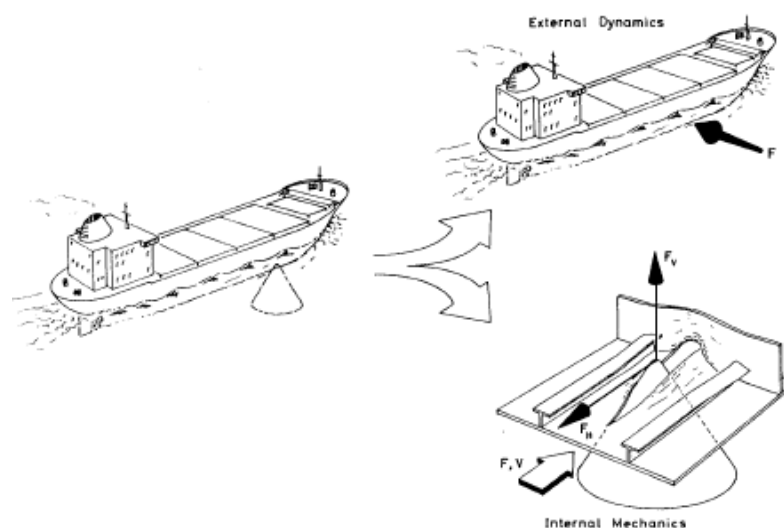


Fig. 5.1 External internal mechanics in grounding problems (Simonsen, 1997)

As the Fig. 5.2, if we consider a striking bow hit on a ship side where we can have the total absorbed energy from bow and ship damages as $W_C = W_{BC} + W_{SC}$.

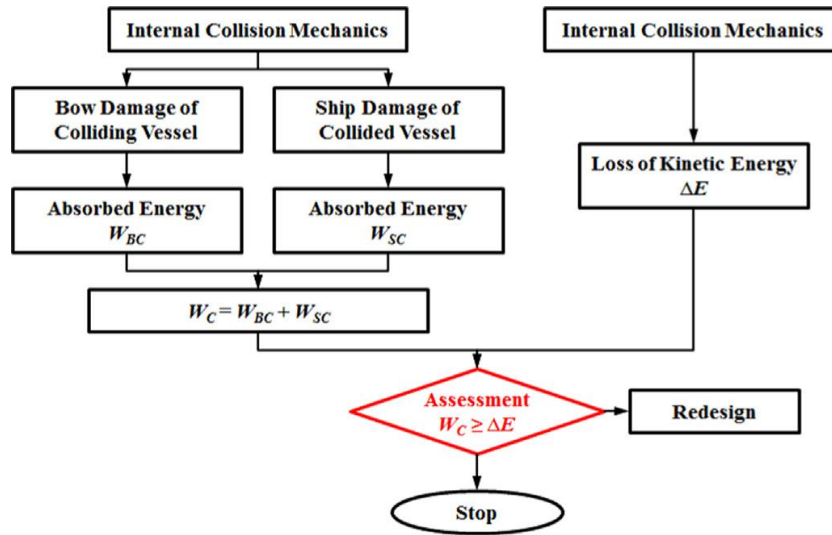


Fig. 5.2 Flow chart for the collision mechanics (Paik, 2007)

For the different method to estimate the internal mechanics, here we simplify to introduce the main five methods of internal mechanics.

5.1 METHODS FOR COLLISION PROBLEMS

(1). Statistical Methods

Minorsky (1959) provide the statically formula below which were according to the 26 collision cases of analysis:

$$W_C = 47.2R_v + 32.7 \text{ (MJ)} \tag{10}$$

$$R_v = \sum_{N=1}^{S1} B_N L_N t_N + \sum_{n=1}^{S2} B_n L_n t_n \text{ (m}^3\text{)} \tag{11}$$

Where the R_v is the ruptured volume of striking and struck ships which represent the factor of crashworthiness. W_C is the total energy absorbed by the large deformation and cracks of ship structures. B_N is the width of the number N structure on striking ship and B_n is the width of the number n structure on struck ship. As same as L_N, L_n, t_N and t_n , which L means the length of structure and t means the thickness. S1 and S2 are the number of structures on striking and struck ship.

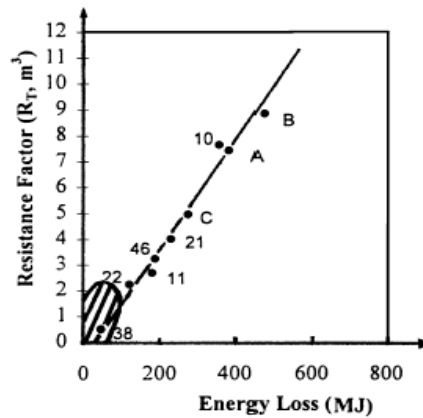


Fig. 5.3 Regression curve based on the collision cases (Minorsky, 1959)

From the Fig. 5.3 that the wide range of low energy cases could be found out in the region of slant lines. The other 8 high energy cases are approached on the regression curve which corresponds that the statically formula from Minorsky is suitable in high energy collision cases. The statically formula from Minorsky is easy and widely used in collision estimation. By trying different factor in the formula that he found out the damage volume of calculating the absorb energy is the better way to get accurate results.

Although the formula is easy to use, the drawback of this method is the formula is based on the database from Card (1975) which studied based on the old ship cases, it should be modified by the database of new ships.

(2). Finite Element Method

Nowadays there are more and more people use the commercial software to solve structure collision problems, such as LS-DYNA, ABAQUS, MSC/DYTRAN...etc..

Kitamura (1997) use the FEM to analyze the collision on side structures of ship, Amdahl and Kavlie (1992), Kuroiwa (1996) solve the grounding problems. The Fig. 5.4 shows the simulation model of ship grounding analysis, Kuroiwa (1996).

There are some important points when using FEM to solve the collision and grounding problems, the reasonable simplified model, settings of boundary conditions, setting of analysis parameter, analysis method should be considered. Some problems for the large deformation dynamic analysis should be verified and proof the reliability by experimental tests.

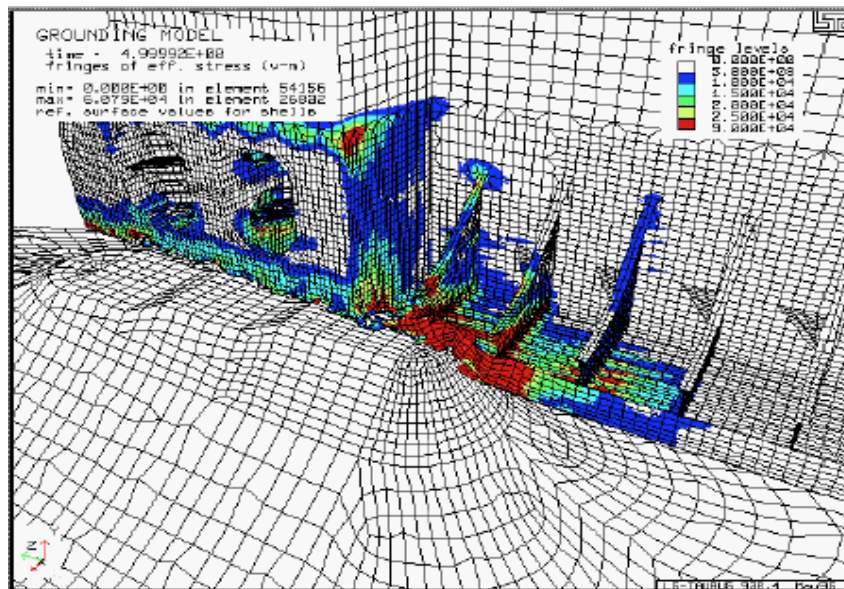


Fig. 5.4 Grounding analysis of VLCC (Kuroiwa, 1996)

(3). Experimental Methods

To understand the internal mechanics, a large amount of researchers tried to do the related experimental test, but most of that were simplified. The cost and time of real ship damage from collision are difficult to estimate, some experiment test with real scale of ship model which supported by government or international institution, normally researchers using the smaller scale size to do this kind of experiment.

To analyse the significant on the local position of ship structures which will be examined by simplified models, for instance the damage mode on the bottom plates can be replaced as a cutting phenomenon by Cone wedges as Fig. 5.5. The principle uncertainty of the experiment is the scale effect, it's not easy to apply the result on the real case by simple scale method, also the differences between real case and experiment of dynamic effects still need to be considered and verified.

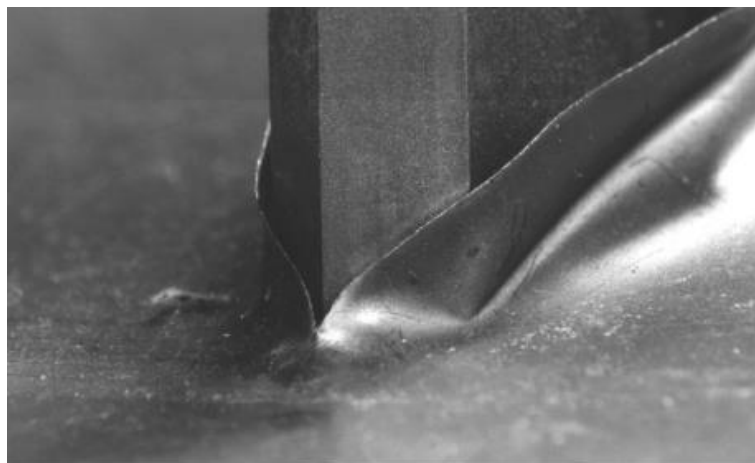


Fig. 5.5 Experiment test of cutting plate by Cone wedges (Simonsen, 1997)

(4). Simplified Analytical Methods

This method is based on the upper-bound theorem and the assumptions from the results of experimental test and real cases. The general idea is the principle of conservation of energy which the energy induced by external force will equal to dissipation energy on structures. Many academic use this method to analyze the internal mechanics of ship collision and grounding which have a good result of it.

Alexander (1959) is the primary person applied this method on collision study of thin plates, as Fig. 5.6 below. The high accuracy of the results can be obtained when considered a simple structure with the understanding of the failure mode, but there are the limitation for complex structures which is hard to identify the failure mode.

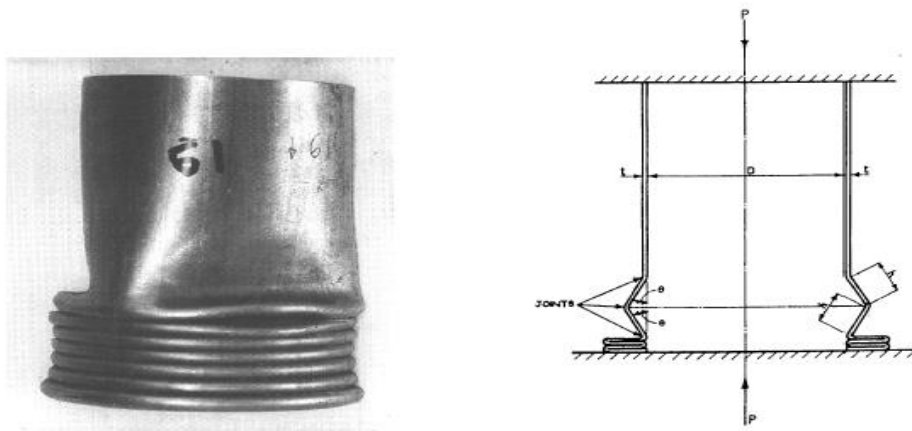


Fig. 5.6 Collision analysis on a cylinder, Alexander (1959)

(5). Idealized Structural Unit Method (ISUM)

The advantage of the previous four methods which are suitable using in different cases. The method of ISUM include all the benefit from these four method which identify the stiffness of element by deformation or stress function that the element size can be larger and need less computation time. Ueda (1975) is the first person to apply it on computation software and affected the following researchers make use of different study on structures. The Fig. 5.7 represents the simulation model of ship structure fracture under an impact which done by Paik and Pedersen (1996).

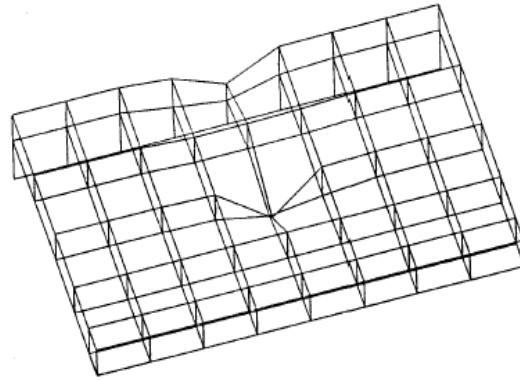


Fig. 5.7 Simulation model of side ship collision by ISUM analysis (Paik and Pedersen, 1996)

5.2 APPLIED EXAMPLES FOR COLLISION

With regard the low temperature will increasing the yielding stress that cause higher ultimate strength, but the brittle fracture of steel under low temperature is equivalent important to effect the structure damage particularly. In this case study that we demonstrate the collision dynamic analysis with three cargo holds which are according to the scantling of midship section as in Chapter 4.

Due to the lack information of striking ship from KOSORI that we could know the similar container ship bow but smaller size of struck ship will be used in this dynamic analysis.

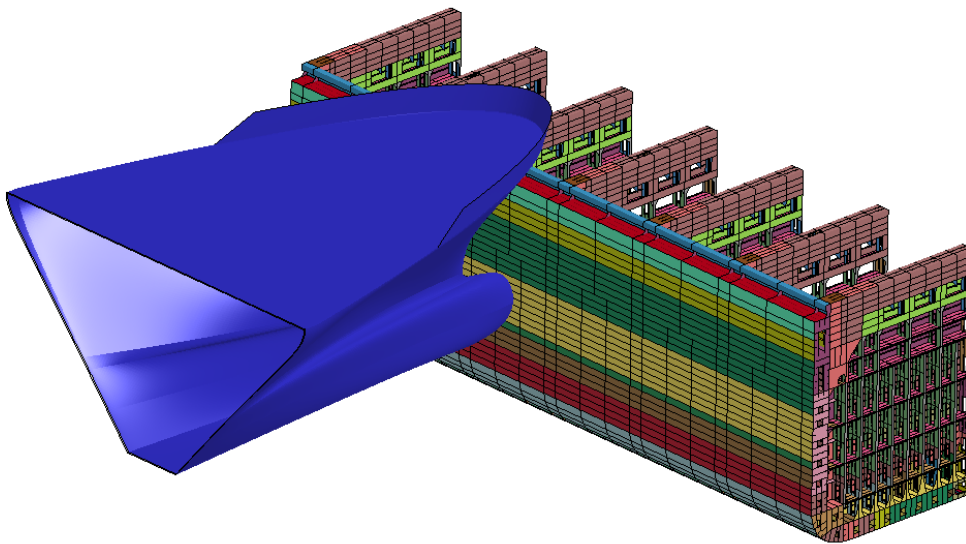


Fig. 5.8 Schematic diagram of collision analysis (isometric view)

To ignore the effect of bow flare impact on the upper part of side of container ship that we assume the striking ship is on the minimum ballast draft and the struck ship is on the full load condition.

To identify the normal situation of collision, we considered the accident occurred around the port when the ship move out from the port after unloaded the cargos with ballast condition consideration. The collision point is in the middle between watertight bulkhead and non-tight bulkhead which consider the critical collision point for the cargos in Fig. 5.9.

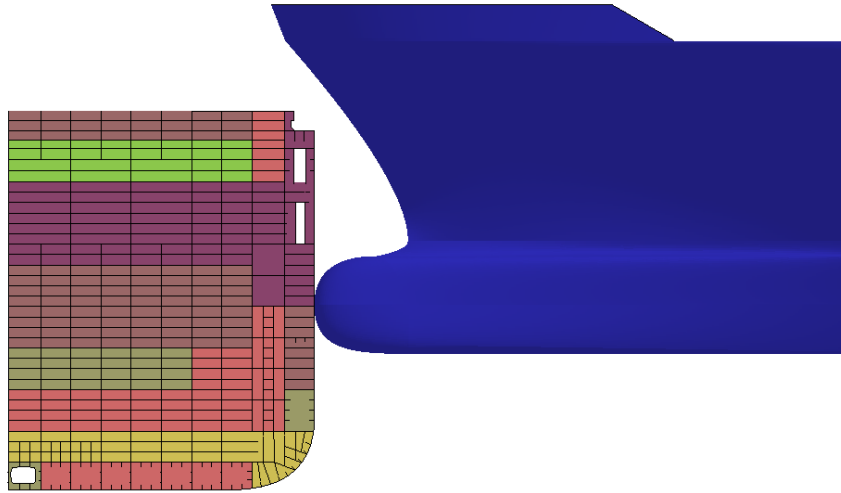


Fig. 5.9 Schematic diagram of collision analysis (Front view)

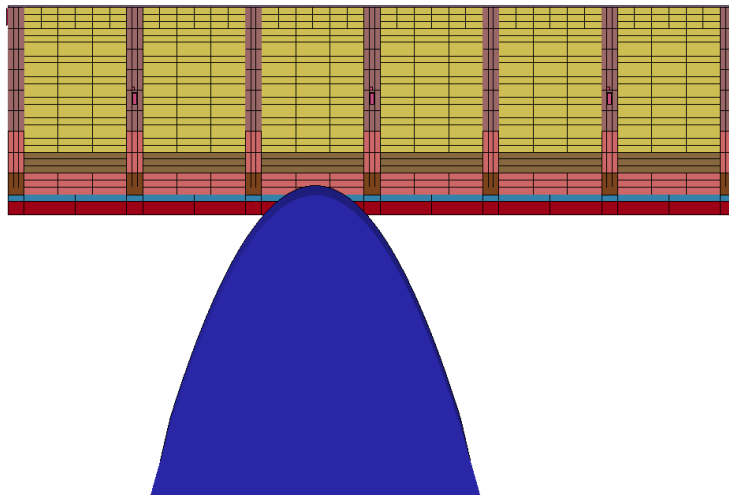


Fig. 5.10 Schematic diagram of collision analysis (Top view)

➤ Settings of the FE model

The mesh size of struck ship is around 200 mm which could represent the local crush and fold of stiffener and plates. To simplified and saved analytical time, the boundary on the two side of cargo hold is fixed, and striking ship is assumed as a rigid body.

Normally the collision accident occurred when entering or exiting to ports. Therefore, the velocity of striking ship in this research considered the real situation that the striking ship will

use the brakes to stop the ship. However due to the large amount of weight of ship that the inertial force will continue as the reason use 2 knots in the dynamic simulation.

➤ Dynamic properties of materials

When simulate a dynamic analysis with LS-DYNA software that we need to consider the dynamic fracture strain and dynamic yielding stress instead of static values.

From the KOSORI experimental test database that we obtained the following stress-strain curve for both mild steel and high tensile steel (AH32) as following Fig. 5.11 and Fig. 5.12. To specified the ratio of fracture strain that we can use the fracture strain (ϵ_F) from these curves with the strain rate ($\dot{\epsilon}$) 2.3.

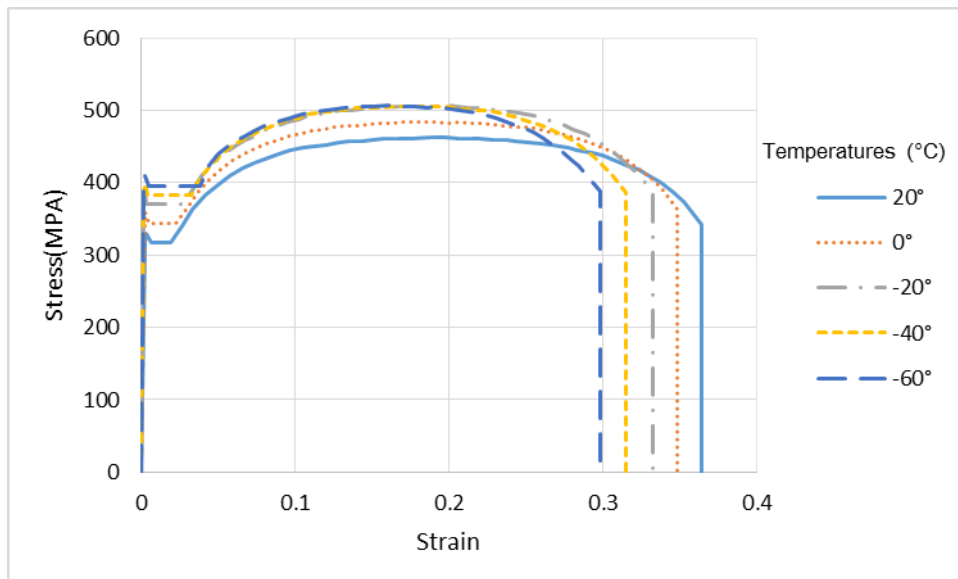


Fig. 5.11 Engineering stress-strain curve of Mild steel

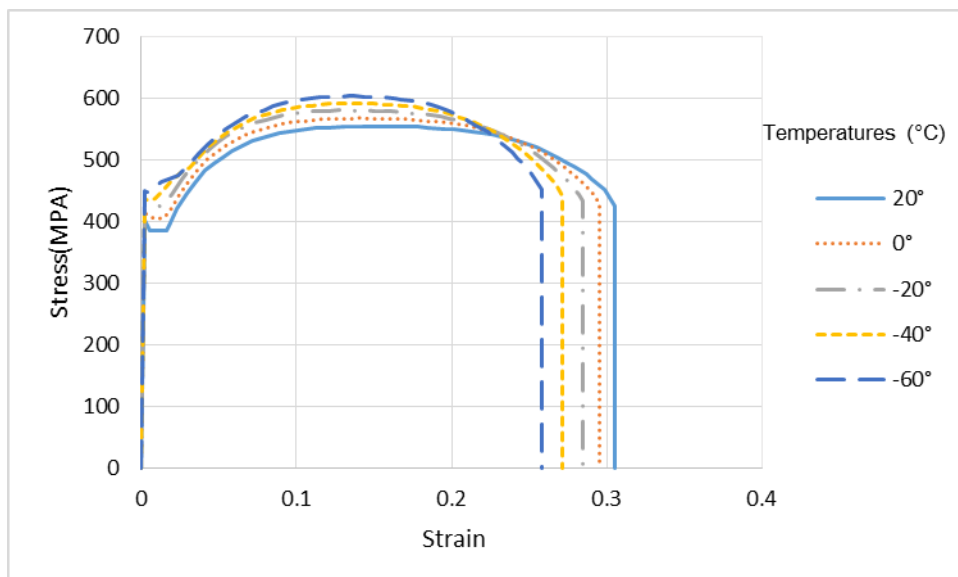


Fig. 5.12 Engineering stress-strain curve of High tensile steel (AH)

To calculate the dynamic material properties as equation (12) to (14) below.

When considering the critical fracture ϵ_{Fc} that we can obtain the fracture strain value on the end of the curve from the figures above. Applied to formula (12) with $\gamma=0.3$, and assumed $\left[d_1 \left(\frac{t}{s} \right)^{d_2} \right]$ is equal to 1.

$$\epsilon_{Fc} = \gamma \left[d_1 \left(\frac{t}{s} \right)^{d_2} \right] \epsilon_F \tag{12}$$

$$\epsilon_{Fd} = \left[1 + \left(\frac{\dot{\epsilon}}{C} \right)^{\frac{1}{q}} \right]^{-1} \epsilon_{Fc} \tag{13}$$

$$\sigma_{Yd} = \left[1 + \left(\frac{\dot{\epsilon}}{C} \right)^{\frac{1}{q}} \right] \sigma_Y \tag{14}$$

Where ϵ_{Fc} is the critical fracture strain, ϵ_{Fd} is the dynamic fracture strain, σ_{Yd} is the dynamic yielding stress. The coefficient of C and q value for mild steel and high tensile steel are listed on the following table which according from Cowper-Symonds constitutive equation (From Ship-Shaped Offshore Installations: Design, Building, and Operation)

Table 5.1 Sample coefficients for the Cowper-Symonds constitutive equation

Material	C (s ⁻¹)	q	Reference
Mild steel	40.4	5	Cowper and Symonds (1957)
	7.39	4.67	Schneider and Jones (2004)
	114	5.56	Hsu and Jones (2004a)
Higher-tensile steel	3,200	5	Paik and Chung (1999)
Aluminum alloy	6,500	4	Bodner and Symonds (1962)
	9.39 × 10 ¹⁰	9.55	Hsu and Jones (2004b)
α-Titanium (Ti 50A)	120	9	Symonds and Chon (1974)
Stainless steel 304	100	10	Forrestal and Sagartz (1978)

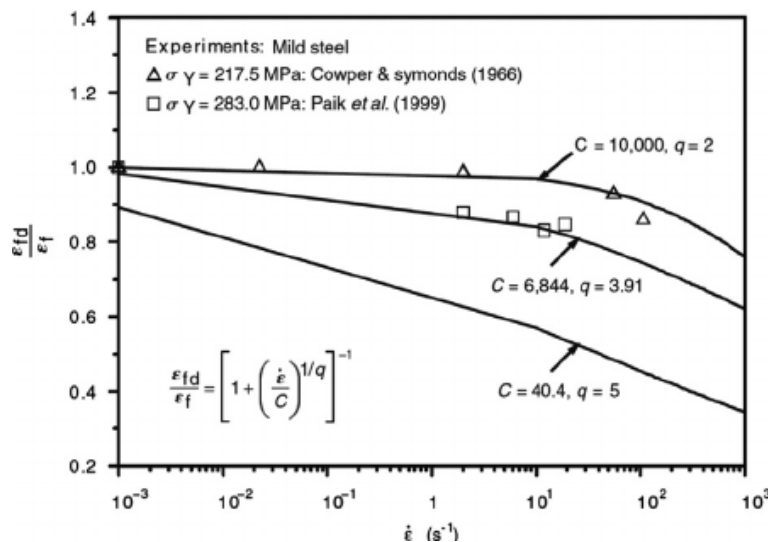


Fig. 5.13 Normalized dynamic failure strain versus strain rate for mild steel (Paik and Thayamballi, 2003)

5.3 COLLISION ANALYSIS RESULTS

Concentrating on the effect of fracture of collision point that due to the large angle of bow flare on striking ship thus during the collision analysis that the contact between bow flare area and struck ship side on the upper deck area will be ignored.

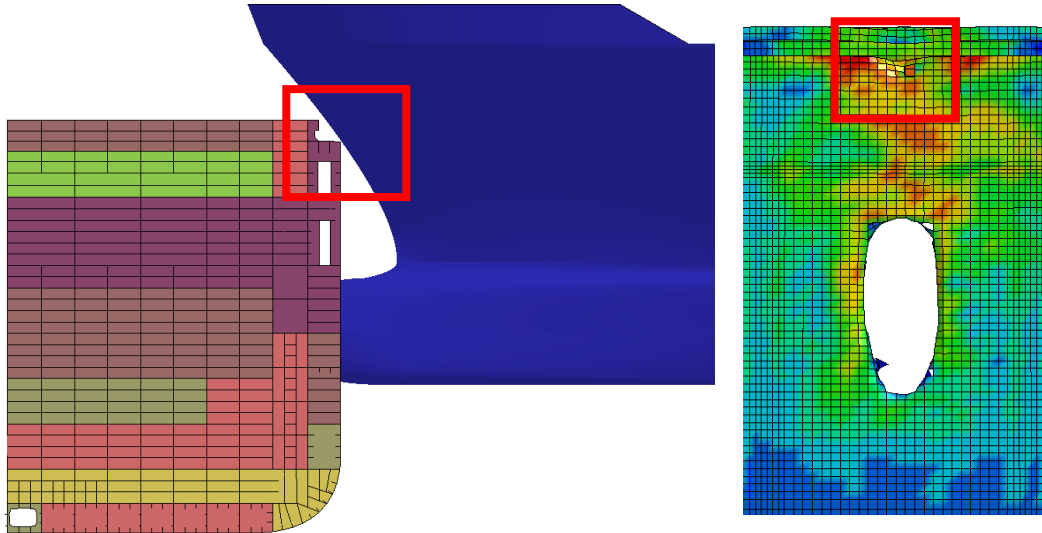
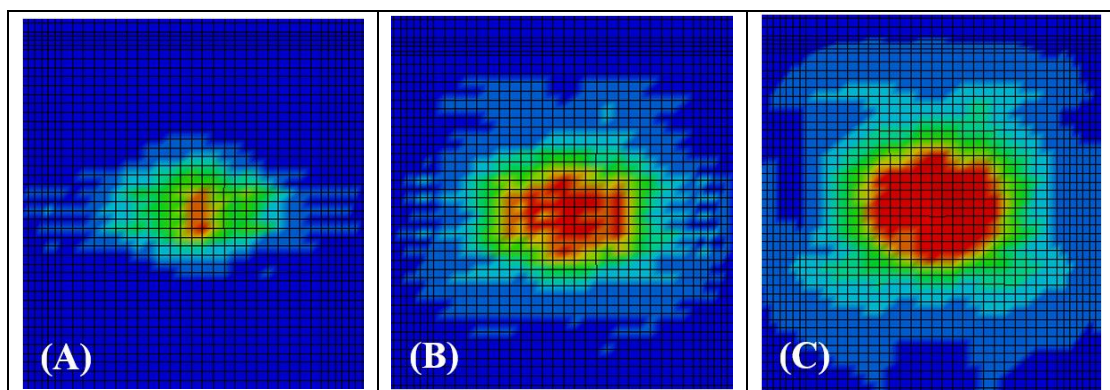


Fig. 5.14 Ignored contact area during collision analysis

The following Fig. 5.15 and Fig. 5.16 represent the collision analysis results for room temperature case and -60°C case during the period of side shell ruptured, and the distribution of Von Mises stress and the process of crack growing have been illustrated. The colors show the different level of Von Mises stress which red is higher and blue is lower.

The tear started from the center of collision point as expectation and according to the sharpness of striking bow structures, and then rapidly increased the size of crack which split by progressing striking bow.



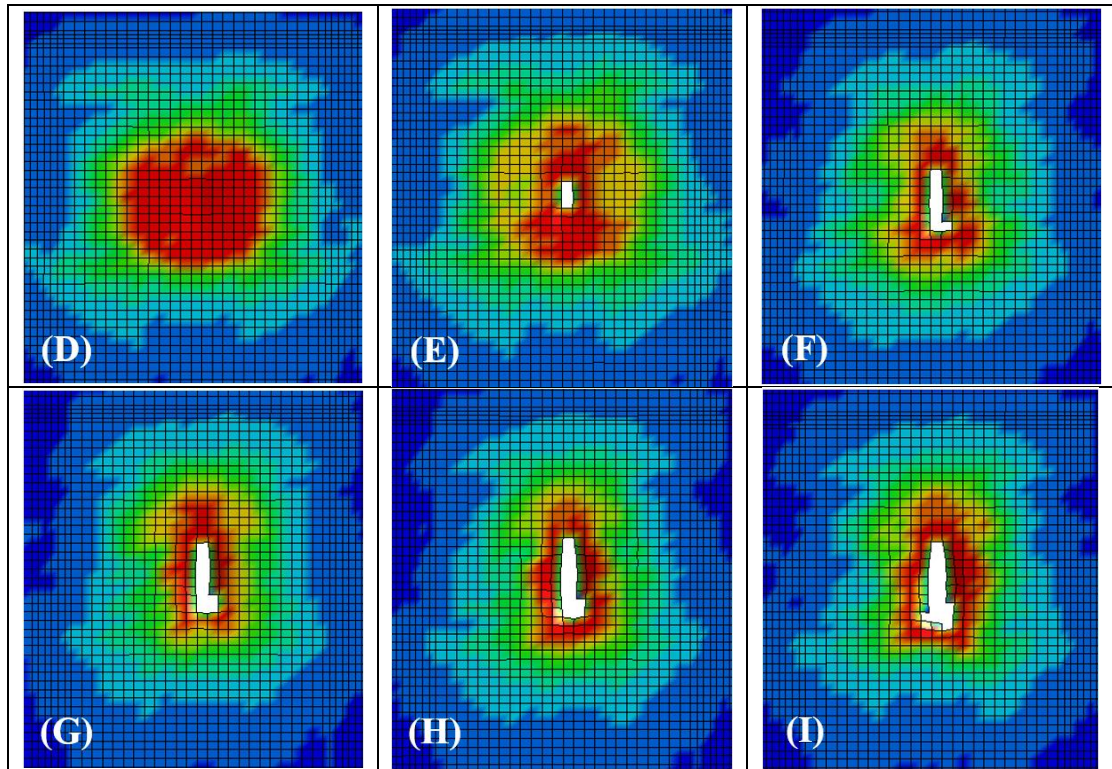
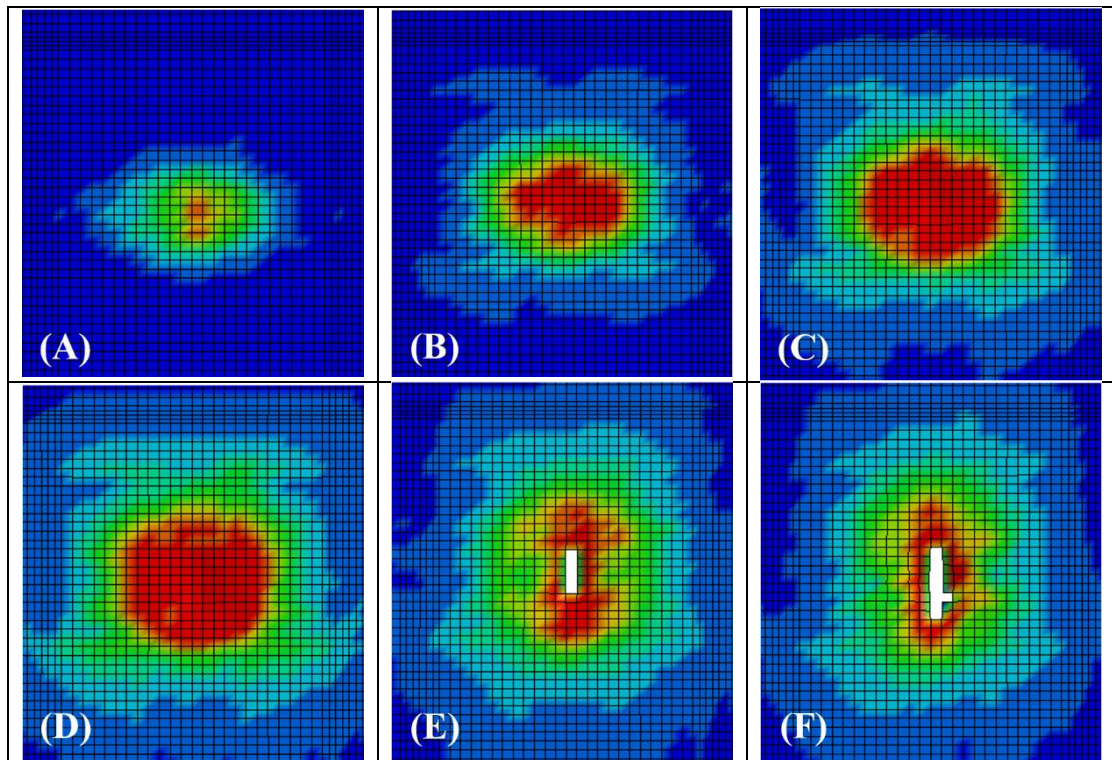


Fig. 5.15 Von Mises stress contours of struck ship on side shell with room temperature (20°C)



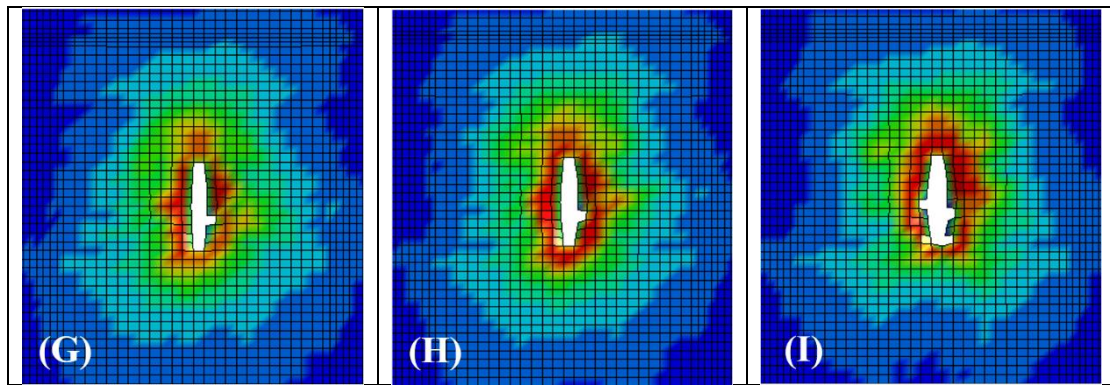
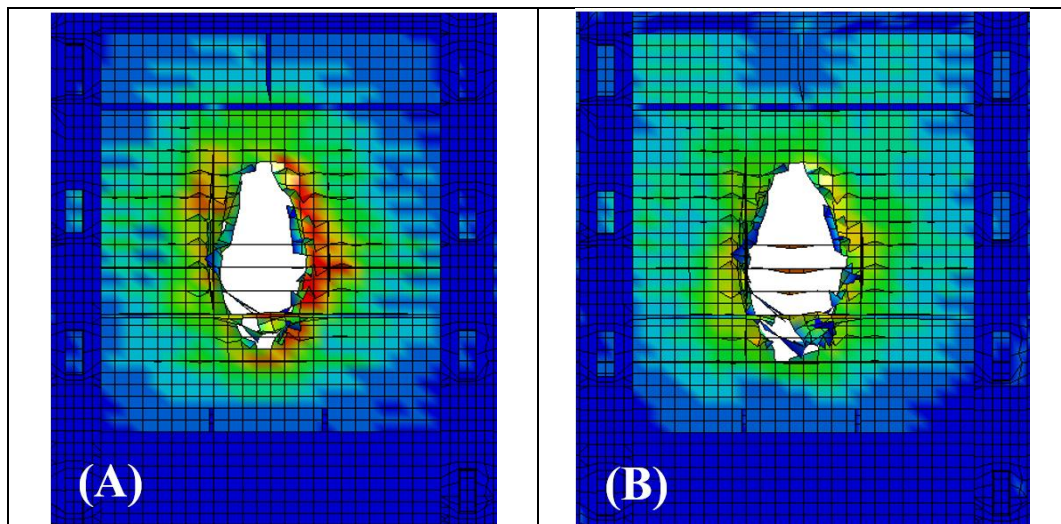


Fig. 5.16 Von Mises stress contours of struck ship on side shell with -60°C

The Fig. 5.17 and Fig. 5.18 below that represent the Von Mises stress, rupture condition of inner shell, and the folded situation of supported stiffeners and plates with room temperature and -60°C . From the sub figure (A) to (C) in Fig. 5.17 and Fig. 5.18 that we can see the collision process of supporting stiffeners on inner shell. The stiffeners resist the collision force, when it can't afford the impact force it will be destroyed and the damage structures can absorb the energy.

The subfigure (D) show the moment of inner shell rupture, which stated from supporting stiffeners failure then move to plate tensile break, and the tears on outer shell are not growing only vertically, but horizontal by the width of progressing striking bow.



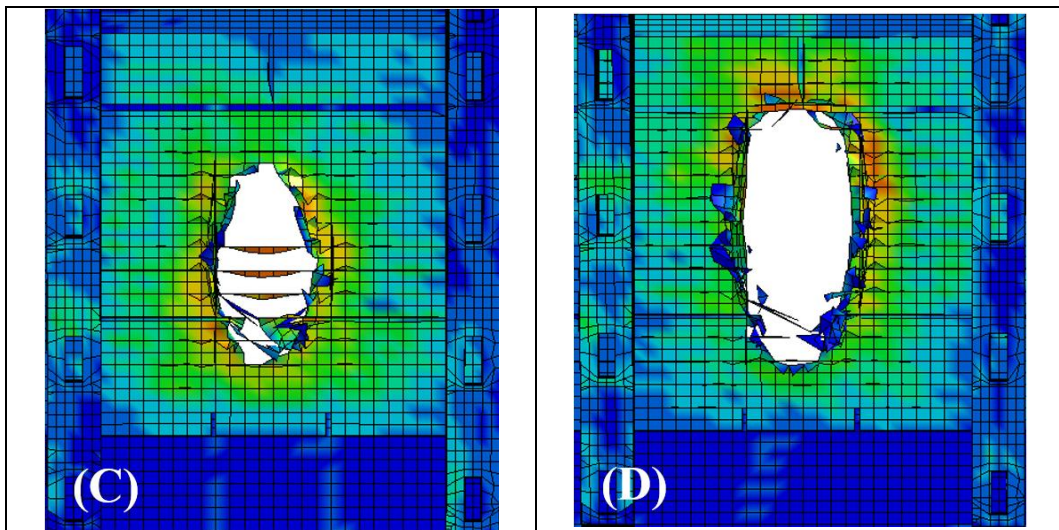


Fig. 5.17 Von Mises stress contours of struck ship on inner shell with room temperature (20°C)

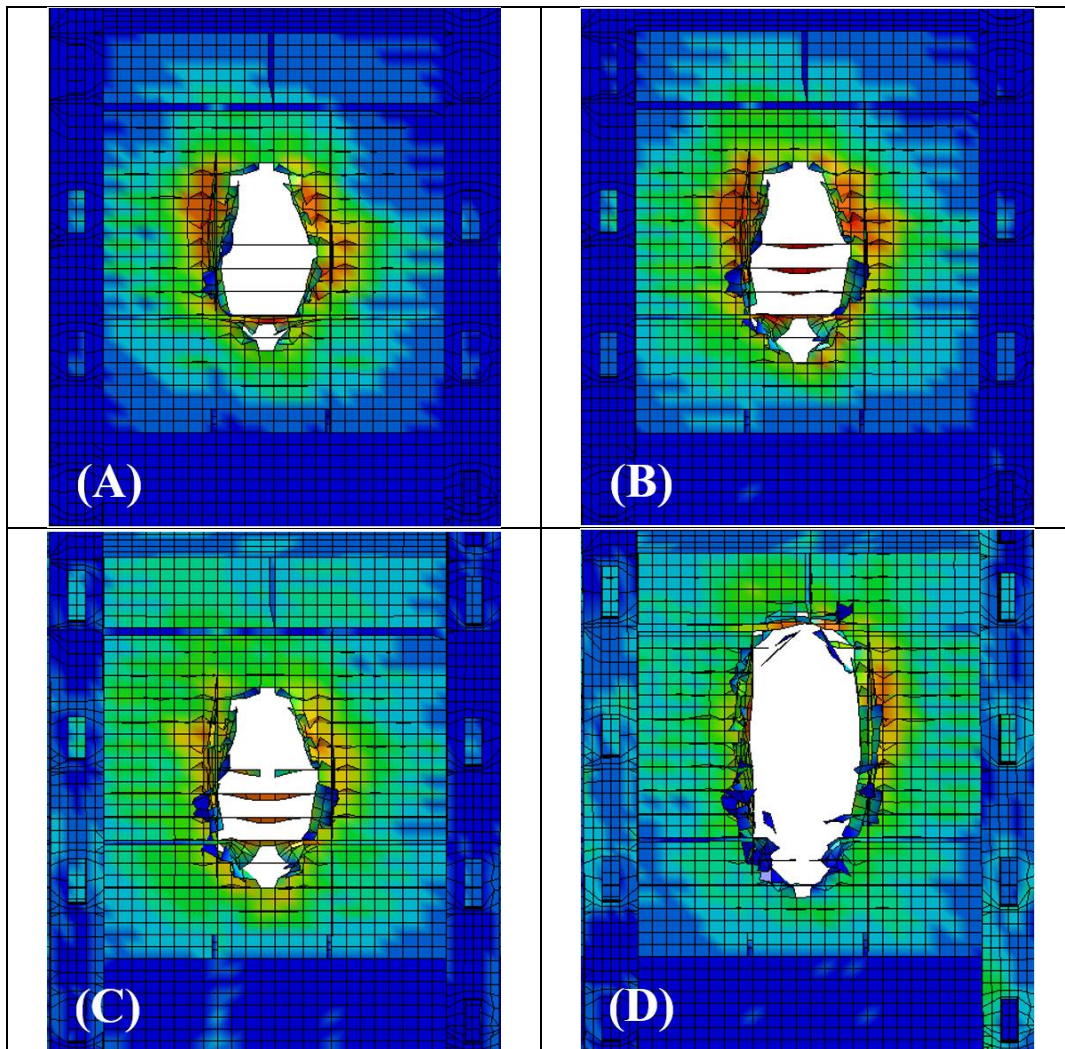


Fig. 5.18 Von Mises stress contours of struck ship on inner shell with -60°C

5.4 DISCUSSION

The differences could be found out in the same step of analysis that the larger ruptured area is on -60°C rather than room temperature in Fig. 5.19.

Compared the outer side shell conditions under Von Mises stress contours between -60°C and room temperature when it started to rupture on struck ship, the deep red color area in -60°C case is smaller than room temperature one, which represent the higher Von Mises stress. Simultaneously, it validated the result from Chapter 4 that the temperature decreased with the increased yielding stresses. On the contrary, the rupture strength at the same analysis step that shows the larger rupture area of lower temperature than room temperatures. Accordingly, we can simply conclude the resistance/ fracture strength of structures will be lower due to low temperatures.

Nevertheless, compared the results of rupture on inner shell, the differences of rupture range between -60°C case and room temperature could not be seen clearly which is larger from Fig. 5.20. The reason might be related to the connection between elements and been folded by different methods during the dynamic analysis. As a result, we estimate the fracture strength by absorbed energy from the start of analysis until the inner shell ruptured.

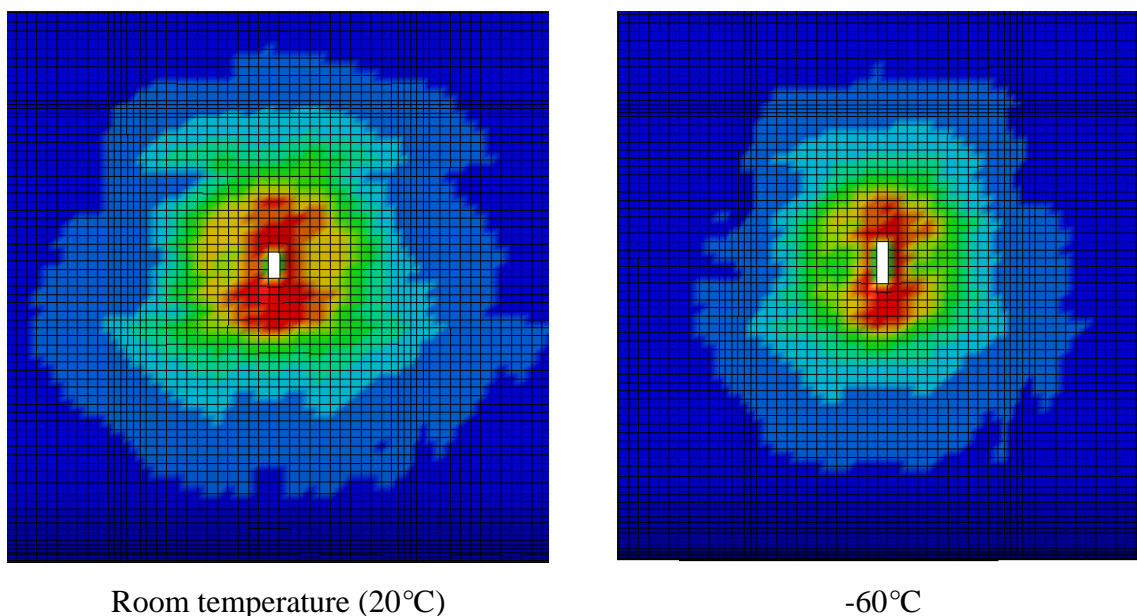


Fig. 5.19 Comparison the start point of rupture on side shell between room temperature and -60°C

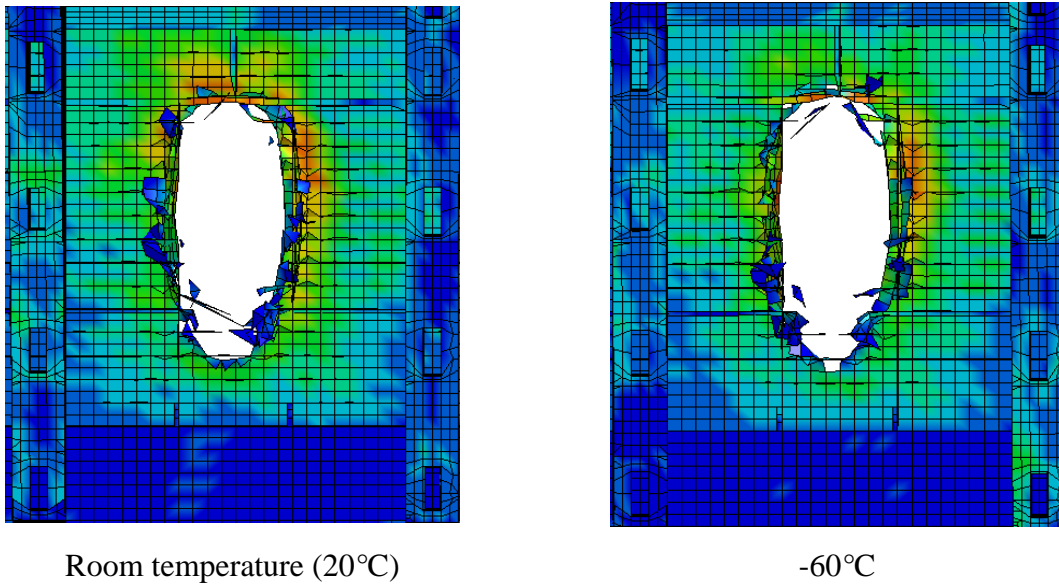


Fig. 5.20 Comparison the start point of rupture on inner shell between room temperature and -60°C

The following Fig. 5.21 represents the analysis results of reaction forces with indentation depths for five different temperatures. The reaction force tendency is similar for five temperatures before indentation 2.3 m, since the bow flare contact display the time delay between different temperatures.

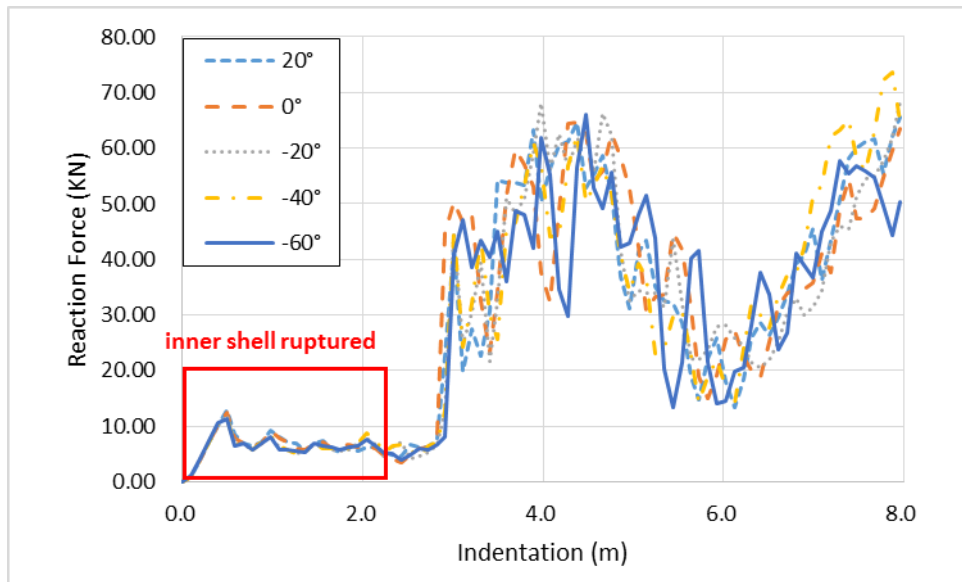


Fig. 5.21 Total reaction force with indentation depth for five different temperatures

Another point of view from the absorb energy with indentation depth for five different temperatures as Fig. 5.22 showed below, the analysis results of absorb energy can be compared

as the structure deformation and damage. During the collision analysis, the absorb energy is increasing with the indentation of striking bow and damage area of struck ship sides.

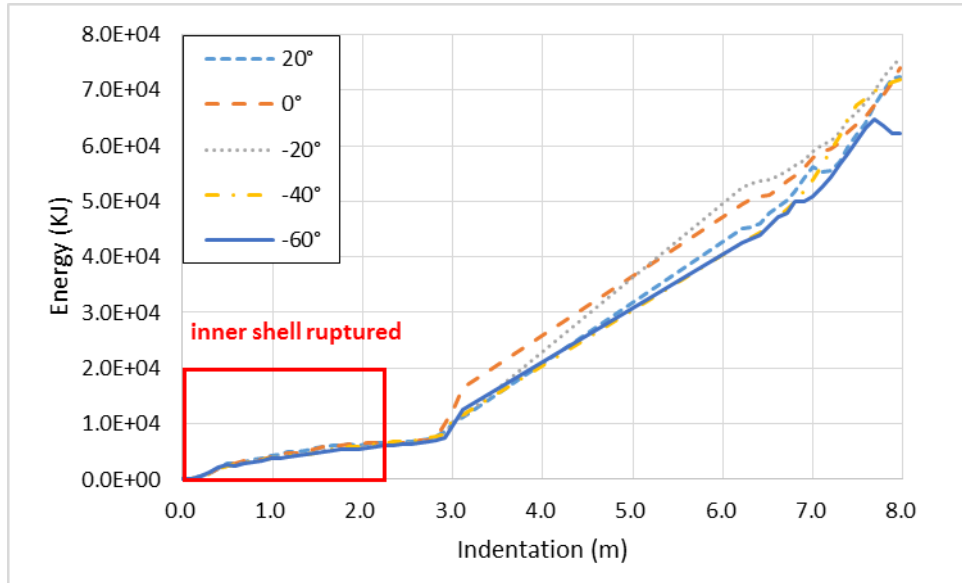


Fig. 5.22 Internal energy with indentation depth for five different temperatures

The Fig. 5.23 shows the history of energy absorption before inner shell ruptured. We could identify the room temperature case has higher absorb energy before 2 m indentation depth and 0°C case has the same tendency with room temperature but a little bit lower. The lowest absorbed energy is occurred on -60°C case which as same with our expect that when the temperature is much lower, the fracture strain will be lower and the structure is getting brittle with lower energy absorption.

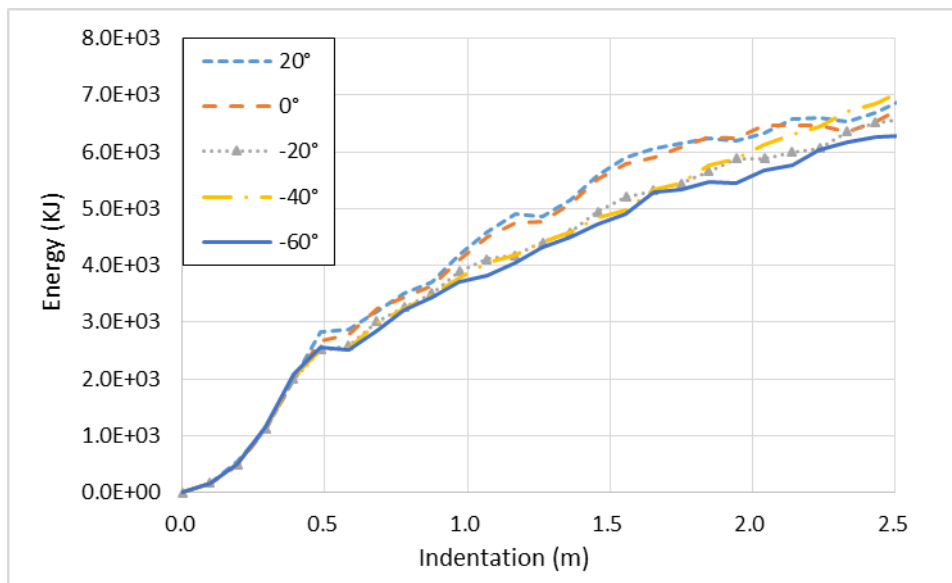


Fig. 5.23 Internal energy history before inner shell ruptured

From the result of the whole process of collision, we focus on the Von Mises stress on the damaged structures and absorb energy on double side shell ruptured. Based on the previous analysis results, the following conclusions could be summarized:

1. The Von Mises stress contours represent the lower stress on -60°C case rather than room temperature which is corresponded with the results in Chapter 4 that the temperature decreased with the increased yielding stresses.
2. From the absorb energy point of view, the energy absorbed by damage structures which included the plate crack, folded structures ...etc.. It means the higher absorbed energy that the structure is stronger and less brittle.

6. CONCLUSION AND FUTURE WORK

From the result of ultimate strength of stiffened plates and hull girder strength in Chapter 4, we could find out a new concept of steel plate or structures in the low temperature environment that under the lower temperature, the material property of yielding stress will be higher.

The material is only provide the yielding stress and the whole structure can be afford is ultimate strength, and after ultimate stress the structure is reached the point of start to collapse.

Accordingly, the ultimate strength is not only related to material properties such as yielding stress and also the structure construction. Which we can find out the differences of ultimate strength between different stiffener types in Chapter 4.1.2.

In addition, when using the similar stiffener scantling and plate thickness that can show the clear difference between different corrosion wastage considerations under same low temperatures which is linear difference as same trend with corrosion assumption and lower temperature will have the higher ultimate strength.

For the effect of ultimate strength between corrosion wastage and increasing yielding stress with low temperatures, we could summarized the majority effect is corrosion wastage from the results of Chapter 4.2.2.

The results that we acquire the increased yielding stress with temperature decreased, critical fracture strain decreased with temperature decreased.

To conclude the safety assessment of non-iced aged structures that the low temperature provide the higher ultimate according to higher yielding stress which is benefit for structures. However the low temperature will cause material from ductile to brittle which related to fracture strain. It is the disadvantage for non-iced aged structures.

➤ **Future work**

The reasonable assumption of corrosion wastage can be apply for a better realistic results, such as nonlinear corrosion wastage with ages, or real corrosion wastage from examination. Moreover, the material property of yielding stress and fracture strain which utilized form experimental test that conducted by the same plate thickness. To obtain the precise and accurate results that should be contain all material properties for different thickness of plates and could distinguish the effect of aged plates of brittle differences under low temperatures which need to be concerned as a factor in the same collision analysis.

DECLARATION OF AUTHORSHIP

I declare that this thesis and the work presented in it are my own and have been generated by me as the result of my own original research.

Where I have consulted the published work of others, this is always clearly attributed.

Where I have quoted from the work of others, the source is always given. With the exception of such quotations, this thesis is entirely my own work.

I have acknowledged all main sources of help.

Where the thesis is based on work done by myself jointly with others, I have made clear exactly what was done by others and what I have contributed myself.

This thesis contains no material that has been submitted previously, in whole or in part, for the award of any other academic degree or diploma.

I cede copyright of the thesis in favour of the University of West Pomeranian University of Technology, Szczecin

Date:

Signature

ACKNOWLEDGEMENTS

Firstly, I would like to express my gratitude to all the people who have been contributed to this thesis. Especially to my supervisor Professor Zbigniew Sekulski from West Pomeranian University of Technology, Szczecin, that spend a lot of time to review and give me useful comments; and I would like to thank Professor Paik and Dr. Kim support me all knowledge and share practical experience with me when I was in Busan. And all the people in KOSORI and Busan University that give me the advice for this research and accompany with me that I have the best time during my internship in Korea.

Secondary, I would like to give my gratitude to Prof. Philippe Rigo, Prof Lionel Gentaz and Prof. Zbigniew Sekulski who instruct and help me during my study in Belgium, France and Poland. Additionally, I want to say thank you for all of my best friends in EMSHIP program, it is my honor to become the one of EMSHIP student and join to 6 cohort.

Finally, I would like to thank my lovely family, they always give supports from Taiwan, and my best friend Kun-Ping who accompany with me to finish this research, it's really important for me to pass the tough time.

This thesis was developed in the frame of the European Master Course in “Integrated Advanced Ship Design” named “EMSHIP” for “European Education in Advanced Ship Design”, Ref.: 159652-1-2009-1-BE-ERA MUNDUS-EMMC.

REFERENCES

American Bureau of Shipping, 2015. Vessels intended to carry containers (130 meters (427 feet) to 450 meters (1476 feet) in length). *In: Rules for building and classing-Steel vessels- Specific vessel types*. Worldwide: American Bureau of Shipping, 601-882.

Chen, D., 2010. *Simplified ship collision model*. Thesis (Master). Virginia Polytechnic Institute and State University.

Emmerson, C., & Lahn, G., Lloyd's Opportunity and Risk in the High North (2012).

Gao, Y., Hu, Z., Ringsberg, J.W. and Wang, J., 2015. An elastic-plastic ice material model for ship-iceberg collision simulations. *Ocean Engineering*, 102 (2015), 27-39.

Hong, L. and Amdahl, J., 2008. Crushing resistance of web girders in ship collision and grounding. *Marine Structures*, 21 (2008), 374-401.

Hughes, O.F. and Paik, J.K., 2010. *Ship structural analysis and design*. New Jersey: The Society of Naval Architects and Marine Engineers.

International Association of Classification Societies LTD., 2015. *S11A Longitudinal strength standard for container ships* [online]. Unified requirements. Available from: <http://www.iacs.org.uk/publications/publications.aspx?pageid=4§ionid=3> [Accessed June 2015].

International Association of Classification Societies LTD., 2016. *Polar class* [online]. Unified requirements. Available from: <http://www.iacs.org.uk/publications/publications.aspx?pageid=4§ionid=3> [Accessed April 2016]

International Marine Organization, 2006. *Resolution MSC.215(82)/Annex 1-Performance standard for protective coatings for dedicated seawater ballast tanks in all types of ships and double-side skin spaces of bulk carriers*. Worldwide: International Marine Organization.

IMO, Adoption of an international code of safety for ships operating in polar waters (Polar Code) <http://www.imo.org/en/mediacentre/hottopics/polar/pages/default.aspx>

Kim, D.K., Kim, H.B., Zhang, X.M., Li, C.G. and Paik, J.K., 2014. Ultimate strength performance of tankers associated with industry corrosion addition practices. *International Journal of Naval Architecture and Ocean Engineering*, 6 (2014), 507-528.

Kim, D.K., Park, D.K., Kim, H.B., Seo, J.K., Kim, B.J., Paik, J.K. and Kim, M.S., 2012. The necessity of applying the common corrosion addition rule to container ships in terms of ultimate longitudinal strength. *Ocean Engineering*, 49 (2012), 43-55.

Kim, Y.S., Park, D.K., Kim, S.J., Lee, D.H., Kim, B.J., Ha, Y.C., Seo, J.K. and Paik, J.K., 2014. Ultimate strength assessment of ship stiffened panel under Arctic conditions. *Journal of the Society of Naval Architects of Korea*, 51 (4), 283-290.

- Lee, S.E., Thayamballi, A.K. and Paik, J.K., 2015. Ultimate strength of steel brackets in ship structures. *International Journal of Ocean Engineering*, 101 (2015), 182-200.
- Lehmann, E. and Peschmann, J., 2002. Energy absorption by the steel structure of ships in the event of collisions. *Marine Structures*, 15 (2002), 429-441.
- Mohd, M.H. and Paik, J.K., 2013. Investigation of the corrosion progress characteristics of offshore subsea oil well tubes. *Corrosion Science*, 67 (2013), 130-141.
- Park, D.K., 2015. *Nonlinear structural response analysis of ship and offshore structures in low temperature*. Thesis (PhD). Pusan National University.
- Park, D.K., Kim, D.K., Seo, J.K., Kim, B.J., Ha, Y.C. and Paik, J.K., 2015. Operability of non-ice class aged ships in the Arctic Ocean-part I: Ultimate limit state approach. *Ocean Engineering*, 102 (2015), 197-205.
- Park, D.K., Kim, D.K., Seo, J.K., Kim, B.J., Ha, Y.C. and Paik, J.K., 2015. Operability of non-ice class aged ships in the Arctic Ocean-part II: Accidental limit state approach. *Ocean Engineering*, 102 (2015), 206-215.
- Paik, J.K., Amlashi, H., Boon, B., Branner K., Caridis, P., Das, P., Fujikubo, M., Huang, C.H., Josefson, L., Kaeding, P., Kim, C.W., Parmentier, G., Pasqualino, I.P., Rizzo, C.M., Vhanmane, S., Wang, X. and Yang, P., 2012. Committee III.1: Ultimate strength. *18th International Ship and Offshore Structures Congress*, 1, 285-363.
- Paik, J.K. and Kim, D.K., 2012. Advanced method for the development of an empirical model to predict time-dependent corrosion wastage. *Corrosion Science*, 63 (2012), 51-58.
- Paik, J.K. and Melchers, R.E., 2008. *Condition assessment of aged structures*. New York: CRC Press.
- Paik J.K., Kim S.J., D.H. Kim & D.C. Kim, P.A. Frieze, M. Abbattista & M. Vallascas, O.F. Hughes, 2011. Benchmark study on use of ALPS/ULSAP method to determine plate and stiffened panel ultimate strength. *Marstruct conference*, 2011
- Paik, J.K. and Thayamballi, A.K., 2003. *Ultimate limit state design of steel-plated structures*. Chichester: John Wiley & Sons.
- Paik, J.K. and Thayamballi, A.K., 2007. *Ship-shaped offshore installations: Design, building, and operation*. Cambridge: Cambridge University Press.
- Paik, J.K., Kim, B.J., Park, D.K. and Jang, B.S., 2011. On quasi-static crushing of thin-walled steel structures in cold temperature: Experimental and numerical studies. *International Journal of Impact Engineering*, 38 (2011), 13-28.
- Paik, J.K., Lee, J.M., Park, Y.I., Hwang, J.S. and Kim, C.W., 2003. Time-variant ultimate longitudinal strength of corroded bulk carriers. *Marine Structures*, 16 (2003), 567-600.
- Paik, J.K., Thayamballi, A.K., Park, Y.I. and Hwang, J.S., 2004. A time-dependent corrosion wastage model for seawater ballast tank structures of ships. *Corrosion Science*, 46 (2004), 471-486.

Qin, S. and Cui, W., 2003. Effect of corrosion models on the time-dependent reliability of steel plated elements. *Marine Structures*, 16 (2003), 15-34.

Soares, C.G., Garbatov, Y., Zayed, A. and Wang, G., 2005. Non-linear corrosion model for immersed steel plates accounting for environmental factors. *ABS Technical Papers*, 193-211.

Tabri, K., Broekhuijsen, J., Matusiak, J. and Varsta, P., 2009. Analytical modelling of ship collision based on full-scale experiments. *Marine Structures*, 22 (2009), 42-61.

Wisniewski, K. and Kolakowski, P., 2003. The effect of selected parameters on ship collision results by dynamic FE simulations. *Finite Elements in Analysis and Design*, 39 (2003), 985-1006.

Xu, L.Y. and Cheng, Y.F., 2012. Reliability and failure pressure prediction of various grades of pipeline steel in the presence of corrosion defects and pre-strain. *International Journal of Pressure Vessels and Piping*, 89 (2012), 75-84.

Zhang, M.Q., Beer, M., Quek, S.T. and Choo, Y.S., 2010. Comparison of uncertainty models in reliability analysis of offshore structures under marine corrosion. *Structural Safety*, 32 (2010), 425-432.

APPENDICES

➤ Initial deflection calculation for 7 cases:

Case 1 (Upper deck):

Temperature 20°C	corrosion wastage (original)	5 years	10 years	15 years	20 years	25 years
UPPER DECK	1.5	0.375	0.75	1.125	1.5	1.875
800	thickness	77.625	77.25	76.875	76.5	76.125
	Initial max. deflection	1.302	1.308	1.315	1.321	1.328
	E, young's modulus	205800	205800	205800	205800	205800
	yielding stress	325.000	325.000	325.000	325.000	325.000
	b, plate breadth	800	800	800	800	800
	β	0.410	0.412	0.414	0.416	0.418

Temperature 0°C	corrosion wastage (original)	5 years	10 years	15 years	20 years	25 years
UPPER DECK	1.5	0.375	0.75	1.125	1.5	1.875
	thickness	77.625	77.25	76.875	76.5	76.125
	Initial max. deflection	1.302	1.308	1.315	1.321	1.328
	E, young's modulus	205800	205800	205800	205800	205800
	yielding stress	325.000	325.000	325.000	325.000	325.000
	b, plate breadth	800	800	800	800	800
	β	0.410	0.412	0.414	0.416	0.418

Temperature -20°C	corrosion wastage (original)	5 years	10 years	15 years	20 years	25 years
UPPER DECK	1.5	0.375	0.75	1.125	1.5	1.875
	thickness	77.625	77.25	76.875	76.5	76.125
	Initial max. deflection	1.303	1.310	1.316	1.322	1.329
	E, young's modulus	205800	205800	205800	205800	205800
	yielding stress	325.325	325.325	325.325	325.325	325.325
	b, plate breadth	800	800	800	800	800
	β	0.410	0.412	0.414	0.416	0.418

Temperature -40°C	corrosion wastage (original)	5 years	10 years	15 years	20 years	25 years
UPPER DECK	1.5	0.375	0.75	1.125	1.5	1.875
	thickness	77.625	77.25	76.875	76.5	76.125
	Initial max. deflection	1.338	1.345	1.352	1.358	1.365
	E, young's modulus	205800	205800	205800	205800	205800
	yielding stress	334.100	334.100	334.100	334.100	334.100
	b, plate breadth	800	800	800	800	800
	β	0.415	0.417	0.419	0.421	0.423

Temperature -60°C	corrosion wastage (original)	5 years	10 years	15 years	20 years	25 years
UPPER DECK	1.5	0.375	0.75	1.125	1.5	1.875
	thickness	77.625	77.25	76.875	76.5	76.125
	Initial max. deflection	1.396	1.403	1.409	1.416	1.423
	E, young's modulus	205800	205800	205800	205800	205800
	yielding stress	348.400	348.400	348.400	348.400	348.400
	b, plate breadth	800	800	800	800	800
	β	0.424	0.426	0.428	0.430	0.432

Case 2 (Bottom plate in pipe duct area):

Temperature 20°C	corrosion wastage (original)	5 years	10 years	15 years	20 years	25 years
BTMPD	1	0.25	0.5	0.75	1	1.25
	thickness	22.75	22.5	22.25	22	21.75
	Initial max. deflection	4.093	4.139	4.185	4.233	4.281
	E, young's modulus	205800	205800	205800	205800	205800
	yielding stress	315.000	315.000	315.000	315.000	315.000
	b, plate breadth	780	780	780	780	780
	β	1.341	1.356	1.372	1.387	1.403

Temperature 0°C	corrosion wastage (original)	5 years	10 years	15 years	20 years	25 years
BTMPD	1	0.25	0.5	0.75	1	1.25
	thickness	22.75	22.5	22.25	22	21.75
	Initial max. deflection	4.093	4.139	4.185	4.233	4.281
	E, young's modulus	205800	205800	205800	205800	205800
	yielding stress	315.000	315.000	315.000	315.000	315.000
	b, plate breadth	780	780	780	780	780
	β	1.341	1.356	1.372	1.387	1.403

Temperature -20°C	corrosion wastage (original)	5 years	10 years	15 years	20 years	25 years
BTMPD	1	0.25	0.5	0.75	1	1.25
	thickness	22.75	22.5	22.25	22	21.75
	Initial max. deflection	4.097	4.143	4.189	4.237	4.286
	E, young's modulus	205800	205800	205800	205800	205800
	yielding stress	315.315	315.315	315.315	315.315	315.315
	b, plate breadth	780	780	780	780	780
	β	1.342	1.357	1.372	1.388	1.404

Temperature -40°C	corrosion wastage (original)	5 years	10 years	15 years	20 years	25 years
BTMPD	1	0.25	0.5	0.75	1	1.25
	thickness	22.75	22.5	22.25	22	21.75
	Initial max. deflection	4.208	4.255	4.302	4.351	4.401
	E, young's modulus	205800	205800	205800	205800	205800
	yielding stress	323.820	323.820	323.820	323.820	323.820
	b, plate breadth	780	780	780	780	780
	β	1.360	1.375	1.391	1.406	1.423

Temperature -60°C	corrosion wastage (original)	5 years	10 years	15 years	20 years	25 years
BTMPD	1	0.25	0.5	0.75	1	1.25
	thickness	22.75	22.5	22.25	22	21.75
	Initial max. deflection	4.388	4.437	4.487	4.538	4.590
	E, young's modulus	205800	205800	205800	205800	205800
	yielding stress	337.680	337.680	337.680	337.680	337.680
	b, plate breadth	780	780	780	780	780
	β	1.389	1.404	1.420	1.436	1.453

Case 3 (Inner bottom plate in pipe duct area):

Temperature 20°C	corrosion wastage (original)	5 years	10 years	15 years	20 years	25 years
INBTMPD	1.00	0.25	0.5	0.75	1	1.25
	thickness	17.75	17.5	17.25	17	16.75
	Initial max. deflection	5.246	5.321	5.398	5.478	5.560
	E, young's modulus	205800	205800	205800	205800	205800
	yielding stress	315.000	315.000	315.000	315.000	315.000
	b, plate breadth	780	780	780	780	780
	β	1.719	1.744	1.769	1.795	1.822

Temperature 0°C	corrosion wastage (original)	5 years	10 years	15 years	20 years	25 years
INBTMPD	1.00	0.25	0.5	0.75	1	1.25
	thickness	17.75	17.5	17.25	17	16.75
	Initial max. deflection	5.246	5.321	5.398	5.478	5.560
	E, young's modulus	205800	205800	205800	205800	205800
	yielding stress	315.000	315.000	315.000	315.000	315.000
	b, plate breadth	780	780	780	780	780
	β	1.719	1.744	1.769	1.795	1.822

Temperature -20°C	corrosion wastage (original)	5 years	10 years	15 years	20 years	25 years
INBTMPD	1	0.25	0.5	0.75	1	1.25
	thickness	17.75	17.5	17.25	17	16.75
	Initial max. deflection	5.252	5.327	5.404	5.483	5.565
	E, young's modulus	205800	205800	205800	205800	205800
	yielding stress	315.315	315.315	315.315	315.315	315.315
	b, plate breadth	780	780	780	780	780
	β	1.720	1.745	1.770	1.796	1.823

Temperature -40°C	corrosion wastage (original)	5 years	10 years	15 years	20 years	25 years
INBTMPD	1	0.25	0.5	0.75	1	1.25
	thickness	17.75	17.5	17.25	17	16.75
	Initial max. deflection	5.393	5.470	5.550	5.631	5.715
	E, young's modulus	205800	205800	205800	205800	205800
	yielding stress	323.820	323.820	323.820	323.820	323.820
	b, plate breadth	780	780	780	780	780
	β	1.743	1.768	1.794	1.820	1.847

Temperature -60°C	corrosion wastage (original)	5 years	10 years	15 years	20 years	25 years
INBTMPD	1	0.25	0.5	0.75	1	1.25
	thickness	17.75	17.5	17.25	17	16.75
	Initial max. deflection	5.624	5.704	5.787	5.872	5.960
	E, young's modulus	205800	205800	205800	205800	205800
	yielding stress	337.680	337.680	337.680	337.680	337.680
	b, plate breadth	780	780	780	780	780
	β	1.780	1.805	1.832	1.859	1.886

Case 4 & Case 5 (Bottom plate with indifferent stiffeners):

Temperature 20°C	corrosion wastage (original)	5 years	10 years	15 years	20 years	25 years
BTM/BTM-2	1	0	0.333	0.667	1	1.333
	thickness	22	21.667	21.333	21	20.667
	Initial max. deflection	4.909	4.985	5.063	5.143	5.226
	E, young's modulus	205800	205800	205800	205800	205800
	yielding stress	315.000	315.000	315.000	315.000	315.000
	b, plate breadth	840	840	840	840	840
	β	1.494	1.517	1.540	1.565	1.590

Temperature -20°C	corrosion wastage (original)	5 years	10 years	15 years	20 years	25 years
BTM/BTM-2	1	0	0.333	0.667	1	1.333
	thickness	22	21.667	21.333	21	20.667
	Initial max. deflection	4.914	4.990	5.068	5.148	5.231
	E, young's modulus	205800	205800	205800	205800	205800
	yielding stress	315.315	315.315	315.315	315.315	315.315
	b, plate breadth	840	840	840	840	840
	β	1.495	1.518	1.541	1.566	1.591
Temperature -40°C	corrosion wastage (original)	5 years	10 years	15 years	20 years	25 years
BTM/BTM-2	1	0	0.333	0.667	1	1.333
	thickness	22	21.667	21.333	21	20.667
	Initial max. deflection	5.047	5.124	5.204	5.287	5.372
	E, young's modulus	205800	205800	205800	205800	205800
	yielding stress	323.820	323.820	323.820	323.820	323.820
	b, plate breadth	840	840	840	840	840
	β	1.515	1.538	1.562	1.587	1.612
Temperature -60°C	corrosion wastage (original)	5 years	10 years	15 years	20 years	25 years
BTM/BTM-2	1	0	0.333	0.667	1	1.333
	thickness	22	21.667	21.333	21	20.667
	Initial max. deflection	5.263	5.344	5.427	5.513	5.602
	E, young's modulus	205800	205800	205800	205800	205800
	yielding stress	337.680	337.680	337.680	337.680	337.680
	b, plate breadth	840	840	840	840	840
	β	1.547	1.570	1.595	1.620	1.646

Case 6 & Case 7 (Inner bottom plate with indifferent stiffeners):

Temperature 20°C	corrosion wastage (original)	5 years	10 years	15 years	20 years	25 years
INBTM/INBTM-2	1.5	0	0.5	1	1.5	2
	thickness	18	17.5	17	16.5	16
	Initial max. deflection	6.000	6.171	6.353	6.545	6.750
	E, young's modulus	205800	205800	205800	205800	205800
	yielding stress	315.000	315.000	315.000	315.000	315.000
	b, plate breadth	840	840	840	840	840
	β	1.826	1.878	1.933	1.992	2.054

Temperature 0°C	corrosion wastage (original)	5 years	10 years	15 years	20 years	25 years
INBTM/INBTM-2	1.5	0	0.5	1	1.5	2
	thickness	18	17.5	17	16.5	16
	Initial max. deflection	6.000	6.171	6.353	6.545	6.750
	E, young's modulus	205800	205800	205800	205800	205800
	yielding stress	315.000	315.000	315.000	315.000	315.000
	b, plate breadth	840	840	840	840	840
	β	1.826	1.878	1.933	1.992	2.054
Temperature -20°C	corrosion wastage (original)	5 years	10 years	15 years	20 years	25 years
INBTM/INBTM-2	1.5	0	0.5	1	1.5	2
	thickness	18	17.5	17	16.5	16
	Initial max. deflection	6.006	6.178	6.359	6.552	6.757
	E, young's modulus	205800	205800	205800	205800	205800
	yielding stress	315.315	315.315	315.315	315.315	315.315
	b, plate breadth	840	840	840	840	840
	β	1.827	1.879	1.934	1.993	2.055
Temperature -40°C	corrosion wastage (original)	5 years	10 years	15 years	20 years	25 years
INBTM/INBTM-2	1.5	0	0.5	1	1.5	2
	thickness	18	17.5	17	16.5	16
	Initial max. deflection	6.168	6.344	6.531	6.729	6.939
	E, young's modulus	205800	205800	205800	205800	205800
	yielding stress	323.820	323.820	323.820	323.820	323.820
	b, plate breadth	840	840	840	840	840
	β	1.851	1.904	1.960	2.019	2.083
Temperature -60°C	corrosion wastage (original)	5 years	10 years	15 years	20 years	25 years
INBTM/INBTM-2	1.5	0	0.5	1	1.5	2
	thickness	18	17.5	17	16.5	16
	Initial max. deflection	6.432	6.616	6.810	7.017	7.236
	E, young's modulus	205800	205800	205800	205800	205800
	yielding stress	337.680	337.680	337.680	337.680	337.680
	b, plate breadth	840	840	840	840	840
	β	1.890	1.944	2.002	2.062	2.127